

MPI-Ph/93-11
CERN-TH-6821/93
TUM-T31-35/93
March 1993

The Anatomy of ε'/ε Beyond Leading Logarithms with Improved Hadronic Matrix Elements*

Andrzej J. BURAS^{1,2}, Matthias JAMIN³ and Markus E. LAUTENBACHER¹

¹ *Physik Department, Technische Universität München, D-8046 Garching, FRG.*

² *Max-Planck-Institut für Physik – Werner-Heisenberg-Institut,
P.O. Box 40 12 12, D-8000 München, FRG.*

³ *Division TH, CERN, 1211 Geneva 23, Switzerland.*

*Supported by the German Bundesministerium für Forschung und Technologie under contract 06 TM 732 and by the CEC Science project SC1-CT91-0729.

ABSTRACT

We use the recently calculated two-loop anomalous dimensions of current-current operators, QCD and electroweak penguin operators to construct the effective Hamiltonian for $\Delta S = 1$ transitions beyond the leading logarithmic approximation. We solve the renormalization group equations involving α_s and α up to two-loop level and we give the numerical values of Wilson coefficient functions $C_i(\mu)$ beyond the leading logarithmic approximation in various renormalization schemes. Numerical results for the Wilson coefficients in $\Delta B = 1$ and $\Delta C = 1$ Hamiltonians are also given. We discuss several aspects of renormalization scheme dependence and demonstrate the scheme independence of physical quantities. We stress that the scheme dependence of the Wilson coefficients $C_i(\mu)$ can only be cancelled by the one present in the hadronic matrix elements $\langle Q_i(\mu) \rangle$. This requires also the calculation of $\mathcal{O}(\alpha)$ corrections to $\langle Q_i(\mu) \rangle$. We propose a new semi-phenomenological approach to hadronic matrix elements which incorporates the data for CP -conserving $K \rightarrow \pi\pi$ amplitudes and allows to determine the matrix elements of all $(V - A) \otimes (V - A)$ operators in any renormalization scheme. Our renormalization group analysis of all hadronic matrix elements $\langle Q_i(\mu) \rangle$ reveals certain interesting features. We compare critically our treatment of these matrix elements with those given in the literature. When matrix elements of dominant QCD penguin (Q_6) and electroweak penguin (Q_8) operators are kept fixed the effect of next-to-leading order corrections is to lower considerably ε'/ε in the 't Hooft-Veltman (HV) renormalization scheme with a smaller effect in the dimensional regularization scheme with anticommuting γ_5 (NDR). Taking $m_t = 130$ GeV, $\Lambda_{\overline{\text{MS}}} = 300$ MeV and calculating $\langle Q_6 \rangle$ and $\langle Q_8 \rangle$ in the $1/N$ approach with $m_s(1 \text{ GeV}) = 175$ MeV, we find in the NDR scheme $\varepsilon'/\varepsilon = (6.7 \pm 2.6) \times 10^{-4}$ in agreement with the experimental findings of E731. We point out however that the increase of $\langle Q_6 \rangle$ by only a factor of two gives $\varepsilon'/\varepsilon = (20.0 \pm 6.5) \times 10^{-4}$ in agreement with the result of NA31. The dependence of ε'/ε on $\Lambda_{\overline{\text{MS}}}$, m_t and $\langle Q_{6,8} \rangle$ is presented. A detailed anatomy of various contributions and comparison with the analyses of Rome and Dortmund groups are given.

Contents

1	Introduction	1
2	Basic Formulae for Wilson Coefficient Functions	6
2.1	Operators	6
2.2	Renormalization Group Equations	7
2.3	Generalized Evolution Matrix	8
2.4	The Pure QCD Evolution Matrix $\hat{U}(m_1, m_2)$	9
2.5	The Evolution Matrix $\hat{R}(m_1, m_2)$	10
2.6	A Different Form of the Evolution Matrix	11
2.7	The Initial Conditions $\vec{C}(M_W)$	12
2.8	Final Formulae for Wilson Coefficient Functions	13
3	Renormalization Scheme Dependence	13
3.1	General Consistency Relations	13
3.2	Relations Between Coefficient Functions	14
3.3	Scheme Independence of Physical Quantities	15
4	$\Delta S = 1$ Hamiltonian Beyond Leading Logarithms	15
4.1	General Remarks	16
4.2	Master Formulae for Wilson Coefficient Functions ($\mu < m_c$)	16
4.3	The Matching Matrix \hat{M}	21
4.4	Master Formulae for Wilson Coefficients ($m_c < \mu < m_b$)	22
4.5	Relations Between Operators	22
4.6	Numerical Results for Wilson Coefficients	23
4.7	Comparison with refs. [12], [13] and [16]	26
5	Hadronic Matrix Elements	27
5.1	General Remarks	27
5.2	Explicit Formulae for the Matrix Elements	30
5.3	Critical Comparison of Various Matrix Elements Estimates	31
6	A Phenomenological Approach to Hadronic Matrix Elements	34
6.1	General Remarks	34
6.2	$\langle Q_i(\mu) \rangle_2$ for $(V - A) \otimes (V - A)$ Operators	35
6.3	$\langle Q_i(\mu) \rangle_0$ for $(V - A) \otimes (V - A)$ Operators	38

6.4	$\langle Q_i(\mu) \rangle_{0,2}$ for $(V - A) \otimes (V + A)$ Operators	40
6.5	The Fate of the Operators $Q_{1,2}^c$	42
6.6	Strategy of the Present Paper	42
7	CKM-Parameters and ε	43
8	ε'/ε Beyond Leading Logarithms	45
8.1	Basic Formulae	45
8.2	B_i -Expansions and the Four Dominant Contributions to ε'/ε	46
8.3	The μ -Dependence of Various Contributions	48
8.4	Final Numerical Results for ε'/ε	49
8.5	Comparison with Other Analyses	50
9	Wilson Coefficients for $\Delta B = 1$ Decays	52
10	Ten Messages from This Paper	53
A	Quark Threshold Matching Matrices	62
B	Numerical Results for Wilson Coefficients, ε'/ε and B_i-Expansion	63
C	Collection of Numerical Input Parameters	74
D	Figures	75

1 Introduction

The CP -violating ratio ε'/ε is governed by penguin contributions [1, 2]. Until 1989 there had been a general belief [3, 4] that ε'/ε is mainly described by the QCD-penguin contributions with the electroweak penguins (γ - and Z^0 -penguins) playing only a secondary role. A new development in this field came in 1989 through the increase of m_t and the work of Flynn and Randall [5] who pointed out that for large m_t the electroweak penguin contributions could become important and, having opposite sign to QCD-penguin contributions, could considerably suppress ε'/ε . A detailed anatomy of ε'/ε in the presence of a heavy top quark has been done by Buchalla, Harlander and one of the authors [6]. It has been found that with increasing m_t the electroweak penguins could indeed compete with QCD penguins to cancel their contribution completely for $m_t \approx \mathcal{O}(220 \text{ GeV})$ so that $\varepsilon'/\varepsilon \approx 0$ like in superweak theories. This rather surprising result has been confirmed in subsequent years by Paschos and Wu [7] and by Lusignoli, Maiani, Martinelli and Reina [8].

On the experimental side, after heroic efforts on both sides of the Atlantic the situation is not yet conclusive [9, 10],

$$\text{Re}(\varepsilon'/\varepsilon) = \begin{cases} (23 \pm 7) \cdot 10^{-4} & \text{NA31} \\ (7.4 \pm 6.0) \cdot 10^{-4} & \text{E731} \end{cases} . \quad (1.1)$$

While the result of NA31 clearly indicates a non-zero ε'/ε , the value of E731 is compatible with superweak theories in which $\varepsilon'/\varepsilon \equiv 0$ [11]. From the point of view of the analyses quoted above the NA31 result points toward a top quark mass of $m_t \approx \mathcal{O}(100 \text{ GeV})$ whereas the E731 result points toward $m_t \gtrsim \mathcal{O}(150 \text{ GeV})$. Hopefully, in the next five years the experimental situation on ε'/ε will be clarified through the new measurements by the two collaborations at the 10^{-4} level and by experiments at the Φ -factory in Frascati.

Since the outcome of the fight between QCD and electroweak penguins is rather sensitive to various approximations used in refs. [6, 7, 8], it is important to improve the theoretical calculations of short distance (Wilson coefficient functions $C_i(\mu)$) and also the estimates of long distance (hadronic matrix elements $\langle Q_i(\mu) \rangle$) contributions. In the present paper we will make progress on both parts of the problem by calculating the Wilson coefficients beyond the leading logarithmic approximation and by extracting several hadronic matrix elements from the existing very accurate data on CP -conserving $K \rightarrow \pi\pi$ amplitudes. Needless to say that many results presented here are not only important for ε'/ε but can also be applied to all $\Delta S = 1$, $\Delta C = 1$ and $\Delta B = 1$ decay processes.

The present paper culminates our extensive studies of $\Delta F = 1$ effective non-leptonic Hamiltonians beyond the leading logarithmic approximation [12]–[15]. In ref. [12] two-loop

anomalous dimensions $\mathcal{O}(\alpha_s^2)$ of current-current operators have been calculated, confirming the previous results of Altarelli et al. [16]. This calculation has been extended to include QCD penguin operators and electroweak penguin operators in ref. [13, 14] where a two-loop 10×10 anomalous dimension matrix $\mathcal{O}(\alpha_s^2)$ has been presented. Subsequently, the corresponding two-loop matrix of order $\mathcal{O}(\alpha \alpha_s)$ has been calculated [15]. The latter is necessary for a consistent treatment of electroweak penguin operators beyond the leading logarithmic approximation.

One of the aims of the present paper is to construct the effective Hamiltonian for $\Delta S = 1$ transitions which incorporates the results of refs. [12]–[15]. This Hamiltonian will take the form

$$\mathcal{H}_{\text{eff}} = \frac{G_F}{\sqrt{2}} \sum_{i=1}^{10} Q_i(\mu) C_i(\mu) \equiv \frac{G_F}{\sqrt{2}} \vec{Q}(\mu)^T \vec{C}(\mu), \quad (1.2)$$

where the Wilson coefficients $C_i(\mu)$ include leading and next-to-leading QCD corrections and leading order corrections in the electromagnetic coupling constant α . Here $Q_{1,2}$ stand for current-current operators, Q_{3-6} for QCD penguin operators and Q_{7-10} for electroweak penguin operators. Explicit expressions for these operators will be given in section 2. A truncated effective Hamiltonian for Q_{1-6} with $\alpha = 0$ has been presented already by us in ref. [13], where an application to the $\Delta I = 1/2$ rule and ε'/ε has been made. The present paper can be considered on one hand as a generalization of ref. [13] to include electroweak penguin operators. On the other hand it can be considered as a generalization of the analyses [5, 6, 7, 8] to include next-to-leading logarithmic effects. Whereas in refs. [5, 6, 7, 8] the logarithms $(\alpha_s t)^n$ and $\alpha t (\alpha_s t)^n$ with $t = \ln(M_W^2/\mu^2)$ have been summed, the present analysis includes also the logarithms $\alpha_s (\alpha_s t)^n$ and $\alpha (\alpha_s t)^n$. Moreover, we improve the treatment of hadronic matrix elements.

The central questions which one would like to address in a paper like this one are as follows:

- Do the complete next-to-leading corrections enhance or suppress the Wilson coefficients of current-current operators ?
- Do the complete next-to-leading corrections enhance or suppress the Wilson coefficient functions of QCD penguin operators ?
- Do these corrections enhance or suppress the Wilson coefficients of electroweak penguin operators relative to the ones of QCD penguin operators ?
- What is the impact of all these effects on ε'/ε and the $\Delta I = 1/2$ rule ?

- How does ε'/ε depend on $\Lambda_{\overline{\text{MS}}}$?

Unfortunately, the answers to these questions are complicated by the fact that the coefficients $C_i(\mu)$ depend at the next-to-leading level on the renormalization scheme for the operators Q_i , and only after the hadronic matrix elements $\langle Q_i(\mu) \rangle$ have been calculated at the same level, can this scheme dependence be removed. This requires also the calculation of $\mathcal{O}(\alpha)$ corrections to $\langle Q_i(\mu) \rangle$. Thus the size of next-to-leading order corrections to $C_i(\mu)$ calculated in the NDR scheme (anticommuting γ_5 in $D \neq 4$ space-time dimensions) differs from the corresponding corrections found in the HV scheme (non-anticommuting γ_5 in $D \neq 4$ space-time dimensions). In order to cancel these dependences one would have to calculate $\langle Q_i(\mu) \rangle$ in a method sensitive to such a scheme dependence. To our knowledge only QCD sum rules could be useful in this respect at present but future lattice calculations also could overcome this difficulty, at least in principle. In spite of this our short distance calculation provides an important and necessary step towards a more accurate estimate of weak decay amplitudes than the one given merely by the leading logarithmic approximation. Moreover, in order to consistently study the m_t -dependence of weak amplitudes it is mandatory to go beyond the leading logarithmic approximation as will be evident from what follows.

The scheme dependence just discussed is an important point which we would like to address here. To this end we will evaluate the Wilson coefficient functions in three different schemes and we will investigate how the scheme dependence affects the answers to the set of questions stated above if no proper scheme dependence is incorporated in the matrix elements $\langle Q_i(\mu) \rangle$. In particular, we find as a rather unexpected result that the next-to-leading QCD corrections to Wilson coefficients of current-current operators Q_1 and Q_2 calculated in the renormalization schemes considered in fact *suppress* slightly the $\Delta I = 1/2$ transitions and *enhance* the $\Delta I = \frac{3}{2}$ transitions. We explain why the authors of refs. [12] and [16] who performed correct calculations reached conclusions opposite to ours.

Other not unrelated issues are the μ -dependence of $\langle Q_i(\mu) \rangle$ and the actual values of these matrix elements. For this reason we have made a critical comparison of the existing estimates of $\langle Q_i(\mu) \rangle$ based on the vacuum insertion, the $1/N$ -expansion and lattice methods. In this connection, we point out that the evolution of $\langle Q_i(\mu) \rangle$ with μ can be calculated within renormalization group improved perturbation theory. Performing to our knowledge the first detailed renormalization group analysis of $\langle Q_i(\mu) \rangle$ we find that due to the asymmetry of the anomalous dimension matrices the μ -dependences of $\langle Q_i(\mu) \rangle$ are quite different from the ones of $C_i(\mu)$. This allowed us to answer the following question:

- Should the parameters B_i entering various $\langle Q_i(\mu) \rangle$ be μ -dependent in order to be consistent with the true QCD evolution ?

Rather unexpectedly, we have found that the B_i parameters of *all* $(V - A) \otimes (V + A)$ operators $Q_5 - Q_8$ show only very weak μ -dependence for $\mu \gtrsim 1$ GeV supporting to some extent the structure of these matrix elements which is common to the three approaches in question. On the other hand the B_i parameters of $(V - A) \otimes (V - A)$ operators show sizeable μ -dependence which is fully missing in the vacuum insertion approach, partly present in the $1/N$ approach and not yet calculable in the lattice approach.

In view of the latter problem and the fact that the present methods are not yet capable of addressing properly the renormalization scheme dependence of $\langle Q_i(\mu) \rangle$, nor fully explain the known data on CP -conserving $K \rightarrow \pi\pi$ decays, we have developed a phenomenological framework in which the matrix elements $\langle Q_i(\mu) \rangle$ necessary for the calculation of ε'/ε are extracted as far as possible from the data on CP -conserving $K \rightarrow \pi\pi$ decays. In this framework the central role is played by the calculable scheme and μ -dependent coefficients $C_i(\mu)$ and the scheme and μ -independence of measured $K \rightarrow \pi\pi$ amplitudes gives us automatically the scheme and μ -dependence of $\langle Q_i(\mu) \rangle$ which are in addition consistent with the CP -conserving $K \rightarrow \pi\pi$ data. Thus the $\Delta I = 1/2$ rule is incorporated in our approach from the beginning. We verify that the scheme and μ -dependences of $\langle Q_i(\mu) \rangle$ found this way are to a very good approximation consistent with the ones given by the renormalization group.

Our approach has the four basic parameters

$$\Lambda_{\overline{\text{MS}}}, \quad B_2^{(1/2)}(m_c), \quad B_6^{(1/2)}(m_c), \quad B_8^{(3/2)}(m_c). \quad (1.3)$$

The choice $\mu = m_c$ turns out to be very convenient but is not necessary. The last three parameterize hadronic matrix elements for $K \rightarrow \pi\pi$, and will be defined in section 5.2. $B_2^{(1/2)}(m_c)$ parameterizes all matrix elements $\langle Q_i \rangle_0$ of $(V - A) \otimes (V - A)$ operators. $B_6^{(1/2)}(m_c)$ and $B_8^{(3/2)}(m_c)$ parameterize the $(V - A) \otimes (V + A)$ operators. In our phenomenological approach all matrix elements are given in terms of these four parameters in such a way that for each set of these parameters all data on CP -conserving $K \rightarrow \pi\pi$ amplitudes are reproduced. Moreover, all the matrix elements $\langle Q_i(\mu) \rangle_2$ of $(V - A) \otimes (V - A)$ operators ($i = 1, 2, 9, 10$) are given in our approach as numerical functions of only $\Lambda_{\overline{\text{MS}}}$, μ and the renormalization scheme considered. With all these matrix elements at hand we can predict the CP -violating quantity

$$\frac{\varepsilon'}{\varepsilon} = 10^{-4} \left[\frac{\text{Im}\lambda_t}{1.7 \cdot 10^{-4}} \right] \left[P^{(1/2)} - P^{(3/2)} \right], \quad (1.4)$$

where $\lambda_t = V_{ts}^* V_{td}$ and

$$P^{(1/2)} = a_0^{(1/2)} + a_2^{(1/2)} B_2^{(1/2)} + a_6^{(1/2)} B_6^{(1/2)}, \quad (1.5)$$

$$P^{(3/2)} = a_0^{(3/2)} + a_8^{(3/2)} B_8^{(3/2)}. \quad (1.6)$$

We calculate the coefficients a_i as functions of $\Lambda_{\overline{\text{MS}}}$ and m_t for the leading order and the two renormalization schemes (NDR, HV) considered.

We hope very much that this novel anatomy of various aspects of ε'/ε including next-to-leading order corrections and an improved treatment of hadronic matrix elements will shed some light on the present uncertainties and on the theoretical prediction of ε'/ε in the Standard Model (SM). By doing this we will attempt to clarify the discrepancy between recent theoretical estimates of ε'/ε which bears some similarity in it to the discrepancy concerning experimental results on ε'/ε given in eq. (1.1). Whereas the Dortmund group [17, 18] found last year ε'/ε to be close to the NA31 result, the very recent analysis of the Rome group [19] favours the experimental result of E731.

Our paper is organized as follows: In section 2, we will present general formulae for $C_i(\mu)$ beyond the leading logarithmic approximation. These formulae generalize the ones given in refs. [13] and [6]. In section 3, the renormalization scheme dependence will be discussed. In section 4, we calculate the coefficients $C_i(M_W)$ and use the known one-loop [2], [20]–[27] and two-loop anomalous dimension matrices [12]–[15] to find $C_i(\mu)$ in various renormalization schemes. In section 5, we collect and compare various existing theoretical estimates of hadronic matrix elements. In section 6, we present the details of our phenomenological approach to the matrix elements, we calculate the matrix elements as functions of the parameters in eq. (1.3) and compare the results with the ones obtained in section 5. Here, we also present the renormalization group evolution of $\langle Q_i(\mu) \rangle$ advertised earlier in this paper. In section 7, we recall the CKM-parameters necessary for our numerical analysis of ε'/ε and we give the $\Delta S = 2$ Hamiltonian which we used to determine the CKM-phase δ from the experimental value of the parameter ε describing indirect CP -violation in the K -system. In section 8, we give the basic expressions for ε'/ε in terms of $C_i(\mu)$ and $\langle Q_i(\mu) \rangle$, and we address all the issues mentioned above. In particular we give the results for ε'/ε as a function of $\Lambda_{\overline{\text{MS}}}$, m_t and the matrix elements $\langle Q_6 \rangle_0$ and $\langle Q_8 \rangle_2$. For completeness, we give in section 9, the numerical values for $C_i(\mu)$ relevant for $\Delta B = 1$ transitions. We end our paper with a list of main messages coming from our new anatomy of ε'/ε .

2 Basic Formulae for Wilson Coefficient Functions

2.1 Operators

In order to illustrate the scheme dependence of Wilson coefficient functions we will use two bases of operators. Our main basis is given as follows

$$\begin{aligned}
Q_1 &= (\bar{s}_\alpha u_\beta)_{V-A} (\bar{u}_\beta d_\alpha)_{V-A} , \\
Q_2 &= (\bar{s}u)_{V-A} (\bar{u}d)_{V-A} , \\
Q_3 &= (\bar{s}d)_{V-A} \sum_q (\bar{q}q)_{V-A} , \\
Q_4 &= (\bar{s}_\alpha d_\beta)_{V-A} \sum_q (\bar{q}_\beta q_\alpha)_{V-A} , \\
Q_5 &= (\bar{s}d)_{V-A} \sum_q (\bar{q}q)_{V+A} , \\
Q_6 &= (\bar{s}_\alpha d_\beta)_{V-A} \sum_q (\bar{q}_\beta q_\alpha)_{V+A} , \\
Q_7 &= \frac{3}{2} (\bar{s}d)_{V-A} \sum_q e_q (\bar{q}q)_{V+A} , \\
Q_8 &= \frac{3}{2} (\bar{s}_\alpha d_\beta)_{V-A} \sum_q e_q (\bar{q}_\beta q_\alpha)_{V+A} , \\
Q_9 &= \frac{3}{2} (\bar{s}d)_{V-A} \sum_q e_q (\bar{q}q)_{V-A} , \\
Q_{10} &= \frac{3}{2} (\bar{s}_\alpha d_\beta)_{V-A} \sum_q e_q (\bar{q}_\beta q_\alpha)_{V-A} ,
\end{aligned} \tag{2.1}$$

where α, β denote colour indices ($\alpha, \beta = 1, \dots, N$) and e_q are quark charges. We omit the colour indices for the colour singlet operators. ($V \pm A$) refer to $\gamma_\mu(1 \pm \gamma_5)$. This basis closes under QCD and QED renormalization.

For $\mu < m_c$ the sums over quark flavours in (2.1) run over u, d and s . However, when $m_b > \mu > m_c$ is considered also $q = c$ has to be included. Moreover, in this case two additional current–current operators have to be taken into account,

$$Q_1^c = (\bar{s}_\alpha c_\beta)_{V-A} (\bar{c}_\beta d_\alpha)_{V-A} , \quad Q_2^c = (\bar{s}c)_{V-A} (\bar{c}d)_{V-A} . \tag{2.2}$$

It should be stressed that this basis differs from the one used by Gilman and Wise [23] and by the Rome group [19] in the form for Q_1, Q_2, Q_1^c and Q_2^c where the corresponding Fierz conjugates have been adopted

$$\tilde{Q}_1 = (\bar{s}d)_{V-A} (\bar{u}u)_{V-A} , \quad \tilde{Q}_2 = (\bar{s}_\alpha d_\beta)_{V-A} (\bar{u}_\beta u_\alpha)_{V-A} , \tag{2.3}$$

$$\tilde{Q}_1^c = (\bar{s}d)_{V-A} (\bar{c}c)_{V-A} , \quad \tilde{Q}_2^c = (\bar{s}_\alpha d_\beta)_{V-A} (\bar{c}_\beta c_\alpha)_{V-A} . \quad (2.4)$$

We will refer to the basis of refs. [23, 19] as the second basis. Both are equally good although we somewhat prefer the basis (2.1), because there Q_2 is taken in the colour singlet form as it appears in the tree level Hamiltonian.

Now, as we have stressed in refs. [13, 14, 15] the two-loop anomalous dimension matrices in the two bases differ when calculated in the NDR scheme. Consequently, the corresponding coefficients $C_i(\mu)$ differ. We will refer to these two possibilities as schemes NDR and $\overline{\text{NDR}}$, respectively. On the other hand in the HV scheme it is immaterial whether the first or the second basis is used but the corresponding HV Wilson coefficient functions differ from those obtained in the NDR and $\overline{\text{NDR}}$ schemes.

In what follows we will present general formulae for Wilson coefficients valid in any scheme leaving the discussion of scheme dependence to section 3.

We should also remark that we do not include in our analysis the operators

$$\tilde{Q}_{11} = (\bar{s}d)_{V-A} (\bar{b}b)_{V-A} , \quad Q_{12} = (\bar{s}b)_{V-A} (\bar{b}d)_{V-A} , \quad (2.5)$$

which have been taken into account in ref. [6, 7]. Even at leading order their effect on ε'/ε is smaller than 1% and in order not to complicate the analysis further, we have decided to drop them. This was also the strategy of the Rome group [19].

2.2 Renormalization Group Equations

The renormalization group equation for $\vec{C}(\mu)$ is given by

$$\left[\mu \frac{\partial}{\partial \mu} + \beta(g) \frac{\partial}{\partial g} \right] \vec{C}\left(\frac{M_W^2}{\mu^2}, g^2, \alpha\right) = \hat{\gamma}^T(g^2, \alpha) \vec{C}\left(\frac{M_W^2}{\mu^2}, g^2, \alpha\right), \quad (2.6)$$

where $\beta(g)$ is the QCD beta function

$$\beta(g) = -\beta_0 \frac{g^3}{16\pi^2} - \beta_1 \frac{g^5}{(16\pi^2)^2} - \beta_{1e} \frac{e^2 g^3}{(16\pi^2)^2}, \quad (2.7)$$

with

$$\beta_0 = 11 - \frac{2}{3}f, \quad \beta_1 = 102 - \frac{38}{3}f, \quad \beta_{1e} = -\frac{8}{9}\left(u + \frac{d}{4}\right), \quad (2.8)$$

and $f = u + d$ denoting the number of active flavours, u and d being the number of u -type and d -type flavours respectively. To the order considered in this paper, in principle we also have to take into account the third term in eq. 2.8. However, we have checked that its contribution to the coefficient functions is negligible, and we will drop it for the rest of this work.

In what follows, we also neglect the running of the electromagnetic coupling constant α . This is a very good approximation because only scales $1 \text{ GeV} \leq \mu \leq M_W$ are involved in our analysis. In the numerical analysis we will take $\alpha = 1/128$. For the effective QCD coupling constant we will use

$$\alpha_s^{(f)}(Q) = \frac{4\pi}{\beta_0 \ln(Q^2/\Lambda_f^2)} \left[1 - \frac{\beta_1 \ln \ln(Q^2/\Lambda_f^2)}{\beta_0^2 \ln(Q^2/\Lambda_f^2)} \right], \quad (2.9)$$

with Λ_f in the $\overline{\text{MS}}$ scheme. Demanding the continuity of $\alpha_s^{(f)}(Q)$ at quark thresholds in the form

$$\alpha_s^{(3)}(m_c) = \alpha_s^{(4)}(m_c), \quad \alpha_s^{(4)}(m_b) = \alpha_s^{(5)}(m_b), \quad (2.10)$$

gives relations between the various values for Λ_f . In what follows we will denote $\Lambda_{\overline{\text{MS}}} \equiv \Lambda_4 \equiv \Lambda_{QCD}$.

Next, $\hat{\gamma}(g^2, \alpha)$ is the full 10×10 anomalous dimension matrix which we expand in the following way

$$\hat{\gamma}(g^2, \alpha) = \hat{\gamma}_s(g^2) + \frac{\alpha}{4\pi} \hat{\Gamma}(g^2), \quad (2.11)$$

where

$$\hat{\gamma}_s(g^2) = \frac{\alpha_s}{4\pi} \hat{\gamma}_s^{(0)} + \frac{\alpha_s^2}{(4\pi)^2} \hat{\gamma}_s^{(1)}, \quad (2.12)$$

and

$$\hat{\Gamma}(g^2) = \hat{\gamma}_e^{(0)} + \frac{\alpha_s}{4\pi} \hat{\gamma}_{se}^{(1)}. \quad (2.13)$$

Explicit expressions for $(\hat{\gamma}_s^{(0)}, \hat{\gamma}_s^{(1)})$ and $(\hat{\gamma}_e^{(0)}, \hat{\gamma}_{se}^{(1)})$ can be found in refs. [14] and [15], respectively. They will not be repeated here.

The solution of the renormalization group equation (2.6) is given by

$$\vec{C}\left(\frac{M_W^2}{\mu^2}, g^2, \alpha\right) = \left[T_g \exp \int_{g(M_W)}^{g(\mu)} dg' \frac{\hat{\gamma}^T(g'^2, \alpha)}{\beta(g')} \right] \vec{C}(1, g^2(M_W), \alpha), \quad (2.14)$$

where T_g denotes the ordering in the QCD coupling constant such that the couplings increase from right to left.

2.3 Generalized Evolution Matrix

Let us next introduce a generalized evolution matrix from m_2 down to $m_1 < m_2$

$$\hat{U}(m_1, m_2, \alpha) \equiv T_g \exp \int_{g(m_2)}^{g(m_1)} dg' \frac{\hat{\gamma}^T(g'^2, \alpha)}{\beta(g')}, \quad (2.15)$$

which is the generalization of eq. (2.3) of ref. [13]. Eq. (2.14) can be now in a short hand notation written as

$$\vec{C}(\mu) = \hat{U}(\mu, M_W, \alpha) \vec{C}(M_W). \quad (2.16)$$

The matrix $\hat{U}(m_1, m_2, \alpha)$ can be decomposed as follows

$$\hat{U}(m_1, m_2, \alpha) = \hat{U}(m_1, m_2) + \frac{\alpha}{4\pi} \hat{R}(m_1, m_2), \quad (2.17)$$

where $\hat{U}(m_1, m_2)$ describes pure QCD evolution and $\hat{R}(m_1, m_2)$ the additional evolution in the presence of the electromagnetic interaction. $\hat{U}(m_1, m_2)$ sums the logarithms $(\alpha_s t)^n$ and $\alpha_s (\alpha_s t)^n$ with $t = \ln(m_2^2/m_1^2)$ whereas $\hat{R}(m_1, m_2)$ sums the logarithms $t(\alpha_s t)^n$ and $(\alpha_s t)^n$. $\hat{U}(m_1, m_2)$ has been given in ref. [13]. The leading order formula for $\hat{R}(m_1, m_2)$ can be found in ref. [6] except that here we used a different overall normalization (an additional factor -4π in \hat{R}). For completeness, we will now recall the formula for $\hat{U}(m_1, m_2)$ and subsequently, we will derive a corresponding expression for $\hat{R}(m_1, m_2)$.

2.4 The Pure QCD Evolution Matrix $\hat{U}(m_1, m_2)$

As shown in [13] the pure QCD evolution can be written as

$$\hat{U}(m_1, m_2) = \left(\hat{1} + \frac{\alpha_s(m_1)}{4\pi} \hat{J} \right) \hat{U}^{(0)}(m_1, m_2) \left(\hat{1} - \frac{\alpha_s(m_2)}{4\pi} \hat{J} \right), \quad (2.18)$$

where $\hat{U}^{(0)}(m_1, m_2)$ denotes the evolution matrix in the leading logarithmic approximation and \hat{J} summarizes the next-to-leading correction to this evolution. If

$$(\hat{\gamma}_s^{(0)})_D \equiv \hat{V}^{-1} \hat{\gamma}_s^{(0)T} \hat{V}, \quad \hat{G} \equiv \hat{V}^{-1} \hat{\gamma}_s^{(1)T} \hat{V}, \quad (2.19)$$

where $(\hat{\gamma}_s^{(0)})_D$ denotes a diagonal matrix whose diagonal elements are the components of the vector $\vec{\gamma}_s^{(0)}$, then

$$\hat{U}^{(0)}(m_1, m_2) = \hat{V} \left[\left(\frac{\alpha_s(m_2)}{\alpha_s(m_1)} \right)^{\vec{a}} \right]_D \hat{V}^{-1} \quad \text{with} \quad \vec{a} = \frac{\vec{\gamma}_s^{(0)}}{2\beta_0}. \quad (2.20)$$

For the matrix \hat{J} one gets

$$\hat{J} = \hat{V} \hat{S} \hat{V}^{-1}, \quad (2.21)$$

where the elements of \hat{S} are given by

$$S_{ij} = \delta_{ij} \gamma_{s,i}^{(0)} \frac{\beta_1}{2\beta_0^2} - \frac{G_{ij}}{2\beta_0 + \gamma_{s,i}^{(0)} - \gamma_{s,j}^{(0)}}, \quad (2.22)$$

with $\gamma_{s,i}^{(0)}$ denoting the components of $\vec{\gamma}_s^{(0)}$ and G_{ij} the elements of \hat{G} . Although eq. (2.22) can develop singularities for certain combinations of the $\gamma_{s,i}^{(0)}$, the physically relevant evolution matrix (2.18) always remains finite after proper combination of relevant terms.

2.5 The Evolution Matrix $\hat{R}(m_1, m_2)$

Inserting (2.11) into (2.15), we find a general expression for $\hat{R}(m_1, m_2)$,

$$\hat{R}(m_1, m_2) = \int_{g(m_2)}^{g(m_1)} dg' \frac{\hat{U}(m_1, m') \Gamma^T(g') \hat{U}(m', m_2)}{\beta(g')}, \quad (2.23)$$

where $\hat{U}(m_1, m_2)$ is given by (2.18), $\Gamma(g)$ has been defined in (2.13) and $g' \equiv g(m')$.

It is instructive to discuss the leading order in (2.23) which is obtained by keeping only the first terms in (2.7) and (2.13) and setting $\hat{J} \equiv 0$ in $\hat{U}(m_1, m_2)$ of eq. (2.18). We then find

$$\hat{R}^{(0)}(m_1, m_2) = -\frac{2\pi}{\beta_0} \hat{V} \hat{K}^{(0)}(m_1, m_2) \hat{V}^{-1}, \quad (2.24)$$

where the matrix $\hat{K}^{(0)}(m_1, m_2)$ is given by

$$(\hat{K}^{(0)}(m_1, m_2))_{ij} = \hat{M}_{ij}^{(0)} \int_{\alpha_s(m_2)}^{\alpha_s(m_1)} d\alpha'_s \left(\frac{\alpha'_s}{\alpha_s(m_1)} \right)^{a_i} \frac{1}{\alpha_s'^2} \left(\frac{\alpha_s(m_2)}{\alpha'_s} \right)^{a_j}, \quad (2.25)$$

with a_i being the components of the vector \vec{a} defined in eq. (2.20). Moreover, the matrix $\hat{M}^{(0)}$ is given by

$$\hat{M}^{(0)} = \hat{V}^{-1} \hat{\gamma}_e^{(0)T} \hat{V}. \quad (2.26)$$

Straightforward integration gives

$$(\hat{K}^{(0)}(m_1, m_2))_{ij} = \frac{\hat{M}_{ij}^{(0)}}{a_i - a_j - 1} \left[\left(\frac{\alpha_s(m_2)}{\alpha_s(m_1)} \right)^{a_j} \frac{1}{\alpha_s(m_1)} - \left(\frac{\alpha_s(m_2)}{\alpha_s(m_1)} \right)^{a_i} \frac{1}{\alpha_s(m_2)} \right], \quad (2.27)$$

which is precisely eq. (3.23) of ref. [6].

Similarly to eq. (2.22), we note an apparent singularity in the element (7, 8) for which $a_7 = a_8 + 1$ when $f = 3$. However, the expression in parenthesis also vanishes in this case and no singularity is present. For numerical calculations it is safer to use in the case $a_i = a_j + 1$ the following formula obtained directly from eq.(2.25)

$$(\hat{K}^{(0)}(m_1, m_2))_{ij} = \hat{M}_{ij}^{(0)} \frac{1}{\alpha_s(m_1)} \left(\frac{\alpha_s(m_2)}{\alpha_s(m_1)} \right)^{a_j} \ln \frac{\alpha_s(m_1)}{\alpha_s(m_2)}. \quad (2.28)$$

It is straightforward to generalize (2.24) beyond the leading logarithmic approximation. We find

$$\hat{R}(m_1, m_2) = -\frac{2\pi}{\beta_0} \hat{V} \hat{K}(m_1, m_2) \hat{V}^{-1} \equiv \hat{R}^{(0)}(m_1, m_2) + \hat{R}^{(1)}(m_1, m_2), \quad (2.29)$$

where

$$\hat{K}(m_1, m_2) = \hat{K}^{(0)}(m_1, m_2) + \frac{1}{4\pi} \sum_{i=1}^3 \hat{K}_i^{(1)}(m_1, m_2). \quad (2.30)$$

The next-to-leading corrections originating in $\hat{J} \neq 0$, $\hat{\gamma}_{se}^{(1)} \neq 0$ and $\beta_1 \neq 0$ are represented by the matrices $\hat{K}_i^{(1)}(m_1, m_2)$ and more globally by $\hat{R}^{(1)}(m_1, m_2)$.

Let us introduce

$$\hat{\Gamma}^{(1)} = \hat{\gamma}_{se}^{(1)T} - \frac{\beta_1}{\beta_0} \hat{\gamma}_e^{(0)T}, \quad (2.31)$$

and

$$\hat{M}^{(1)} = \hat{V}^{-1} \left(\hat{\Gamma}^{(1)} + [\hat{\gamma}_e^{(0)T}, \hat{J}] \right) \hat{V}. \quad (2.32)$$

The matrices $\hat{K}_i^{(1)}(m_1, m_2)$ are then given as follows

$$\left(\hat{K}_1^{(1)}(m_1, m_2) \right)_{ij} = \begin{cases} \frac{M_{ij}^{(1)}}{a_i - a_j} \left[\left(\frac{\alpha_s(m_2)}{\alpha_s(m_1)} \right)^{a_j} - \left(\frac{\alpha_s(m_2)}{\alpha_s(m_1)} \right)^{a_i} \right] & i \neq j \\ M_{ii}^{(1)} \left(\frac{\alpha_s(m_2)}{\alpha_s(m_1)} \right)^{a_i} \ln \frac{\alpha_s(m_1)}{\alpha_s(m_2)} & i = j \end{cases}, \quad (2.33)$$

$$\hat{K}_2^{(1)}(m_1, m_2) = -\alpha_s(m_2) \hat{K}^{(0)}(m_1, m_2) \hat{S}, \quad (2.34)$$

$$\hat{K}_3^{(1)}(m_1, m_2) = \alpha_s(m_1) \hat{S} \hat{K}^{(0)}(m_1, m_2). \quad (2.35)$$

Comparison of (2.27) with (2.33) and the additional factors of $\alpha_s(m_i)$ in (2.34) and (2.35) make it clear that $\hat{R}^{(1)}(m_1, m_2)$ is by one logarithm lower or by one order in α_s higher than $\hat{R}^{(0)}(m_1, m_2)$. For later purposes it will be useful to introduce “ α_s -counting” in which $\hat{R}^{(0)}(m_1, m_2)$ is $\mathcal{O}(1/\alpha_s)$ and $\hat{R}^{(1)}(m_1, m_2)$ is $\mathcal{O}(1)$.

2.6 A Different Form of the Evolution Matrix

The evolution matrix $\hat{U}(m_1, m_2, \alpha)$ can also be written in a form which nicely generalizes the pure QCD evolution matrix of eq. (2.18),

$$\hat{U}(m_1, m_2, \alpha) = \hat{W}(m_1) \hat{U}^{(0)}(m_1, m_2) \hat{W}'(m_2) \quad (2.36)$$

where

$$\hat{W}(m_1) = \left(1 + \frac{\alpha}{4\pi} \hat{J}_{se} \right) \left(1 + \frac{\alpha_s(m_1)}{4\pi} \hat{J}_s \right) \left(1 + \frac{\alpha}{\alpha_s(m_1)} \hat{J}_e \right), \quad (2.37)$$

$$\hat{W}'(m_2) = \left(1 - \frac{\alpha}{\alpha_s(m_2)} \hat{J}_e \right) \left(1 - \frac{\alpha_s(m_2)}{4\pi} \hat{J}_s \right) \left(1 - \frac{\alpha}{4\pi} \hat{J}_{se} \right). \quad (2.38)$$

This is in fact the form used in ref. [19], where only implicit equations for the matrices \hat{J}_s , \hat{J}_e , and \hat{J}_{se} have been given. Here, we give explicit expressions for the \hat{J}_i which can be easily found from the previous subsections. \hat{J}_s is simply given by \hat{J} of (2.21) and \hat{J}_e , \hat{J}_{se} are found to be

$$\hat{J}_e = \hat{V} \hat{S}_e \hat{V}^{-1}, \quad \hat{J}_{se} = \hat{V} \hat{S}_{se} \hat{V}^{-1}, \quad (2.39)$$

where

$$(\hat{S}_e)_{ij} = \frac{1}{2\beta_0} \frac{\hat{M}_{ij}^{(0)}}{(1+a_j-a_i)}, \quad (\hat{S}_{se})_{ij} = \frac{1}{2\beta_0} \frac{\hat{M}_{ij}^{(1)}}{(a_j-a_i)}, \quad (2.40)$$

with $\hat{M}_{ij}^{(0)}$ and $\hat{M}_{ij}^{(1)}$ defined in eqs. (2.26) and (2.32), respectively. We note that \hat{S}_e can develop singularities for certain combinations of a_j and a_i , and \hat{S}_{se} is singular for $i = j$. All these singularities cancel in the final expression for $\hat{U}(m_1, m_2, \alpha)$ when all contributing terms are combined. This is seen for instance in (2.33). Thus although formula (2.36) is more elegant than the evolution matrix presented in sections 2.4 and 2.5, the former formulation in terms of the evolution matrices $\hat{U}(m_1, m_2)$ and $\hat{R}(m_1, m_2)$, which is non-singular at all stages, is more suitable for numerical calculations.

2.7 The Initial Conditions $\vec{C}(M_W)$

In order to complete the analysis, we have to discuss the structure of $\vec{C}(M_W)$. This discussion generalizes the one given in section 2 of ref. [13]. In order to find $\vec{C}(M_W)$ the one-loop current-current and penguin diagrams of fig. 1 with the full W and Z propagators and internal top quark exchanges have to be calculated first. Subsequently, the result of this calculation should be expressed in terms of matrix elements $\langle \vec{Q}(M_W) \rangle$. The latter are found by inserting the operators \vec{Q} in the one-loop current-current and penguin diagrams of fig. 2 and calculating the finite contributions in some renormalization scheme. We note the absence of Z^0 -contributions to $\langle \vec{Q}(M_W) \rangle$. Indeed, in the mass independent renormalization schemes used here such contributions are zero.

If

$$T = \langle \vec{Q}^{(0)T} \rangle \left[\vec{T}^{(0)} + \frac{\alpha_s(M_W)}{4\pi} \vec{T}_s^{(1)} + \frac{\alpha}{4\pi} \vec{T}_e^{(1)} \right] \equiv \langle \vec{Q}(M_W)^T \rangle \vec{C}(M_W), \quad (2.41)$$

denotes the result of evaluating the diagrams of fig. 1 with $\langle \vec{Q}^{(0)} \rangle$ being the tree level matrix elements and

$$\langle \vec{Q}(M_W) \rangle = \left[\hat{1} + \frac{\alpha_s(M_W)}{4\pi} \hat{r}_s + \frac{\alpha}{4\pi} \hat{r}_e \right] \langle \vec{Q}^{(0)} \rangle, \quad (2.42)$$

obtained from fig. 2, then

$$\vec{C}(M_W) = \vec{T}^{(0)} + \frac{\alpha_s(M_W)}{4\pi} [\vec{T}_s^{(1)} - \hat{r}_s^T \vec{T}^{(0)}] + \frac{\alpha}{4\pi} [\vec{T}_e^{(1)} - \hat{r}_e^T \vec{T}^{(0)}]. \quad (2.43)$$

It should be stressed that $\vec{T}_e^{(1)}$, $\vec{T}_s^{(1)}$, \hat{r}_s and \hat{r}_e depend on the assumptions made about the properties of the external lines in figs. 1 and 2, i.e., on the infrared structure of the theory. This dependence cancels however in (2.43) so that $\mathcal{O}(\alpha_s)$ and $\mathcal{O}(\alpha)$ corrections

in (2.43) do not depend on external states as it should be. They depend however on the renormalization scheme through the matrices \hat{r}_s and \hat{r}_e .

The formulae (2.41)-(2.43) are general and apply also to situations in which several operators are present in the limit $\alpha = \alpha_s = 0$ represented by the first term in (2.43). In the case at hand only the operator Q_2 is present in this limit and the vector $\vec{T}^{(0)}$ is the transposed of $(0, 1, 0, \dots, 0)$. This implies that only $\langle Q_2(M_W) \rangle$ has to be calculated in order to find $\vec{C}(M_W)$. This is evident from (2.43) and the discussion in appendix C of ref. [13]. Yet, this more general formulation is very useful for the analysis of scheme dependences as we will see below.

2.8 Final Formulae for Wilson Coefficient Functions

Let us define

$$\vec{C}(\mu) = \vec{C}_s(\mu) + \frac{\alpha}{4\pi} \vec{C}_e(\mu). \quad (2.44)$$

Inserting (2.17) and (2.43) into (2.16), we find

$$\vec{C}_s(\mu) = \left(\hat{1} + \frac{\alpha_s(\mu)}{4\pi} \hat{J} \right) \hat{U}^{(0)}(\mu, M_W) \left(\vec{T}^{(0)} + \frac{\alpha_s(M_W)}{4\pi} \vec{T}_s^{(1)} - \frac{\alpha_s(M_W)}{4\pi} (\hat{r}_s^T + \hat{J}) \vec{T}^{(0)} \right), \quad (2.45)$$

and

$$\begin{aligned} \vec{C}_e(\mu) &= \hat{U}^{(0)}(\mu, M_W) \left[\vec{T}_e^{(1)} - \hat{r}_e^T \vec{T}^{(0)} \right] \\ &+ \hat{R}^{(0)}(\mu, M_W) \left[\vec{T}^{(0)} + \frac{\alpha_s(M_W)}{4\pi} (\vec{T}_s^{(1)} - \hat{r}_s^T \vec{T}^{(0)}) \right] \\ &+ \hat{R}^{(1)}(\mu, M_W) \vec{T}^{(0)}. \end{aligned} \quad (2.46)$$

3 Renormalization Scheme Dependence

3.1 General Consistency Relations

The two-loop anomalous dimensions depend on the renormalization scheme for operators and in particular on the treatment of γ_5 in $D \neq 4$ dimensions. In refs. [13] and [15], we have derived two relations between $\hat{\gamma}_a^{(1)}$ and $\hat{\gamma}_b^{(1)}$ calculated in two different renormalization schemes a and b .

$$(\hat{\gamma}_s^{(1)})_b = (\hat{\gamma}_s^{(1)})_a + \left[\Delta \hat{r}_s, \hat{\gamma}_s^{(0)} \right] + 2 \beta_0 \Delta \hat{r}_s, \quad (3.1)$$

$$(\hat{\gamma}_{se}^{(1)})_b = (\hat{\gamma}_{se}^{(1)})_a + \left[\Delta \hat{r}_s, \hat{\gamma}_e^{(0)} \right] + \left[\Delta \hat{r}_e, \hat{\gamma}_s^{(0)} \right], \quad (3.2)$$

with

$$\Delta\hat{r}_i = (\hat{r}_i)_b - (\hat{r}_i)_a, \quad i = s, e, \quad (3.3)$$

and \hat{r}_i defined in (2.42). It follows that the combinations

$$\hat{W}_s = \hat{\gamma}_s^{(1)} - [\hat{r}_s, \hat{\gamma}_s^{(0)}] - 2\beta_0 \hat{r}_s, \quad (3.4)$$

and

$$\hat{W}_{se} = \hat{\gamma}_{se}^{(1)} - [\hat{r}_s, \hat{\gamma}_e^{(0)}] - [\hat{r}_e, \hat{\gamma}_s^{(0)}], \quad (3.5)$$

are independent of the renormalization scheme considered. We should also point out that $\Delta\hat{r}_s$ and $\Delta\hat{r}_e$ do not depend on the infrared structure of the theory, whereas this is not the case for \hat{r}_s and \hat{r}_e as has been stressed in section 2.

Relations (3.1)-(3.4) turned out to be very useful in testing the two-loop anomalous dimension matrices found in refs. [14] and [15]. They also play a central role in demonstrating the scheme independence of physical quantities. For the pure QCD case this has been discussed in ref. [13]. Below we will extend these considerations to $\mathcal{O}(\alpha)$ corrections.

3.2 Relations Between Coefficient Functions

The relations between coefficient functions obtained in two different schemes a and b are entirely given in terms of the matrices $\Delta\hat{r}_i$ of eq. (3.3) which follow from the evaluation of the one-loop diagrams of fig. 2.

One has

$$\vec{C}_b(\mu) = \left[\hat{1} - \frac{\alpha_s(\mu)}{4\pi} \Delta\hat{r}_s^T - \frac{\alpha}{4\pi} \Delta\hat{r}_e^T \right] \vec{C}_a(\mu), \quad (3.6)$$

with the corresponding relation for the hadronic matrix elements

$$\langle \vec{Q}(\mu) \rangle_b^T = \langle \vec{Q}(\mu) \rangle_a^T \left[\hat{1} + \frac{\alpha_s(\mu)}{4\pi} \Delta\hat{r}_s^T + \frac{\alpha}{4\pi} \Delta\hat{r}_e^T \right]. \quad (3.7)$$

The scheme independence of the effective Hamiltonian (1.2) follows directly from these relations.

The matrices $\Delta\hat{r}_s$ and $\Delta\hat{r}_e$ relating HV and NDR schemes can be found in sections 3.3 and 3.4 of ref. [14] and in section 6.2 of ref. [15], respectively. The corresponding matrices relating $\overline{\text{NDR}}$ and NDR schemes are given in eq. (5.14) of ref. [15]. See however eq. (4.25) of the present paper.

3.3 Scheme Independence of Physical Quantities

Let us return to the general formulae (2.45) and (2.46) for the coefficients $\vec{C}(\mu)$. In ref. [13], we have shown that the combination $\hat{r}_s^T + \hat{J}$ in eq. (2.45) is renormalization scheme independent, implying that the next-to-leading QCD corrections to $\vec{C}_s(\mu)$ are only scheme dependent through the matrix \hat{J} at the lower end of the evolution which involves $\alpha_s(\mu)$. This scheme dependence is cancelled by the one of $\mathcal{O}(\alpha_s)$ corrections to $\langle \vec{Q}(\mu) \rangle$ so that the resulting decay amplitudes do not depend on the renormalization scheme as it should be. We would like now to demonstrate that an analogous proof can be made in the case of $\vec{C}_e(\mu)$ given by (2.46). This can certainly be done, but it turns out that a much more elegant proof can be made by using the form of (2.36).

First we want to demonstrate the scheme independence of terms at the upper end of the evolution. Inserting (2.36) and (2.43) into (2.16) and recalling that $\vec{T}^{(0)}$, $\vec{T}^{(1)}$ and \hat{J}_e are scheme independent we find that it is sufficient to consider the combination

$$\hat{X} = \left(\frac{\alpha_s(M_W)}{4\pi} \hat{1} + \frac{\alpha}{4\pi} \hat{J}_e \right) [\hat{r}_s^T + \hat{J}_s] + \frac{\alpha}{4\pi} [\hat{r}_e^T + \hat{J}_{se}]. \quad (3.8)$$

The first part of this expression is scheme independent due to scheme independence of \hat{J}_e and $\hat{r}_s^T + \hat{J}_s$ as shown in [13]. It remains therefore to show that also $\hat{r}_e^T + \hat{J}_{se}$ is scheme independent.

Now the scheme independence of \hat{W}_{se} and $\hat{r}_s^T + \hat{J}_s$ allows to extract the scheme dependent part of $\hat{M}^{(1)}$:

$$\hat{M}_{ij}^{(1)}(\text{scheme dependent}) = \left(\gamma_{s,i}^{(0)} - \gamma_{s,j}^{(0)} \right) (\hat{P}_e)_{ij} \quad (3.9)$$

where $\hat{P}_e \equiv \hat{V}^{-1} \hat{r}_e^T \hat{V}$. Therefore using (2.39) and (2.40) we conclude that the scheme dependent part of \hat{J}_{se} is simply $-\hat{r}_e^T$ which ends the proof.

In a very similar way one can show that the scheme dependence around the μ scale present in $\hat{W}(\mu)$ of (2.37) is cancelled by the scheme dependence of the $\mathcal{O}(\alpha_s(\mu))$ and $\mathcal{O}(\alpha)$ corrections to the matrix elements $\langle \vec{Q}^T(\mu) \rangle$. This ends the proof of the scheme independence of physical amplitudes.

4 $\Delta S = 1$ Hamiltonian Beyond Leading Logarithms

4.1 General Remarks

In the absence of strong and electromagnetic interactions the effective tree-level Hamiltonian for $\Delta S = 1$ non-leptonic decays can be written as follows

$$\mathcal{H}_{\text{eff}}(\Delta S = 1) = \frac{G_F}{\sqrt{2}} V_{\text{ud}} V_{\text{us}}^* \left\{ (1 - \tau)(Q_2^u - Q_2^c) + \tau(Q_2^u - Q_2^t) \right\}, \quad (4.1)$$

where

$$\tau \equiv -\frac{V_{\text{td}} V_{\text{ts}}^*}{V_{\text{ud}} V_{\text{us}}^*} \quad \text{and} \quad Q_2^q = (\bar{s}q)_{V-A} (\bar{q}d)_{V-A}, \quad q = u, c, t. \quad (4.2)$$

If the $\overline{\text{NDR}}$ scheme is adopted the Fierz conjugates \tilde{Q}_2^q of (2.3) and (2.4) are present in (4.1). For the HV scheme it is immaterial whether Q_2^q or \tilde{Q}_2^q are used.

The inclusion of QCD corrections and the evolution of \mathcal{H}_{eff} from M_W down to $\mu \ll M_W$ has been discussed in the leading logarithmic approximation at length in [6]. The next-to-leading order formulae involving $Q_1 - Q_6$ have already been given in ref. [13]. Here, we generalize the results of [13] to include also the electroweak penguin operators $Q_7 - Q_{10}$ together with $\mathcal{O}(\alpha)$ corrections using the formalism developed in previous sections. A similar though less explicit generalization has been made by the authors of ref. [19]. In the latter paper however mainly the Wilson coefficients relevant for ε'/ε have been considered. Here, we present also the results for the coefficients relevant for the real parts of $K \rightarrow \pi\pi$ amplitudes which enter the discussion of the $\Delta I = 1/2$ rule. Moreover, it will be useful to discuss the cases $\mu < m_c$ and $m_c < \mu < m_b$ separately, as well as the interesting case $\mu = m_c$ on the border line of effective 4- and 3-flavour theories. This case is simultaneously relevant for $\Delta C = 1$ transitions after proper replacement of quark flavours and is a useful renormalization point for our approach to hadronic matrix elements. The case $\mu \approx \mathcal{O}(m_b)$, relevant for $\Delta B = 1$ decays, is considered in section 9.

4.2 Master Formulae for Wilson Coefficient Functions ($\mu < m_c$)

The transformation of \mathcal{H}_{eff} of (4.1) from M_W down to $\mu < m_c$ involves 5-, 4- and 3-flavour effective theories and can be compactly described as follows

$$Q_2^u - Q_2^c \rightarrow \sum_{i=1}^{10} z_i(\mu) Q_i, \quad Q_2^u - Q_2^t \rightarrow \sum_{i=1}^{10} v_i(\mu) Q_i, \quad (4.3)$$

where Q_i are the operators given in (2.1), with $q = u, d, s$. Consequently, we find the familiar expression

$$\mathcal{H}_{\text{eff}}(\Delta S = 1) = \frac{G_F}{\sqrt{2}} V_{\text{ud}} V_{\text{us}}^* \sum_{i=1}^{10} (z_i(\mu) + \tau y_i(\mu)) Q_i(\mu), \quad (4.4)$$

where

$$y_i(\mu) = v_i(\mu) - z_i(\mu). \quad (4.5)$$

The coefficients z_i and v_i are the components of the ten dimensional column vectors \vec{z} and \vec{v}

$$\vec{z}(\mu) = \hat{U}_3(\mu, m_c, \alpha) \vec{z}(m_c), \quad (4.6)$$

and

$$\vec{v}(\mu) = \hat{U}_3(\mu, m_c, \alpha) \hat{M}(m_c) \hat{U}_4(m_c, m_b, \alpha) \hat{M}(m_b) \hat{U}_5(m_b, M_W, \alpha) \vec{C}(M_W). \quad (4.7)$$

The full evolution matrices $\hat{U}_f(m_1, m_2, \alpha)$ are given by (2.17) with f denoting the number of effective flavours. $\hat{M}(m_i)$ is the matching matrix at quark threshold m_i . Its origin and structure is discussed separately in section 4.3.

Using (4.6) and (4.7), care must be taken to remove consistently higher order terms in α_s and α resulting from the multiplication of the evolution matrices and initial values. To this end one should remember our discussion of the “ α_s -counting” in the case of the evolution matrix $\hat{R}(m_1, m_2)$. From this counting it is evident that e.g. terms involving products $\hat{J}\hat{R}^{(1)}$ should be discarded to the order considered here.

The initial values $\vec{C}(M_W)$ necessary for the evaluation of $v_i(\mu)$ are found according to the procedure outlined in section 2. For the case $\alpha = 0$ they have already been given in [13]. For the NDR scheme we find

$$C_1(M_W) = \frac{\alpha_s(M_W)}{4\pi} B_{s,1}^{\text{NDR}} + \frac{\alpha}{4\pi} B_{e,1}^{\text{NDR}}, \quad (4.8)$$

$$C_2(M_W) = 1 + \frac{\alpha_s(M_W)}{4\pi} B_{s,2}^{\text{NDR}} + \frac{\alpha}{4\pi} B_{e,2}^{\text{NDR}}, \quad (4.9)$$

$$C_3(M_W) = -\frac{\alpha_s(M_W)}{24\pi} \tilde{E}(x_t) + \frac{\alpha}{6\pi \sin^2 \theta_W} [2B(x_t) + C(x_t)], \quad (4.10)$$

$$C_4(M_W) = \frac{\alpha_s(M_W)}{8\pi} \tilde{E}(x_t), \quad (4.11)$$

$$C_5(M_W) = -\frac{\alpha_s(M_W)}{24\pi} \tilde{E}(x_t), \quad (4.12)$$

$$C_6(M_W) = \frac{\alpha_s(M_W)}{8\pi} \tilde{E}(x_t), \quad (4.13)$$

$$C_7(M_W) = \frac{\alpha}{6\pi} [4C(x_t) + \tilde{D}(x_t)], \quad (4.14)$$

$$C_8(M_W) = 0, \quad (4.15)$$

$$C_9(M_W) = \frac{\alpha}{6\pi} \left[4C(x_t) + \tilde{D}(x_t) + \frac{1}{\sin^2 \theta_W} (10B(x_t) - 4C(x_t)) \right], \quad (4.16)$$

$$C_{10}(M_W) = 0, \quad (4.17)$$

where

$$\begin{aligned} B_{s,1}^{\text{NDR}} &= 11/2, & B_{s,2}^{\text{NDR}} &= -11/6, \\ B_{e,1}^{\text{NDR}} &= 0, & B_{e,2}^{\text{NDR}} &= -35/18, \end{aligned} \quad (4.18)$$

$$\tilde{E}(x_t) = E(x_t) - \frac{2}{3}, \quad \tilde{D}(x_t) = D(x_t) - \frac{4}{9}, \quad (4.19)$$

$$x_t = \frac{m_t^2}{M_W^2}, \quad (4.20)$$

and

$$B(x) = \frac{1}{4} \left[\frac{x}{1-x} + \frac{x \ln x}{(x-1)^2} \right], \quad (4.21)$$

$$C(x) = \frac{x}{8} \left[\frac{x-6}{x-1} + \frac{3x+2}{(x-1)^2} \ln x \right], \quad (4.22)$$

$$D(x) = -\frac{4}{9} \ln x + \frac{-19x^3 + 25x^2}{36(x-1)^3} + \frac{x^2(5x^2 - 2x - 6)}{18(x-1)^4} \ln x, \quad (4.23)$$

$$E(x) = -\frac{2}{3} \ln x + \frac{x(18 - 11x - x^2)}{12(1-x)^3} + \frac{x^2(15 - 16x + 4x^2)}{6(1-x)^4} \ln x. \quad (4.24)$$

Comparing with eqs. (3.26)-(3.35) of ref. [6], we observe that the initial conditions for the penguin operators given here differ from the ones used in ref. [6]. There the leading order evolution matrices have been used but in the initial conditions the m_t -dependent next-to-leading terms have been already taken into account. These m_t -dependent terms represented by the functions $B(x_t)$, $C(x_t)$, $D(x_t)$ and $E(x_t)$ are renormalization scheme independent. Yet, the initial conditions may also contain scheme dependent next-to-leading terms which of course were not present in the analysis of ref. [6]. In the NDR scheme these scheme dependent terms enter the initial conditions for Q_1 and Q_2 and also modify the functions $E(x_t)$ and $D(x_t)$ by constant terms as given in (4.19).

The initial values for the $\overline{\text{NDR}}$ and HV schemes can be found by using the relations (3.6). It is then interesting to observe that in these schemes the additional terms in (4.19) are absent and the initial conditions for Q_1 and Q_2 are changed. The corresponding two-loop anomalous dimensions also change so that the final result for \mathcal{H}_{eff} remains scheme independent. This clarifies the observation made by Flynn and Randall [5] that the initial conditions for penguin operators do depend on the form of the operators. As already emphasized in [13], the inclusion of two-loop anomalous dimensions cancels this dependence. Compared to ref. [13], we have however slightly changed our treatment of the HV scheme. Since in the HV scheme the anomalous dimension of the weak current γ_J is non-zero at $\mathcal{O}(\alpha_s^2)$ [12], an additional contribution arises which can be either included in the anomalous dimension matrix as $\hat{\gamma}_s - 2\gamma_J \hat{1}$ [12] or in the initial condition. In [13] we choose to work

with the latter treatment, which however introduces an unnecessarily large scheme dependence at the lower end of the evolution. Therefore, here we have included the anomalous dimension of the weak current in the anomalous dimension matrix. This also changes the initial conditions in the HV scheme, as was already discussed in ref. [13]. Moreover, $\Delta\hat{r}_s$ given in [13, 14] has to be changed to

$$\Delta\hat{r}_s \rightarrow \Delta\hat{r}_s - 4 C_F \hat{1}. \quad (4.25)$$

In order to calculate $z_i(\mu)$ one has to consider the difference $Q_2^u - Q_2^c$. Then due to the GIM mechanism the coefficients $z_i(\mu)$ of penguin operators Q_i , $i \neq 1, 2$ are zero in 5- and 4-flavour theories. The evolution in this range of μ ($\mu > m_c$) involves then only current-current operators $Q_{1,2} \equiv Q_{1,2}^u$ and $Q_{1,2}^c$ with the initial conditions

$$z_1(M_W) = \frac{\alpha_s(M_W)}{4\pi} B_{s,1}^{\text{NDR}} + \frac{\alpha(M_W)}{4\pi} B_{e,1}^{\text{NDR}}, \quad (4.26)$$

$$z_2(M_W) = 1 + \frac{\alpha_s(M_W)}{4\pi} B_{s,2}^{\text{NDR}} + \frac{\alpha(M_W)}{4\pi} B_{e,2}^{\text{NDR}}, \quad (4.27)$$

as in (4.8) and (4.9). $Q_{1,2}^u$ and $Q_{1,2}^c$ do not mix under renormalization with each other and the initial conditions for the coefficients of $Q_{1,2}^c$ to be denoted by $z_{1,2}^c(\mu)$ are identical to the ones given above. We then find

$$\begin{pmatrix} z_1(m_c) \\ z_2(m_c) \end{pmatrix} = \hat{U}_4(m_c, m_b, \alpha) \hat{M}(m_b) \hat{U}_5(m_b, M_W, \alpha) \begin{pmatrix} z_1(M_W) \\ z_2(M_W) \end{pmatrix}, \quad (4.28)$$

where this time the evolution matrices $\hat{U}_{4,5}$ contain only the (2, 2) anomalous dimension matrices describing the mixing between current-current operators. When the charm quark is integrated out the operators $Q_{1,2}^c$ disappear from the effective Hamiltonian and the coefficients $z_i(\mu)$, $i \neq 1, 2$ for penguin operators become non-zero. In order to calculate $z_i(m_c)$ for penguin operators a proper matching between effective 4- and 3-quark theories has to be made. This matching has been already discussed in detail in ref. [13]. However, there we have set $q^2 = -m_c^2$ in evaluating the penguin diagrams of fig. 2. Meanwhile, we have realized that in the effective 3-quark theory, q being related to external light quarks must be much smaller than m_c and the consistent procedure within the operator product expansion is to set it identically to zero in the full expression. Numerically, the difference between coefficients calculated with $q^2 = -m_c^2$ and $q^2 = 0$ is small, however, the resulting modified expressions represent this time correct matching. Proceeding this way and applying an analogous procedure to QED penguin diagrams we are able to calculate

$\vec{z}(m_c)$ of (4.6). We have in the NDR scheme

$$\vec{z}^{\text{NDR}}(m_c) = \begin{pmatrix} z_1^{\text{NDR}}(m_c) \\ z_2^{\text{NDR}}(m_c) \\ -\alpha_s/(24\pi)F_s^{\text{NDR}}(m_c) \\ \alpha_s/(8\pi)F_s^{\text{NDR}}(m_c) \\ -\alpha_s/(24\pi)F_s^{\text{NDR}}(m_c) \\ \alpha_s/(8\pi)F_s^{\text{NDR}}(m_c) \\ \alpha/(6\pi)F_e^{\text{NDR}}(m_c) \\ 0 \\ \alpha/(6\pi)F_e^{\text{NDR}}(m_c) \\ 0 \end{pmatrix}, \quad (4.29)$$

where

$$F_s^{\text{NDR}}(\mu) = -\frac{2}{3} \left(\ln\left(\frac{m_c^2}{\mu^2}\right) + 1 \right) z_2(\mu), \quad (4.30)$$

$$F_e^{\text{NDR}}(\mu) = -\frac{4}{9} \left(\ln\left(\frac{m_c^2}{\mu^2}\right) + 1 \right) (3z_1(\mu) + z_2(\mu)), \quad (4.31)$$

with $\mu \approx \mathcal{O}(m_c)$. In the $\overline{\text{NDR}}$ and HV schemes the “1” in (4.30) and (4.31) is absent. Consequently, in the $\overline{\text{NDR}}$ and HV schemes one has $z_i(m_c) = 0$ for $i \neq 1, 2$ but in the case of the NDR scheme these coefficients are non-vanishing.

Due to the fact that z_1 and z_2 have opposite sign and $|z_1(m_c)| \approx \frac{1}{3}|z_2(m_c)|$ the coefficients $z_7(m_c)$ and $z_9(m_c)$ are very small. This is reminiscent of the situation in exclusive two-body decays such as $D^0 \rightarrow \pi^0 K^0$, for which such a cancellation between Q_1 and Q_2 contributions takes place. In the context of the $\Delta S = 1$ Hamiltonian such a cancellation has already been pointed out in ref. [28].

Again, when using the formulae above one has to take care that $\mathcal{O}(\alpha^2)$ terms are omitted as well as terms $\mathcal{O}(\alpha_s^2)$ and $\mathcal{O}(\alpha\alpha_s)$

At this stage it is mandatory for us to compare the results in (4.30) and (4.31) with the ones of [29], [30] and [28] where the effects of incomplete GIM mechanism resulting from $m_u \neq m_c$ for $\mu > m_c$ has been calculated. These analyses resulted in a scheme independent constant “ $\frac{5}{3}$ ” in place of “1” in (4.30) and (4.31). Yet, the proper matching must involve a scheme dependent constant. Our interpretation of this difference is as follows. It is intuitively clear that an incomplete GIM cancellation in the $Q_2^u - Q_2^c$ sector must take place for $\mu > m_c$. Yet, this effect is at the next-to-leading level at which other scheme dependent contributions are present. From our analysis it turns out that in the HV and $\overline{\text{NDR}}$ schemes the latter effects cancel exactly the term “ $\frac{5}{3}$ ” found in [29], [30] so that

$z_i(\mu) = 0$ for $\mu \geq m_c$. In the NDR scheme however $z_i(m_c) \neq 0$, although as we will see also in this schemes the penguin coefficients are smaller than found in ref. [29].

4.3 The Matching Matrix \hat{M}

In order to show that a non-trivial matching matrix \hat{M} has to be included in the evolution¹⁾, when going from an f -flavour effective theory to an $(f-1)$ -flavour effective theory, we write an amplitude A for some process as follows

$$A = \langle \vec{Q}_f(m) \rangle^T \vec{C}_f(m) = \langle \vec{Q}_{f-1}(m) \rangle^T \vec{C}_{f-1}(m), \quad (4.32)$$

where m is the threshold scale between the two effective theories in question. \vec{Q}_f , \vec{C}_f , \vec{Q}_{f-1} , and \vec{C}_{f-1} are the operators and coefficients in these two theories, respectively.

In analogy to (2.42), one finds from fig. 2

$$\langle \vec{Q}_f(m) \rangle = \left(\hat{1} + \frac{\alpha_s(m)}{4\pi} \delta \hat{r}_s + \frac{\alpha}{4\pi} \delta \hat{r}_e \right) \langle \vec{Q}_{f-1}(m) \rangle, \quad (4.33)$$

where

$$\delta \hat{r}_i = \hat{r}_i(f) - \hat{r}_i(f-1). \quad (4.34)$$

The matrices $\delta \hat{r}$ receive only contributions from penguin diagrams which for certain operator insertions depend on the number of effective flavours. Inserting (4.33) in (4.32), we find

$$\vec{C}_{f-1}(m) = \hat{M}(m) \vec{C}_f(m), \quad (4.35)$$

where

$$\hat{M}(m) = \hat{1} + \frac{\alpha_s(m)}{4\pi} \delta \hat{r}_s^T + \frac{\alpha}{4\pi} \delta \hat{r}_e^T. \quad (4.36)$$

A simple consequence of the presence of a non-trivial matching matrix at the next-to-leading level is the appearance of small discontinuities in the Wilson coefficient functions, and consequently, in the matrix elements of certain penguin operators at the thresholds between effective theories. This is not surprising because after all for penguin operators $\vec{Q}_f \neq \vec{Q}_{f-1}$, as explicitly seen in (2.1). An example of such a discontinuity is given also by the initial conditions in (4.29), since for $\mu > m_c$ one has $z_i(\mu) = 0$ ($i \neq 1, 2$). The matrices $\hat{M}(m)$ are renormalization scheme independent. They are given in appendix A.

¹⁾This has been pointed out by J.-M. Schwarz and has been briefly discussed in an addendum to [13].

4.4 Master Formulae for Wilson Coefficients ($m_c < \mu < m_b$)

If μ is chosen above m_c only operators $Q_{1,2}$ and $Q_{1,2}^c$ are present in the $u - c$ sector. For Q_i , $i = 1, \dots, 10$, we simply find the Hamiltonian in (4.4) with

$$\begin{pmatrix} z_1(\mu) \\ z_2(\mu) \end{pmatrix} = \hat{U}_4(\mu, m_b, \alpha) \hat{M}(m_b) \hat{U}_5(m_b, M_W, \alpha) \begin{pmatrix} z_1(M_W) \\ z_2(M_W) \end{pmatrix}, \quad (4.37)$$

$$\vec{v}(\mu) = \hat{U}_4(\mu, m_b, \alpha) \hat{M}(m_b) \hat{U}_5(m_b, M_W, \alpha) \vec{v}(M_W), \quad (4.38)$$

and $z_i = 0$ for $i \neq 1, 2$. Since $Q_{1,2}^c$ enter the effective Hamiltonian with the opposite sign to $Q_{1,2}^u$ and are only present in the $(1 - \tau)$ term in (4.1), we find

$$z_1^c(\mu) = -z_1(\mu), \quad z_2^c(\mu) = -z_2(\mu), \quad (4.39)$$

and

$$y_1^c(\mu) = z_1(\mu), \quad y_2^c(\mu) = z_2(\mu). \quad (4.40)$$

On the other hand it is evident from the formulae above that

$$y_1(\mu) = y_2(\mu) = 0, \quad (4.41)$$

for arbitrary μ . We note that the coefficients y_1^c and y_2^c are large.

4.5 Relations Between Operators

The operators Q_i given in (2.1) are linearly dependent for $f = 4$ or equivalently $m_c < \mu < m_b$. One has the relations

$$\begin{aligned} Q_4 &= Q_3 + Q_2 - Q_1 + Q_2^c - Q_1^c, \\ Q_9 &= \frac{1}{2}(3Q_1 - Q_3) + \frac{3}{2}Q_1^c, \\ Q_{10} &= Q_9 + Q_4 - Q_3. \end{aligned} \quad (4.42)$$

For $f = 3$, i.e., $\mu < m_c$ when the charm quark is integrated out these relations reduce to

$$\begin{aligned} Q_4 &= Q_3 + Q_2 - Q_1, \\ Q_9 &= \frac{1}{2}(3Q_1 - Q_3), \\ Q_{10} &= Q_2 + \frac{1}{2}(Q_1 - Q_3). \end{aligned} \quad (4.43)$$

It should be however emphasized that these relations have been obtained by performing Fierz transformations. Consequently, they cannot be used a priori in regularization or

renormalization schemes in which the operators Q_i and their Fierz conjugates \tilde{Q}_i are not equivalent in $D \neq 4$ dimensions. Thus, although they can be used in the HV scheme, they receive additional contributions in the NDR and $\overline{\text{NDR}}$ schemes. An inspection of the relation (3.7) reveals that in the limit $\alpha = 0$ only the relation for Q_4 receives additional α_s corrections so that e.g. in the NDR scheme we find

$$Q_4 = Q_3 + Q_2 - Q_1 - \frac{\alpha_s}{4\pi} \left(Q_6 + Q_4 - \frac{1}{3}Q_3 - \frac{1}{3}Q_5 \right), \quad (4.44)$$

which of course then has to be solved for Q_4 . Yet, we have decided to work with all operators and not to use the relations (4.42)–(4.44) in evaluating the coefficients $C_i(\mu)$. As discussed at length in [6] one can without any problems work with linearly dependent operators. The advantage of such a strategy is a much clearer picture of contributions coming from different sources. On the other hand the relations above will turn out to be useful in the analysis of hadronic matrix elements.

4.6 Numerical Results for Wilson Coefficients

In tabs. 1, 2, 3 we give the numerical values for the coefficients z_i and y_i for $\Lambda_{\overline{\text{MS}}}^{(4)} = 200, 300, 400$ MeV, in the NDR and HV schemes for $\mu = 1$ GeV, $\mu = m_c = 1.4$ GeV, and $\mu = 2$ GeV, at a fixed value of $m_t = 130$ GeV. In tabs. 4, 5, 6, we give the m_t -dependence of the coefficients $y_7 - y_{10}$ of the electroweak penguin operators for $\mu = 1.0$ GeV, different values of $\Lambda_{\overline{\text{MS}}}$ and the two schemes in question. The coefficients z_i do not depend on m_t . The m_t -dependence of $y_3 - y_6$ is so weak, that it has not been shown explicitly. The corresponding results for $\mu = m_c = 1.4$ GeV and $\mu = 2.0$ GeV are given in tabs. 7, 8, 9 and 10, 11, 12 respectively. The reason for giving many tables for several values of μ is as follows: For $\mu \approx 1$ GeV the calculation of hadronic matrix elements in an approach like the $1/N$ approach can in principle be performed as discussed in the next section. The scale $\mu = 2.0$ GeV is very suitable for present lattice calculations. Finally, $\mu = m_c$ is a very convenient scale for the semi-phenomenological approach developed in section 6. Simultaneously, $\mu = m_c$ can be used in the case of $\Delta C = 1$ decays.

For comparison, we give in the tables mentioned above the corresponding “leading order” results. These have been obtained using the strategy of ref. [6]. Thus we have set all the m_t -independent terms in (4.8) – (4.19) to zero²⁾ and we have used the leading order evolution matrix, i.e., one-loop anomalous dimension matrices and one-loop β -function. Clearly, the scale Λ_{LO} in the leading order expressions cannot be identified with $\Lambda_{\overline{\text{MS}}}$ which

²⁾We should warn the reader that the authors of ref. [19] keep these scheme dependent terms in their leading order evaluation.

enters the next-to-leading formulae. In addition, α_s at the next-to-leading level is smaller than α_s in the leading order when $\Lambda_{LO} = \Lambda_{\overline{\text{MS}}}$ is taken. In spite of this we have given the leading order results for $\Lambda_{LO} = \Lambda_{\overline{\text{MS}}}$, because the range of values for $\Lambda_{\overline{\text{MS}}}$ used in these tables overlaps considerably with the range used for the QCD scale in the leading order analyses. In any case what is really relevant here are the results for z_i and y_i with next-to-leading order corrections taken into account, because in this case $\Lambda_{\overline{\text{MS}}}$ is exactly the scale as extracted from next-to-leading order analyses in other processes [31].

We make the following observations:

- i) The coefficients z_1 and z_2 are suppressed through next-to-leading order corrections in both schemes considered, with the effect being stronger in the NDR scheme. Consequently, the ratio z_-/z_+ relevant for the $\Delta I = 1/2$ rule is smaller than in the leading order, in contrast to the statements made in refs. [12, 16]. We will clarify this separately below. The μ -dependence of z_{\pm} is shown for $\Lambda_{\overline{\text{MS}}} = 300$ MeV in fig. 3.
- ii) For $\mu > m_c$ the coefficients z_i ($i \neq 1, 2$) are zero. For $\mu = m_c$ they vanish in the HV scheme and in the NDR scheme they are so small that we do not show them in tab. 2. They remain small in both schemes for $\mu = 1$ GeV although considerable enhancements are observed in the case of $z_3 - z_6$ for the NDR scheme. The coefficients $z_7 - z_{10}$ being $\mathcal{O}(\alpha)$, can be neglected for all practical purposes.
- iii) The coefficients $y_3 - y_6$ are very weakly dependent on m_t and only their values for $m_t = 130$ GeV are shown. The coefficients y_6 and y_4 are larger than y_3 and y_5 . We notice considerable dependence of y_6 on μ , $\Lambda_{\overline{\text{MS}}}$ and the scheme considered. Whereas in the HV scheme y_6 is *suppressed* by $\approx 15\%$ relative to the leading order result, in the case of NDR a $\approx 10\%$ *enhancement* of y_6 for $\Lambda_{\overline{\text{MS}}} \geq 300$ MeV and $\mu > m_c$ is observed. For $\mu \leq m_c$ however, y_6 in the NDR scheme is slightly suppressed relatively to the leading order result although its absolute value is always larger than in the HV scheme as shown in fig. 4. The small discontinuity in y_6 for $\mu = m_c$ in the HV scheme is related to the matching discussed in section 4.3. In the NDR scheme this discontinuity is larger because in addition z_6 becoming non-zero at $\mu = m_c$ suppresses visibly $|y_6|$ in view of the formula (4.5). All these changes are compensated by the corresponding changes in the hadronic matrix elements and the contributions of other operators such as $Q_{1,2}^c$ so that the physical amplitudes remain μ -independent. We note that these effects are essentially invisible in the case of y_8 as shown in fig. 4.
- iv) The coefficients y_7 and y_8 show strong m_t -dependence as illustrated in fig. 5 and in the tables. Also as shown in fig. 6 a sizable m_t -dependence is seen in the case of y_9

and y_{10} . As seen in the tables y_7 and y_9 show only a weak dependence on μ and $\Lambda_{\overline{\text{MS}}}$. The corresponding dependences of y_8 and y_{10} are much stronger.

- v) We note that y_9 and y_{10} are substantially larger than y_7 and y_8 and essentially do not change when going from NDR to HV. y_9 is unaffected by next-to-leading order corrections, but y_{10} is considerably suppressed. In ref. [6], where Q_9 and Q_{10} have been eliminated, the effect of y_9 and y_{10} has been transferred to y_1 and y_2 which vanish in our case. In tabs. 6, 9 and 12 we give only the m_t dependence of the sum $y_9 + y_{10}$ which is relevant for ε'/ε . We observe that for $m_t < 150$ GeV the sum $|y_9 + y_{10}|$ is enhanced by roughly 20% over its leading order value but for higher values of m_t this enhancement is smaller.
- vi) The coefficient y_7 is essentially the same in the schemes considered. As noticed in [5, 6], y_7 vanishes for $m_t \approx 145$ GeV in the leading order, and becomes positive for larger m_t -values. The inclusion of next-to-leading order corrections shifts this zero-point to higher values of m_t , such as $m_t \approx 190$ GeV for both schemes. Consequently, y_7 remains negative for $m_t \approx \mathcal{O}(150 \text{ GeV})$, and is roughly of the same order of magnitude as y_8 . Hence for these values of m_t it is substantially enhanced over its leading order value. However, for $m_t \approx \mathcal{O}(200 \text{ GeV})$ the coefficient y_7 is so small in both schemes that the contribution of Q_7 to ε'/ε can be safely neglected for such high values of m_t .
- vii) Most interesting is however the *enhancement* of y_8 through next-to-leading corrections as noticed already in ref. [19], where only the HV scheme has been considered. We find that this enhancement is smaller in the NDR scheme. We also note that with increasing m_t the enhancement of y_8 over its leading order values becomes smaller so that for $m_t \approx \mathcal{O}(200 \text{ GeV})$ the NDR result is very close to its leading order value.
- viii) As a result of different impacts of next-to-leading order corrections on y_6 and y_8 in the schemes considered, there is a strong scheme dependence in the ratio $(y_7/3 + y_8)/y_6$, which roughly measures the relative importance of the dominant electroweak and QCD-penguins in the evaluation of ε'/ε . We show this in table 13 for $\mu = m_c$. We observe a large enhancement of this ratio in the HV scheme which however decreases with increasing m_t . In the NDR scheme this enhancement is substantially smaller and for $m_t \approx 190$ GeV the LO and NDR results are very close to each other.
- ix) The coefficients in the $\overline{\text{NDR}}$ scheme are either equal to the NDR coefficients or only slightly different from them. The largest differences are found for z_6 at $\mu < m_c$ and

for y_6 at $\mu > m_c$. This has to be kept in mind.

4.7 Comparison with refs. [12], [13] and [16]

In refs. [20, 21], the enhancement of z_-/z_+ from 1 to roughly 3 for $\mu \approx 1$ GeV has been found by calculating QCD effects in the leading logarithmic approximation. Subsequently, it has been stated in refs. [16] and [12] that z_-/z_+ is further enhanced by next-to-leading logarithmic corrections. Although the calculations in [12] and [16] are certainly correct, the coefficients on which this conclusion was based, are really not the coefficients z_\pm of the operators O_\pm , but the scheme independent coefficients given by

$$\tilde{z}_\pm(\mu) = z_\pm(\mu) \left[1 - \frac{\alpha_s(\mu)}{4\pi} B_\pm \right], \quad (4.45)$$

which correspond to

$$\langle \tilde{O}_\pm(\mu) \rangle \equiv \langle O_\pm(\mu) \rangle \left[1 + \frac{\alpha_s(\mu)}{4\pi} B_\pm \right]. \quad (4.46)$$

The coefficients B_\pm for the schemes considered in [16] (DRED) and [12] (NDR,HV), are as follows

$$\begin{aligned} B_+ &= \frac{2}{3}, & B_- &= -\frac{16}{3}, & \text{DRED} \\ B_+ &= \frac{11}{3}, & B_- &= -\frac{22}{3}, & \text{NDR} \\ B_+ &= \frac{7}{3}, & B_- &= -\frac{14}{3}, & \text{HV} \end{aligned} \quad (4.47)$$

The removal of the $\mathcal{O}(\alpha_s)$ corrections in (4.45) and (4.46) changes the conclusions reached in [12, 16], so that agreement with our paper is obtained. As stressed already in [12], the procedure of [12, 16] can be used, but then also the calculation of hadronic matrix elements should include the compensating factors given in (4.46) so that in both treatments the same amplitude is obtained.

At this stage it should be recalled that similar correction factors are included in the case of the parameter B_K in the QCD analysis of the ε_K -parameter [32]. However, there these corrections are so small that it is irrelevant how they are treated. In the case at hand the corrections are larger, and different conclusions about the signs of next-to-leading order corrections can be reached, dependently whether z_\pm or \tilde{z}_\pm are considered. Similar comments apply to our paper of ref. [13], where scheme independent coefficients $\tilde{z}_1 - \tilde{z}_6$ and $\tilde{y}_1 - \tilde{y}_6$ have been used.

Although the introduction of these additional corrections may in principle identify the full physical effect, as discussed in [13], it seems to us at present that for the future treatment of hadronic matrix elements it is more elegant, more convenient, and more transparent not to perform additional “rotations” to scheme independent bases. Indeed,

on one hand such a procedure is not unique and on the other hand it may in certain cases cause misleading conclusions. The observed suppression of z_-/z_+ through next-to-leading order corrections in the scheme considered must of course be compensated by the corresponding effects in the hadronic matrix elements, in order to explain the $\Delta I = 1/2$ rule as we will discuss in more detail in section 6.

5 Hadronic Matrix Elements

5.1 General Remarks

An important ingredient of any analysis of non-leptonic K -decays are the hadronic matrix elements of operators Q_i which we denote by

$$\langle Q_i \rangle_I \equiv \langle (\pi\pi)_I | Q_i | K \rangle, \quad I = 0, 2. \quad (5.1)$$

These matrix elements depend generally on the scale μ and on the renormalization scheme used for the operators. These two dependences are cancelled by those present in the coefficients $C_i(\mu)$ so that the effective Hamiltonian and the resulting amplitudes do not depend on μ and on the scheme used to renormalize the operators.

At this point, it should be emphasized that eq. (1.2) is valid beyond perturbation theory so that in principle μ can be chosen completely arbitrary. It can even be set to $\mu = 0$. In the spirit of ref. [33], we can then divide the renormalization group evolution into a *short distance evolution* from M_W to μ described by

$$\vec{C}(\mu) = \hat{U}(\mu, M_W, \alpha) \vec{C}(M_W), \quad (5.2)$$

and a *long distance evolution* from scale 0 *up to* μ , described by

$$\langle \vec{Q}^T(\mu) \rangle = \langle \vec{Q}^T(0) \rangle \hat{U}(0, \mu, \alpha), \quad (5.3)$$

where $\hat{U}(0, \mu, \alpha)$ is the evolution matrix in the long distance regime. Although this evolution cannot be evaluated at the lower end in a perturbative framework, it has general features similar to the evolution in the short distance regime as demonstrated in [33]. In particular, the μ and scheme dependences at the *upper* end of the evolution (around μ) must match the ones present in the coefficients $C_i(\mu)$ in such a way that these dependences are not present in the physical amplitudes. In other words it is a matter of choice what belongs to the matrix element and what to the coefficient function.

From this discussion it is evident that the scheme dependence of $\langle Q_i(\mu) \rangle$ is only present at the upper end of the long distance evolution. Consequently, for sufficiently high μ this

dependence can be calculated together with the μ -dependence in a perturbative framework. The relation between the matrix elements calculated in two different schemes is given in (3.7). The relation between matrix elements evaluated at two scales $m_1 < m_2$ is simply given by

$$\langle \vec{Q}^T(m_2) \rangle = \langle \vec{Q}^T(m_1) \rangle \hat{U}(m_1, m_2, \alpha), \quad (5.4)$$

where \hat{U} is the evolution matrix of section 2.3. Thus, if there is a method to calculate $\langle \vec{Q}(\mu) \rangle$ at a single scale $\mu = m_1$, the renormalization group will give us these matrix elements at any other scale $\mu \neq m_1$. Unfortunately, the full long distance evolution involves all scales down to $\mu = 0$ and consequently, the actual evaluation of $\langle Q_i(m_1) \rangle$ can only be done in a non-perturbative framework. In spite of this, it turns out to be very instructive to analyze the evolution of $\langle \vec{Q}(\mu) \rangle$ given in (5.4) in a range of μ for which $\hat{U}(m_1, m_2, \alpha)$ can be calculated as in section 4. Since this has not been studied so far in the literature let us recall that whereas the evolution of $\vec{C}(\mu)$ in (5.2) is governed by $\hat{\gamma}^T$, the evolution of $\langle \vec{Q}(\mu) \rangle$ is determined by $\hat{\gamma}$. Now the matrix $\hat{\gamma}$ is rather asymmetric [12]–[15]. In particular the elements $\hat{\gamma}_{i1} = \hat{\gamma}_{i2}$ for $i = 3, \dots, 10$ vanish. Consequently, the structure of the evolution in (5.4) is rather different from the evolution in (5.2). Thus, whereas the evolution of $C_{1,2}(\mu)$ is unaffected by the presence of penguin contributions, the evolution of $\langle Q_{1,2}(\mu) \rangle$ depends on the size of $\langle Q_i(\mu) \rangle$, $i \neq 1, 2$. Conversely, whereas the evolution of $C_i(\mu)$, $i \neq 1, 2$ depends on the size of $C_{1,2}(\mu)$, the evolution of the matrix elements of penguin operators $\langle Q_i(\mu) \rangle$, $i \neq 1, 2$ is a sole penguin affair. This different structure brings certain surprises as we will see in section 6.

During the last years there have been many attempts to calculate the matrix elements $\langle Q_i \rangle$ by using the lattice approach, $1/N$ -approach, QCD sum rules, hadronic sum rules, effective QCD action [34], chiral perturbation theory [35] and vacuum insertion. Yet, it is fair to say that only in the $1/N$ -expansion of refs. [33, 36] and in the vacuum insertion approach have all matrix elements $\langle Q_i \rangle$ been calculated. Some subset of the $\langle Q_i \rangle$ is also known from the lattice method, sum rules and effective QCD action approach of ref. [34].

At this stage it should be stressed that the $1/N$ -approach, although bearing some similarities to the vacuum insertion (factorization) method, is really a systematic non-perturbative method for QCD calculations, whereas this cannot be said about the vacuum insertion approach. Moreover, there are important quantitative differences between these two methods in the (Q_1, Q_2) sector. Whereas the $1/N$ approach offers a plausible description of CP -conserving $K \rightarrow \pi\pi$ amplitudes such a description is not possible in the vacuum insertion approach. In particular, the understanding of the $\Delta I = 1/2$ rule is completely missing in the factorization approach. Next, one should mention a complete failure of the

factorization method in a large class of exclusive non-leptonic B - and D -decays, whereas a reasonable description of these decays can be achieved in the $1/N$ -approach [37, 38]. Finally, the value for $B_K \approx 0.70 \pm 0.10$ obtained in the $1/N$ -approach is rather close to the present “world average” value given in (7.7) which should be contrasted with $B_K = 1$ obtained in the vacuum insertion approach.

Concerning the matrix elements of the dominant penguin operators the structure of the $1/N$ and the vacuum insertion formulae is similar. However, it should be stressed that whereas the scale Λ_χ entering these formulae can in the $1/N$ method be related to the ratio F_K/F_π [39, 36], no such relation exists in the vacuum insertion approach. Consequently, a quantitative estimate of these matrix elements in the latter approach is essentially impossible.

Concerning the μ -dependence it is well known that the matrix elements of (Q_1, Q_2) calculated in the vacuum insertion method are μ -independent in contradiction with one of the general properties of the hadronic matrix elements of operators carrying anomalous dimensions. In the $1/N$ -approach of ref. [33], the μ -dependence in $\langle Q_i(\mu) \rangle$, $i = 1, 2$ arises through loop effects in a meson theory and at the semi-quantitative level the matching in μ between long and short distance calculations is indeed possible. A problem exists however because in the approach of ref. [33] the long distance evolution in (5.3) can only be extended to scales $\mu \approx 0.6$ GeV at which perturbative evaluation of the Wilson coefficients $C_i(\mu)$ is questionable. There is a hope that by including vector meson contributions to the long distance evolution the scale μ could be increased to $\mu \approx 1$ GeV [40]. However, such a calculation is very difficult and in any case not available for $K \rightarrow \pi\pi$ at present.

On the other hand, the μ -dependence of the for $K \rightarrow \pi\pi$ dominant penguin operators $\langle Q_6(\mu) \rangle$ and $\langle Q_8(\mu) \rangle$ is to a large extend under control in both approaches. It is to a very good approximation given by the μ -dependence of the running strange quark mass $1/m_s^2(\mu)$ as we will demonstrate below. This μ -dependence cancels to a very good approximation the μ -dependence of $C_6(\mu)$ and $C_8(\mu)$ so that in quantities in which Q_6 and Q_8 dominate, the left-over μ -dependence is rather weak. The actual issue then however is what the value of m_s at a fixed value of μ , say $\mu \approx 1$ GeV is. We will return to this question as well as to the μ -dependence of other penguin operators below.

Next, the renormalization scheme dependence of $\langle Q_i(\mu) \rangle$ should be addressed. The vacuum insertion method is certainly insensitive to this dependence. It appears at present that this is also the case of the $1/N$ approach. Evidently, in these two approaches the scheme dependence of $C_i(\mu)$ cannot be cancelled and this feature introduces an additional theoretical uncertainty. We will investigate the size of this uncertainty below.

At this stage a few remarks about the lattice approach are in order [41]– [46]. In

this approach the μ -dependence and the scheme dependence of $\langle Q_i(\mu) \rangle$ is in principle calculable [47]–[52]. However, the accuracy of the lattice methods is insufficient at present to contribute very much to the issue of the μ - and scheme dependence at a quantitative level. This is evident from the strategy of ref. [19] which we will discuss in more detail below. Moreover, the matrix elements $\langle Q_1 \rangle_0$ and $\langle Q_2 \rangle_0$ have not been calculated on the lattice yet.

It will be useful in what follows to recall the matrix elements used in refs. [6, 17, 18, 19], and to compare them with each other. In section 6, we will go beyond these approaches to find matrix elements which we believe are closer to the true QCD matrix elements than these given by the methods just discussed.

5.2 Explicit Formulae for the Matrix Elements

Here, we will give explicit formulae for $\langle Q_i \rangle_I$ which are general enough that the matrix elements used in refs. [6, 17, 18, 19] could be compared with each other. In order to simplify the presentation, we will use the relations between operators given in section 4.5. As discussed there care must be taken when using these relations in the NDR and $\overline{\text{NDR}}$ schemes. In section 6, we will outline our strategy in using the formulae given below.

Taking first $\mu < m_c$, we have

$$\langle Q_1 \rangle_0 = -\frac{1}{9} X B_1^{(1/2)}, \quad (5.5)$$

$$\langle Q_2 \rangle_0 = \frac{5}{9} X B_2^{(1/2)}, \quad (5.6)$$

$$\langle Q_3 \rangle_0 = \frac{1}{3} X B_3^{(1/2)}, \quad (5.7)$$

$$\langle Q_4 \rangle_0 = \langle Q_3 \rangle_0 + \langle Q_2 \rangle_0 - \langle Q_1 \rangle_0, \quad (5.8)$$

$$\langle Q_5 \rangle_0 = \frac{1}{3} B_5^{(1/2)} \langle \overline{Q_6} \rangle_0, \quad (5.9)$$

$$\langle Q_6 \rangle_0 = -4 \sqrt{\frac{3}{2}} \left[\frac{m_K^2}{m_s(\mu) + m_d(\mu)} \right]^2 \frac{F_\pi}{\kappa} B_6^{(1/2)}, \quad (5.10)$$

$$\langle Q_7 \rangle_0 = - \left[\frac{1}{6} \langle \overline{Q_6} \rangle_0 (\kappa + 1) - \frac{X}{2} \right] B_7^{(1/2)}, \quad (5.11)$$

$$\langle Q_8 \rangle_0 = - \left[\frac{1}{2} \langle \overline{Q_6} \rangle_0 (\kappa + 1) - \frac{X}{6} \right] B_8^{(1/2)}, \quad (5.12)$$

$$\langle Q_9 \rangle_0 = \frac{3}{2} \langle Q_1 \rangle_0 - \frac{1}{2} \langle Q_3 \rangle_0, \quad (5.13)$$

$$\langle Q_{10} \rangle_0 = \langle Q_2 \rangle_0 + \frac{1}{2} \langle Q_1 \rangle_0 - \frac{1}{2} \langle Q_3 \rangle_0, \quad (5.14)$$

$$\langle Q_1 \rangle_2 = \langle Q_2 \rangle_2 = \frac{4\sqrt{2}}{9} X B_1^{(3/2)}, \quad (5.15)$$

$$\langle Q_i \rangle_2 = 0, \quad i = 3, \dots, 6, \quad (5.16)$$

$$\langle Q_7 \rangle_2 = - \left[\frac{\kappa}{6\sqrt{2}} \langle \overline{Q_6} \rangle_0 + \frac{X}{\sqrt{2}} \right] B_7^{(3/2)}, \quad (5.17)$$

$$\langle Q_8 \rangle_2 = - \left[\frac{\kappa}{2\sqrt{2}} \langle \overline{Q_6} \rangle_0 + \frac{\sqrt{2}}{6} X \right] B_8^{(3/2)}, \quad (5.18)$$

$$\langle Q_9 \rangle_2 = \langle Q_{10} \rangle_2 = \frac{3}{2} \langle Q_1 \rangle_2, \quad (5.19)$$

where

$$\kappa = \frac{\Lambda_\chi^2}{m_K^2 - m_\pi^2} = \frac{F_\pi}{F_K - F_\pi} = 4.55, \quad (5.20)$$

$$X = \sqrt{\frac{3}{2}} F_\pi (m_K^2 - m_\pi^2) = 3.71 \cdot 10^{-2} \text{ GeV}^3, \quad (5.21)$$

and

$$\langle \overline{Q_6} \rangle_0 = \frac{\langle Q_6 \rangle_0}{B_6^{(1/2)}}. \quad (5.22)$$

For the ease of the reader, we give all the actual numerical values for Λ_χ , m_K , m_π , F_K , F_π that produce these “magic numbers” above in appendix C.

The overall normalization in eqs. (5.5)–(5.22) agrees with [6], but differs by a factor $\sqrt{3/2}$ relative to the normalization used in [19]. This difference cancels however in the final result for ε'/ε and other physical quantities.

For $m_c < \mu < m_b$ the relations (4.42) are valid and the formulae for $\langle Q_4 \rangle_0$, $\langle Q_9 \rangle_0$ and $\langle Q_{10} \rangle_0$ change:

$$\langle Q_4 \rangle_0 = \langle Q_3 \rangle_0 + \langle Q_2 \rangle_0 - \langle Q_1 \rangle_0 + \langle Q_2^c \rangle_0 - \langle Q_1^c \rangle_0, \quad (5.23)$$

$$\langle Q_9 \rangle_0 = \frac{3}{2} \langle Q_1 \rangle_0 - \frac{1}{2} \langle Q_3 \rangle_0 + \frac{3}{2} \langle Q_1^c \rangle_0, \quad (5.24)$$

$$\langle Q_{10} \rangle_0 = \langle Q_4 \rangle_0 + \langle Q_9 \rangle_0 - \langle Q_3 \rangle_0. \quad (5.25)$$

The matrix elements $\langle Q_{1,2}^c \rangle_{0,2}$ although vanishing in the vacuum insertion method may be non-zero in general as discussed below. Also eq. (5.16) is modified by $\mathcal{O}(\alpha)$ corrections. In the vacuum insertion method $B_i \equiv 1$.

5.3 Critical Comparison of Various Matrix Elements Estimates

Having formulae (5.5)–(5.25) at hand, we can compare these matrix elements with the ones used in refs. [6, 17, 18, 19].

In ref. [6], eqs. (5.5)–(5.22) have been used with the terms “1” and X in (5.11), (5.12) and X in (5.17), (5.18) omitted and $B_i^{(\Delta I)} \equiv 1$ except for

$$B_1^{(1/2)} = 5.2, \quad B_2^{(1/2)} = 2.2, \quad B_1^{(3/2)} = 0.55, \quad (5.26)$$

in accordance with the $1/N$ -approach of ref. [33]. The fact that $B_i^{(1/2)} > 1$ for $i = 1, 2$ and $B_1^{(3/2)} < 1$ allows to come closer to the $\Delta I = 1/2$ rule than it is possible in the vacuum insertion method. Furthermore, $\mu = 1$ GeV and $125 \text{ MeV} \leq m_s(1 \text{ GeV}) \leq 200 \text{ MeV}$ have been used. At this point we should mention that the approach of Pich and de Rafael [34] gives similar results to [33] for $K \rightarrow \pi\pi$ amplitudes.

The Dortmund group [17, 18] uses essentially the above formulae with $0.6 \text{ GeV} \leq \mu \leq 1 \text{ GeV}$. The main difference with respect to [6] is the modified factor $B_6^{(1/2)}$ for the operator Q_6 . Using the tables of ref. [17, 18], we find

$$B_6^{(1/2)} \approx 2.4 \pm 0.2. \quad (5.27)$$

The authors of [17, 18] also use $100 \text{ MeV} \leq m_s(1 \text{ GeV}) \leq 175 \text{ MeV}$. The difference of $B_6^{(1/2)}$ from unity follows according to ref. [17, 18] from next-to-leading $1/N$ corrections for which the details are unfortunately not available. $B_8^{(3/2)}$ extracted from [17, 18] remains very close to unity.

The Rome group [19] uses the set of matrix elements relevant for $\mu = 2 \text{ GeV}$ with

$$\begin{aligned} B_{3,4}^{(1/2)} &= 1 - 6^{(*)}, & B_{5,6}^{(1/2)} &= 1.0 \pm 0.2, \\ B_{7,8,9}^{(1/2)} &= 1^{(*)}, & B_{7,8}^{(3/2)} &= 1.0 \pm 0.2, \\ B_{1,2}^c &= 0 - 0.15^{(*)}, & B_9^{(3/2)} &= 0.8 \pm 0.2, \end{aligned} \quad (5.28)$$

where entries with $(*)$ are educated guesses and the remaining values are taken from lattice calculations [41]–[46]. Here, $B_{1,2}^c$ enters the matrix elements $\langle Q_{1,2}^c \rangle_0$ as follows

$$\langle Q_1^c \rangle_0 = -\frac{1}{3} X B_1^c, \quad \langle Q_2^c \rangle_0 = X B_2^c, \quad (5.29)$$

where we have introduced the minus sign in order to make B_1^c positive. In the vacuum insertion approximation $B_{1,2}^c = 0$ holds. However, in QCD it could certainly be non-zero. The range of values for $B_{1,2}^c$ in (5.28) is an educated guess by the authors of ref. [19]. As we will demonstrate in section 6, the size of $\langle Q_{1,2}^c \rangle_0$ is related to the size of $\langle Q_i \rangle_0$, $i = 3, \dots, 6$, and it is possible to go beyond educated guesses and calculate $B_{1,2}^c$. Since as seen in (4.40) and stressed in ref. [19] the coefficients $y_{1,2}^c$ are large the operators $Q_{1,2}^c$ could have in principle some impact on ε'/ε . Our calculations in section 6 show that the educated guess

of [19] overestimates $B_{1,2}^c$ by a factor of four, and consequently, $Q_{1,2}^c$ play only a minor role for $\mu \leq 2$ GeV. A detailed comparison with ref. [19] will be given later on.

Furthermore, the Rome group uses

$$m_s(2 \text{ GeV}) = (170 \pm 30) \text{ MeV} . \quad (5.30)$$

which corresponds to

$$m_s(1 \text{ GeV}) = (225 \pm 30) \text{ MeV} , \quad (5.31)$$

and is considerably higher than the values used in the other two papers. Consequently, the matrix elements $\langle Q_6 \rangle$ and $\langle Q_8 \rangle$ evaluated at $\mu = 1$ GeV are smaller than in ref. [6] and substantially smaller than in [17, 18]. Equivalently, the matrix elements used by the Rome group at $\mu = 2$ GeV are close to the matrix elements used in [6] where $\mu = 1$ GeV has been taken. But since the coefficients $C_i(\mu)$ of penguin operators decrease with increasing μ the penguin contributions to ε'/ε in ref. [19] are bound to be smaller than in the remaining two papers. We will return to this point below.

It should also be remarked that whether the terms “1” and X are kept or dropped in the matrix elements of Q_7 and Q_8 is essentially immaterial for ε'/ε . Although $\langle Q_7 \rangle_0$, $\langle Q_7 \rangle_2$ and $\langle Q_8 \rangle_0$ are modified by roughly 15%, these matrix elements do not play a considerable role in ε'/ε . On the other hand $\langle Q_8 \rangle_2$ which is important is modified by only 2%.

Next, we would like to point out one additional problem with the matrix elements given above. They have been calculated in QCD without taking order $\mathcal{O}(\alpha)$ corrections into account. It is a simple matter to convince oneself that all the matrix elements listed in (5.5)–(5.19) and (5.29) receive $\mathcal{O}(\alpha)$ contributions because at $\mathcal{O}(\alpha)$ they mix under renormalization with the operators Q_7 and Q_9 which have $\mathcal{O}(1)$ matrix elements. In particular one has

$$\langle Q_{3-6} \rangle_2 = \mathcal{O}(\alpha) \quad \langle Q_{1,2}^c \rangle_2 = \mathcal{O}(\alpha) \quad (5.32)$$

to be compared with (5.16) and $\langle Q_{1,2}^c \rangle_2 = 0$ used in ref. [19]. The $\mathcal{O}(\alpha)$ corrections to these matrix elements are necessary in order to cancel the scheme dependence present in the Wilson coefficients as discussed in detail in section 3. The $\mathcal{O}(\alpha)$ corrections to penguin matrix elements should be dropped because they contribute $\mathcal{O}(\alpha \alpha_s)$ or $\mathcal{O}(\alpha^2)$ effects to the amplitudes. On the other hand the $\mathcal{O}(\alpha)$ corrections to the matrix elements of Q_1 and Q_2 should be taken into account because they are exactly at the same level as the $\mathcal{O}(\alpha)$ effects which have been taken into account when evaluating the initial conditions at $\mu \approx M_W$ in section 4. Similarly $\mathcal{O}(\alpha)$ effects to $\langle Q_{1,2}^c \rangle_0$ and $\langle Q_{1,2}^c \rangle_2$ have to be included.

After this rather critical presentation of the existing estimates of hadronic matrix elements, we will now turn to an approach which overcomes several difficulties of the methods just discussed.

6 A Phenomenological Approach to Hadronic Matrix Elements

6.1 General Remarks

We have seen that the present estimates of hadronic matrix elements by means of existing non-perturbative methods suffer from many deficiencies, in particular:

- The hadronic matrix elements of the dominant penguin operators Q_6 and Q_8 are poorly known due to the poor knowledge of $m_s(1 \text{ GeV})$.
- The size of hadronic matrix elements of Q_1 and Q_2 is not fully in accordance with the known data for $K \rightarrow \pi\pi$.
- The renormalization and μ -dependences of the hadronic matrix elements are not under control.

These deficiencies imply another weak point of the ε'/ε analyses of refs. [6, 17, 18]. The usual practice is to vary $m_s(1 \text{ GeV})$ in eq. (5.10), while keeping the matrix elements of current-current operators fixed. Yet, such a procedure fails to fit the data on CP -conserving $K \rightarrow \pi\pi$ amplitudes since for a given value of m_s only certain matrix elements of current-current operators can fit these data.

We would like to propose here a phenomenological approach to obtain the hadronic matrix elements which incorporates properly the renormalization scheme and μ -dependences of the hadronic matrix elements as given by QCD, and at the same time assures that the theoretical CP -conserving $K \rightarrow \pi\pi$ amplitudes are in agreement with the data. The basic ingredients in this approach are

- the assumption that \mathcal{H}_{eff} of (4.4) properly describes the existing data on CP -conserving $K \rightarrow \pi\pi$ amplitudes.
- the Wilson coefficient functions calculated reliably in QCD and QED in section 4.
- some relations between matrix elements which are valid in QCD and are consistent with the renormalization group properties.

Our phenomenological approach to the hadronic matrix elements involves four basic parameters:

- the QCD scale parameter $\Lambda_{\overline{\text{MS}}}$ in the $\overline{\text{MS}}$ renormalization scheme,

- the B -factors $B_2^{(1/2)}(m_c)$, $B_6^{(1/2)}(m_c)$, and $B_8^{(3/2)}(m_c)$, parameterizing the matrix elements $\langle Q_2(m_c) \rangle_0$, $\langle Q_6(m_c) \rangle_0$, and $\langle Q_8(m_c) \rangle_2$ respectively, as defined in eqs. (5.6), (5.10), and (5.18).

The choice $\mu = m_c$ turns out to be very convenient as we will see soon, but is not necessary.

For given values of these four parameters and the chosen renormalization scheme for operators our semi-phenomenological approach gives all the hadronic matrix elements of the dominant operators while being consistent with the measured CP -conserving $K \rightarrow \pi\pi$ amplitudes. In this way an interesting correlation between matrix elements of current-current and penguin operators absent in the analyses of refs. [6, 17, 18, 19] arises.

Having calculated all matrix elements this way, we will be able to give predictions for ε'/ε as functions of the four basic parameters listed above and of m_t .

In what follows, we will first give the basic formulae of our phenomenological approach. Subsequently, we will calculate the hadronic matrix elements $\langle Q_i \rangle_{0,2}$ and we will compare our results with those discussed in the previous section.

In our numerical analysis we use the following experimental data [53]

$$\text{Re}A_0 = 33.3 \cdot 10^{-8} \text{ GeV}, \quad \text{Re}A_2 = 1.50 \cdot 10^{-8} \text{ GeV}, \quad (6.1)$$

which express the $\Delta I = 1/2$ rule

$$\frac{\text{Re}A_0}{\text{Re}A_2} \equiv \frac{1}{\omega} = 22.2. \quad (6.2)$$

6.2 $\langle Q_i(\mu) \rangle_2$ for $(V - A) \otimes (V - A)$ Operators

It turns out that to a very good approximation all the matrix elements $\langle Q_i(\mu) \rangle_2$ can be determined from $\text{Re}A_2$ in (6.1) as functions of $\Lambda_{\overline{\text{MS}}}$, μ and the renormalization scheme considered.

We first introduce the Q_{\pm} operators

$$Q_{\pm} = \frac{1}{2}(Q_2 \pm Q_1), \quad z_{\pm} = z_2 \pm z_1, \quad (6.3)$$

and using (4.1), we find

$$\text{Re}A_2 = cz_+(\mu)\langle Q_+(\mu) \rangle_2, \quad (6.4)$$

where

$$c \equiv \frac{G_F}{\sqrt{2}} V_{ud}V_{us}^* = 1.77 \cdot 10^{-6} \text{ GeV}^{-2}. \quad (6.5)$$

In obtaining (6.4), we have set $\tau y_i = 0$ in view of $z_i \gg \tau y_i$, and we have neglected the contributions of the electroweak penguin operators which having $z_i \approx \mathcal{O}(\alpha)$ play only a

secondary role in CP -conserving amplitudes. Recall also that $\langle Q_i \rangle_2 = \mathcal{O}(\alpha)$ for $i = 3, \dots, 6$ and also $\langle Q_{1,2}^c \rangle_2 = \mathcal{O}(\alpha)$. Consequently, (6.4) is valid for any scale μ in the limit $\alpha = 0$. Moreover for $\mu = m_c$ the contributions of penguin operators and of $Q_{1,2}^c$ (see below) is either zero (HV,LO) or very small (NDR) and at this scale (6.4) is an excellent approximation even for $\alpha \neq 0$.

We note next that (see (5.15))

$$\langle Q_1(\mu) \rangle_2 = \langle Q_2(\mu) \rangle_2 = \langle Q_+(\mu) \rangle_2. \quad (6.6)$$

This relation is valid in pure QCD in which isospin is conserved. It is consistent with the QCD renormalization group evolution. This follows from the fact that the anomalous dimension matrix $\hat{\gamma}_s$ in the (Q_1, Q_2) sector is symmetric with equal diagonal entries and the fact that $\langle Q_i \rangle_2 = 0$ for $i = 3, \dots, 6$. Here, we neglect the mixing with electroweak penguin operators which is $\mathcal{O}(\alpha)$. The effect of this mixing will be analyzed below.

Using the experimental value for $\text{Re}A_2$, together with (6.4) and (6.6), we find the matrix elements $\langle Q_{1,2} \rangle_2$,

$$\langle Q_1(\mu) \rangle_2 = \langle Q_2(\mu) \rangle_2 = \frac{\text{Re}A_2}{c z_+(\mu)}. \quad (6.7)$$

Since $z_+(\mu)$ depends on μ and the renormalization scheme used, (6.7) gives us automatically the scheme and μ -dependence of the matrix elements in question. It also gives the $\Lambda_{\overline{\text{MS}}}$ dependence of $\langle Q_{1,2} \rangle_2$.

Using the relation (5.19) and (6.7), we find the matrix elements $\langle Q_{9,10} \rangle_2$

$$\langle Q_9(\mu) \rangle_2 = \langle Q_{10}(\mu) \rangle_2 = \frac{3\text{Re}A_2}{2c z_+(\mu)}. \quad (6.8)$$

As discussed in section 4.5, eq. (5.19) is valid in all schemes for $\alpha = 0$, and so is (6.8) in this limit.

A numerical analysis shows that the μ -dependence in (6.8) does not cancel the μ -dependence of $z_9(\mu)$ and $z_{10}(\mu)$. This is not surprising, because due to the mixing of Q_9 and Q_{10} with other operators the cancellation of the μ -dependence involves more operators. It should be stressed that the matrix elements in (6.7) and (6.8) do not involve any parameters except for $\Lambda_{\overline{\text{MS}}}$. Although the impact of $\mathcal{O}(\alpha)$ corrections to the determination of these matrix elements is very small we would like to discuss here the matrix elements $\langle Q_{1,2}^c \rangle_2$ which as stated in (5.32) are $\mathcal{O}(\alpha)$. The point is that these matrix elements can be calculated! First they can only be non-zero for $\mu \geq m_c$ because for $\mu \leq m_c$ the operators $Q_{1,2}^c$ disappear from the effective theory. Requiring the μ -independence of $\text{Re}A_2$ and noting

that in the HV and NDR schemes $z_i(m_c) = 0$ for $i = 3, \dots, 10$ we find the following “initial conditions”

$$\langle Q_1^c(m_c) \rangle_2 = \langle Q_2^c(m_c) \rangle_2 = 0 \quad (6.9)$$

valid in these schemes. The evolution (5.4) of these matrix elements to scales $\mu > m_c$ generates calculable non-vanishing values of $\mathcal{O}(\alpha)$. Using (3.7) one can also find the corresponding initial conditions in the NDR scheme. The inclusion of these operators is necessary if one want to keep $\text{Re}A_2$ μ -independent. These points will be illustrated more explicitly in the case of $\langle Q_i^c(\mu) \rangle_0$.

Comparing (6.7) and (6.8) with the general formulae (5.15) and (5.19), respectively, we can extract $B_1^{(3/2)}(\mu)$ which with the approximation used is common for Q_1, Q_2, Q_9 and Q_{10} . The result is represented by the solid lines in figs. 7 and 8 for $Q_{1,2}$ and $Q_{9,10}$, respectively. The remaining lines in these figures represent exact RG evolution. They are obtained by evaluating first the matrix elements at $\mu = m_c$ with the help of (6.7) and (6.8), and evolving subsequently to other values of μ by means of the evolution equation (5.4). In the evolution we have used $\Lambda_{\overline{\text{MS}}} = 300$ MeV.

We observe the following points:

- Our formulae (5.7) and (5.8) are good approximations to the exact evolution including $\mathcal{O}(\alpha)$ effects for $1 \text{ GeV} \leq \mu \leq 2 \text{ GeV}$, considered mainly in this paper. For $\langle Q_1 \rangle_2$ and $\langle Q_9 \rangle_2$ the approximations become slightly worse when μ is increased beyond this range.
- We observe a sizable μ -dependence of $B_1^{(3/2)}(\mu)$.
- The next-to-leading order corrections to $z_{1,2}(\mu)$ decrease $B_1^{(3/2)}(\mu)$ relative to the leading order determination with the effect being stronger in the case of the NDR scheme.
- Most importantly however, we find $B_{\text{HV}}^{(3/2)}(\mu \approx 2 \text{ GeV}) \approx 0.44$, to be compared with $B_9^{(3/2)} \approx 0.8 \pm 0.2$ in (5.28). We conclude therefore that the lattice estimate for $\langle Q_{9,10}(2 \text{ GeV}) \rangle$ of ref. [19] overestimates these matrix elements by almost a factor of two. We will investigate the impact of this on ε'/ε in section 8. The $1/N$ approach used in [6] is in a much better shape here because for low μ , $B_1^{(3/2)} \approx 0.55$ in (5.26) is quite consistent with figs. 7 and 8 for $\mu \approx 1 \text{ GeV}$.

6.3 $\langle Q_i(\mu) \rangle_0$ for $(V - A) \otimes (V - A)$ Operators

The determination of $\langle Q_i(\mu) \rangle_0$ operators is more involved because several operators may contribute to $\text{Re}A_0$ and a relation like (6.6) does not exist in this case. Yet, some progress beyond the approaches of section 5 can also be made in this case. As we will see the choice $\mu = m_c$ is again very helpful in this respect.

Let us begin with $\mu > m_c$. In this case the Wilson coefficients z_i of penguin operators are zero and $\text{Re}A_0$ is given as follows

$$\text{Re}A_0 = c \left[z_-(\mu) \left(\langle Q_- \rangle_0 - \langle Q_-^c \rangle_0 \right) + z_+(\mu) \left(\langle Q_+ \rangle_0 - \langle Q_+^c \rangle_0 \right) \right], \quad (6.10)$$

where similarly to (6.4), τy_i have been set to zero. On the other hand, for $\mu < m_c$ the operators Q_\pm^c disappear from the effective theory but instead the QCD penguin operators contribute

$$\text{Re}A_0 = c \left[z_-(\mu) \langle Q_-(\mu) \rangle_0 + z_+(\mu) \langle Q_+(\mu) \rangle_0 \right] + \text{Re}A_0^P, \quad (6.11)$$

where

$$\text{Re}A_0^P = c \sum_{i=3}^6 z_i(\mu) \langle Q_i(\mu) \rangle_0. \quad (6.12)$$

We again neglect the contributions of electroweak penguin operators Q_i , $i = 7, \dots, 10$.

Since $\text{Re}A_0$ cannot depend on μ , expressions (6.10) and (6.11) have to be matched properly at $\mu = m_c$, the transition point at which one goes from $f = 4$ to $f = 3$ effective theory. This matching gives the following relation between $\langle Q_\pm^c(m_c) \rangle_0$ and $\langle Q_i(m_c) \rangle_0$, $i = 3, \dots, 6$ operators

$$\sum_{i=3}^6 z_i(m_c) \langle Q_i(m_c) \rangle_0 = - \left[z_-(m_c) \langle Q_-^c(m_c) \rangle_0 + z_+(m_c) \langle Q_+^c(m_c) \rangle_0 \right], \quad (6.13)$$

which clearly shows that the role of penguin operators in the $\Delta I = 1/2$ rule is for $\mu > m_c$ played by the operators $Q_{1,2}^c$. There is a very immediate consequence of this observation. The size of the matrix elements $\langle Q_\pm^c \rangle_0$ is correlated with the size of $\langle Q_i \rangle_0$, $i = 3, \dots, 6$.

Now, as discussed in section 4, in the HV and $\overline{\text{NDR}}$ schemes $z_i(m_c) = 0$ holds for $i = 3, \dots, 6$. Consequently, in these schemes we have the relation

$$z_-(m_c) \langle Q_-^c(m_c) \rangle_0 + z_+(m_c) \langle Q_+^c(m_c) \rangle_0 = 0, \quad (6.14)$$

which is also valid for $\alpha \neq 0$.

If we next make a very plausible assumption consistent with all existing non-perturbative methods that $\langle Q_\pm^c \rangle_0 \geq 0$, we find the following “initial” conditions for the matrix elements of $Q_{1,2}^c$:

$$\langle Q_1^c(m_c) \rangle_0 = \langle Q_2^c(m_c) \rangle_0 = 0, \quad (6.15)$$

valid in the HV and $\overline{\text{NDR}}$ schemes. Using (3.7) with $\alpha = 0$, we then find the corresponding result for the NDR scheme

$$\begin{aligned}\langle Q_1^c(m_c) \rangle_0 &= 0, \\ \langle Q_2^c(m_c) \rangle_0 &= \frac{\alpha_s(m_c)}{12\pi} \left[\langle Q_6(m_c) \rangle_0 + \langle Q_4(m_c) \rangle_0 - \frac{1}{3} \langle Q_3(m_c) \rangle_0 - \frac{1}{3} \langle Q_5(m_c) \rangle_0 \right].\end{aligned}\tag{6.16}$$

One can easily check that this result is consistent with (6.13) and with the initial conditions for $z_i(m_c)$, $i = 3, \dots, 6$, given for the NDR scheme in (4.29). The effect of $\mathcal{O}(\alpha)$ corrections can easily be taken into account by using (3.7). It has been included in our numerical analysis. With the initial conditions (6.15) and (6.16) at hand we can calculate $\langle Q_i^c(\mu) \rangle_0$ for any $\mu > m_c$. The result is given in section 6.5.

We now want to constrain the matrix elements by the experimental value of $\text{Re}A_0$. To this end it is useful to set $\mu = m_c$ in (6.11). Since in the HV scheme for $\mu = m_c$ only Q_1 and Q_2 operators contribute to $\text{Re}A_0$, we find the relation

$$z_1(m_c) \langle Q_1(m_c) \rangle_0 + z_2(m_c) \langle Q_2(m_c) \rangle_0 = \frac{\text{Re}A_0}{c},\tag{6.17}$$

from which the following expression for the matrix element $\langle Q_1(m_c) \rangle_0$ as a function of $\langle Q_2(m_c) \rangle_0$ can be found

$$\langle Q_1(m_c) \rangle_0 = \frac{\text{Re}A_0}{c z_1(m_c)} - \frac{z_2(m_c)}{z_1(m_c)} \langle Q_2(m_c) \rangle_0,\tag{6.18}$$

Using next the relations (5.8), (5.13), and (5.14), we are able to obtain $\langle Q_4(m_c) \rangle_0$, $\langle Q_9(m_c) \rangle_0$, and $\langle Q_{10}(m_c) \rangle_0$. Because $\langle Q_3(m_c) \rangle_0$ is colour suppressed, we could set it to zero or just use the expression of eq. (5.7). Since Q_3 has small Wilson coefficients it does not play any role in our analysis. On the other hand $\langle Q_4(m_c) \rangle_0$ plays a substantial role in the analysis of ε'/ε and the assumptions about $\langle Q_3(m_c) \rangle_0$ entering (5.8) matter to some extent. In the following, we will therefore take $\langle Q_3(m_c) \rangle_0$ according to eq. (5.7). $\langle Q_9(m_c) \rangle_0$ and $\langle Q_{10}(m_c) \rangle_0$ are much less important for ε'/ε than $\langle Q_4(m_c) \rangle_0$.

In the case of the NDR scheme there is a small contribution of the penguin operators to (6.15). Moreover, the determination of $\langle Q_4(m_c) \rangle_0$ requires the use of the relation (4.44). Thus, we need some assumptions about $(V - A) \otimes (V + A)$ operators which are discussed below. For $\mu = m_c$ however the issue of $(V - A) \otimes (V + A)$ operators has only very small impact on (6.18) even in the NDR scheme. Equivalently, the matrix elements of $(V - A) \otimes (V - A)$ operators in the NDR scheme can be obtained from the HV matrix elements by means of (3.7).

With all this formalism at hand, we can now calculate the parameters $B_1^{(1/2)}(m_c)$ and $B_4^{(1/2)}(m_c)$ as functions of $B_2^{(1/2)}(m_c)$. If we in addition make the very plausible assumption valid in all known non-perturbative approaches that $\langle Q_-(m_c) \rangle \geq \langle Q_+(m_c) \rangle \geq 0$ the experimental value of $\text{Re}A_0$ implies

$$B_{2,LO}^{(1/2)}(m_c) = 5.8 \pm 1.1, \quad B_{2,NDR}^{(1/2)}(m_c) = 6.7 \pm 0.9, \quad B_{2,HV}^{(1/2)}(m_c) = 6.3 \pm 1.0. \quad (6.19)$$

This should be compared with the vacuum insertion result $B_2^{(1/2)} = 1$, and $B_2^{(1/2)} \approx 2.2$ in the $1/N$ approach. The latter value corresponds to $\mu \approx 0.6$ GeV, and when extrapolated to $\mu = m_c$ would give $B_2^{(1/2)}(m_c) \approx 2.8$. Yet, it is clear that the imposition of the $\Delta I = 1/2$ rule enhances the role of $(V - A) \otimes (V - A)$ operators. Using (6.18), we plot $B_1^{(1/2)}(m_c)$ in fig. 9 as a function of $B_2^{(1/2)}(m_c)$. We note that if the $\Delta I = 1/2$ rule is imposed, the parameters $B_1^{(1/2)}(m_c)$ and $B_2^{(1/2)}(m_c)$ are strongly correlated. A similar plot for $B_4^{(1/2)}(m_c)$ is given in fig. 10. Here, the dependence on $B_3^{(1/2)}(m_c)$ has been shown. These values are consistent with the upper end of the range for $B_4^{(1/2)}$ used by the Rome group [19]. The strong deviation of $B_4^{(1/2)}$ from unity will have interesting consequences for ε'/ε as already pointed out in [6], and even stronger emphasized in [19].

6.4 $\langle Q_i(\mu) \rangle_{0,2}$ for $(V - A) \otimes (V + A)$ Operators

We have seen that by setting $\mu = m_c$, we have decoupled the penguin operators from the question of the $\Delta I = 1/2$ rule. The matrix elements of $(V - A) \otimes (V - A)$ penguin operators could still be determined due to the operator relations of section 4.5. On the other hand the matrix elements of $(V - A) \otimes (V + A)$ operators cannot be constrained by CP -conserving data unless new relations between $(V - A) \otimes (V - A)$ and $(V - A) \otimes (V + A)$ operators are found. Some relations of this type have been suggested in ref. [17, 18, 54]. However, in our opinion these relations are suspect as we will see below and therefore, we will not use them here.

For $\langle Q_6(m_c) \rangle_0$, we simply use the formula (5.10), and for $\langle Q_5(m_c) \rangle_0$ the relation (5.9), however setting $B_5^{(1/2)} \equiv B_6^{(1/2)}$. The assumption about $\langle Q_5(m_c) \rangle_0$ is of little importance because this matrix element, similarly to $\langle Q_3(m_c) \rangle_0$, is colour suppressed and has very small Wilson coefficients. Some support for this strategy will be given soon.

For the matrix elements of the $(V - A) \otimes (V + A)$ electroweak penguin operators Q_7 and Q_8 , we will simply use the relations (5.11), (5.12), as well as (5.17) and (5.18), modified by setting $B_7^{(1/2)} \equiv B_8^{(1/2)}$ and $B_7^{(3/2)} \equiv B_8^{(3/2)}$. Since mainly $\langle Q_8(m_c) \rangle_2$ is of importance for ε'/ε , the simplification of identifying these B -parameters is immaterial. Again our analysis presented below supports this strategy.

At this point, a remark on the strange quark mass is in order. Throughout our analysis, we have used the value $m_s(m_c) = 150$ MeV, which corresponds to $m_s(1 \text{ GeV}) = 175$ MeV. This value is somewhat lower than the central value cited by the Particle Data Group [53]. However, the values there have been obtained with lower values of $\Lambda_{\overline{\text{MS}}}$ than are used in this work, and since $m_s(1 \text{ GeV})$ decreases for larger values of $\Lambda_{\overline{\text{MS}}}$, we expect the above value of m_s to be in the right range [55]. Nevertheless, due to the existing uncertainty in the value of m_s , we have allowed for a larger variation of $B_6^{(1/2)}$ and $B_8^{(1/2)}$, which in this way include a possible variation in the strange quark mass.

As seen in (5.28) the parameters $B_{5,6}^{(1/2)}$ and $B_{7,8}^{(3/2)}$ calculated in the lattice approach [41]–[46], agree very well with the vacuum insertion value and in the case of $B_6^{(1/2)}$ and $B_8^{(3/2)}$ with the $1/N$ approach of ref. [25, 29]. The question arises however, whether this result is valid for a large range of μ . It has been stressed in ref. [6], that the μ -dependence of $\langle Q_6(\mu) \rangle_0$ and $\langle Q_8(\mu) \rangle_2$ is governed in the $1/N$ approach by the μ -dependence of m_s . However, to our knowledge it has never been checked whether $B_6^{(1/2)}$ and $B_8^{(3/2)}$ are indeed μ -independent when μ is varied say in the range $1 \text{ GeV} \leq \mu \leq 4 \text{ GeV}$. With the evolution equation (5.4) at hand, we can answer this question. Taking $B_6^{(1/2)}(m_c) = 1$ and $B_8^{(3/2)}(m_c) = 1$, we have calculated the μ -dependence of these parameters in the case of LO, NDR and HV. As seen in figs. 11 and 12, $B_6^{(1/2)}$ and $B_8^{(3/2)}$ are only weakly dependent on μ , demonstrating that at least for these matrix elements the results of present non-perturbative approaches are consistent with the renormalization group evolution. On the other hand, one would naively expect that the μ -dependence of the colour suppressed matrix elements $\langle Q_5(\mu) \rangle_0$ and $\langle Q_7(\mu) \rangle_2$ should be quite different from the other two matrix elements implying strong μ -dependence of $B_{5,7}^{(1/2)}$. After all, the Wilson coefficients y_5 and y_7 have a μ -dependence very different from y_6 and y_8 . This naive expectation turns out to be completely wrong! As shown in figs. 13 and 14 also $B_5^{(1/2)}(\mu)$ and $B_7^{(1/2)}(\mu)$ are only weakly dependent on μ . Moreover the ratios $B_6^{(1/2)}(\mu)/B_5^{(1/2)}(\mu)$ and $B_8^{(3/2)}(\mu)/B_7^{(3/2)}(\mu)$ are almost independent of μ . In our opinion this is a non-trivial result which gives some support to the lattice results of [41]–[46].

In this connection it is interesting to investigate whether the relations between various operators proposed in refs. [17, 18] are consistent with the renormalization group evolution. Taking the relations of Wu [54] at face value and using the general expressions (5.5)–(5.19), one can derive relations between the B_i -parameters. The most interesting among these relations are

$$B_1^{(1/2)} = \frac{5}{2} B_2^{(1/2)}, \quad B_4^{(1/2)} = B_6^{(1/2)} = \frac{5}{6} B_2^{(1/2)}, \quad B_8^{(3/2)} = \frac{4}{3} B_1^{(3/2)}. \quad (6.20)$$

It is easy to verify by using (5.4) that the relations (6.20) are incompatible with the

renormalization group evolution and can only be valid at a single value of μ . The question then is at which one ?

6.5 The Fate of the Operators $Q_{1,2}^c$

The authors of ref. [19] presented an educated guess for the size of the matrix elements $\langle Q_{1,2}^c(2 \text{ GeV}) \rangle_0$, and emphasized the possible importance of these operators. Having the initial conditions for these matrix elements at $\mu = m_c$ given in (6.15) and (6.16) for the HV and NDR scheme, respectively, we can verify whether this is indeed true. In fig. 15, we show $B_{1,2}^c(\mu)$ defined in (5.29) as functions of $B_6^{(1/2)}(m_c)$ for $\mu = 2, 3$, and 4 GeV in the HV scheme. For $\mu = 2$ GeV and $B_6^{(1/2)}(m_c) = 1.0 \pm 0.2$, as used in [19], $B_{1,2}^c$ turn out to be at the lower end of the range in (5.28). We conclude therefore that at least at $\mu = 2$ GeV the role of the operators $Q_{1,2}^c$ is rather minor in spite of large coefficients $y_{1,2}^c$ given in (4.40). They are more important for $\mu = 4$ GeV, but since for $\mu < m_c$ they do not contribute at all, the fate and the role of these operators depends rather strongly on the choice of μ and also as seen in fig. 15 on $B_6^{(1/2)}$. Similar conclusions are reached in the NDR scheme.

6.6 Strategy of the Present Paper

Making plausible approximations, using the experimental data for CP -conserving amplitudes, and having calculated the Wilson coefficients $z_i(\mu)$ in section 4, we were in a position to calculate the matrix elements $\langle Q_i(\mu) \rangle_{0,2}$ and $\langle Q_{1,2}^c(\mu) \rangle_{0,2}$ for any $\mu \geq 1$ GeV, and any renormalization scheme in terms of the four basic parameters

$$\Lambda_{\overline{\text{MS}}}, \quad B_2^{(1/2)}(m_c), \quad B_6^{(1/2)}(m_c), \quad B_8^{(3/2)}(m_c). \quad (6.21)$$

The remaining two B -parameters $B_3^{(1/2)}$ and $B_8^{(1/2)}$, play only a minor role in the analysis of ε'/ε and will be set to 1.

Let us summarize the basic ingredients of this approach: Having fixed the basic parameters in (6.21) the calculation of the hadronic matrix elements in a given scheme proceeds in several steps as follows.

Step 1:

$$\langle Q_1(\mu) \rangle_2, \langle Q_2(\mu) \rangle_2, \langle Q_9(\mu) \rangle_2 \text{ and } \langle Q_{10}(\mu) \rangle_2 \text{ are given directly by (6.7) and (6.8).}$$

Step 2:

The initial conditions for matrix elements $\langle Q_i(\mu) \rangle_0$ at $\mu = m_c$ can be calculated as described in section 6.3 with the coefficients $z_i(m_c)$ calculated in section 4.

Step 3:

Matrix elements $\langle Q_i(\mu) \rangle_0$ for $\mu \neq m_c$ can be found by using the evolution for the operators given in (5.4). This can also be done for $\langle Q_i(\mu) \rangle_2$ starting at $\mu = m_c$ where (6.7) and (6.8) are most accurate.

Step 4:

The matrix elements $\langle Q_i(\mu) \rangle_{0,2}$ in any other scheme can be calculated by using the relation (3.7).

In performing this program, care must be taken as in the case of the Wilson coefficients, that higher order terms in α_s and α generated in steps 3 and 4 are discarded. When this is done, it is an easy matter to convince oneself that the resulting physical quantities such as A_0 , A_2 and ε'/ε are independent of μ and the scheme considered.

Now, whereas $B_2^{(1/2)}(m_c)$ and the related $(V-A) \otimes (V-A)$ parameters taken in a given scheme can be extracted from CP conserving data as seen in (6.19) and in figs. 7–10 this is not the case for $B_6^{(1/2)}(m_c)$ and $B_8^{(3/2)}(m_c)$. From (3.7), we know that if $B_6^{(1/2)}(m_c) = B_8^{(3/2)}(m_c) = 1$ in the HV scheme then for $\Lambda_{\overline{MS}} = 300$ MeV, we find $B_6^{(1/2)}(m_c) = 0.84$ and $B_8^{(3/2)}(m_c) = 0.85$ in the NDR scheme. Yet, since we do not know at present which renormalization scheme exactly gives the vacuum insertion results, we decided to proceed in the phenomenology of ε'/ε as follows. For all the cases considered (LO, NDR, HV), we will take universal values for the parameters $B_6^{(1/2)}(m_c)$ and $B_8^{(3/2)}(m_c)$. This will necessarily introduce a scheme dependence in our results for ε'/ε because the Wilson coefficients are scheme dependent. This left-over scheme dependence in ε'/ε will give us some idea about the uncertainty in this ratio resulting from the poor knowledge of the scheme dependence for $\langle Q_6(m_c) \rangle_0$ and $\langle Q_8(m_c) \rangle_2$. On the other hand the scheme dependence of the matrix elements of the $(V-A) \otimes (V-A)$ operators will be properly taken into account by means of our approach.

7 CKM–Parameters and ε

In the analysis of ε'/ε we will need the values of various CKM–parameters. We use the standard parameterization of the quark mixing matrix [53] in which the four basic parameters are

$$s_{12} = |V_{us}|, \quad s_{13} = |V_{ub}|, \quad s_{23} = |V_{cb}|, \quad \delta, \quad (7.1)$$

with δ denoting the sole complex phase of this matrix.

In our numerical analysis we will set

$$|V_{\text{us}}| = 0.221, \quad |V_{\text{cb}}| = 0.043 \pm 0.004, \quad (7.2)$$

$$|V_{\text{ub}}/V_{\text{cb}}| = 0.10 \pm 0.03, \quad (7.3)$$

and as usual we will extract δ by fitting the theoretical expression for the parameter ε of the indirect CP -violation to the data. To this end, we use

$$\varepsilon = \frac{\exp(i\pi/4)}{\sqrt{2} \Delta M} (\text{Im}M_{12} + 2\xi \text{Re}M_{12}), \quad (7.4)$$

where

$$\xi = \frac{\text{Im}A_0}{\text{Re}A_0}, \quad \Delta M = 3.5 \cdot 10^{-15} \text{ GeV}, \quad (7.5)$$

with the amplitude $A_0 \equiv A(K \rightarrow (\pi\pi)_{I=0})$ and M_{12} obtained from the standard box diagrams

$$M_{12} = \frac{G_{\text{F}}^2}{12 \pi^2} F_{\text{K}}^2 B_{\text{K}} m_{\text{K}} M_{\text{W}}^2 \left[\lambda_{\text{c}}^{*2} \eta_1 S(x_{\text{c}}) + \lambda_{\text{t}}^{*2} \eta_2 S(x_{\text{t}}) + 2\lambda_{\text{c}}^* \lambda_{\text{t}}^* \eta_3 S(x_{\text{c}}, x_{\text{t}}) \right]. \quad (7.6)$$

Here $S(x_i)$ and $S(x_{\text{c}}, x_{\text{t}})$ are the Inami-Lim functions for which explicit formulae are given e.g. in ref. [6]. Next, $F_{\text{K}} = 161 \text{ MeV}$, $\lambda_i = V_{\text{id}} V_{\text{is}}^*$ and B_{K} is the renormalization group invariant parameter describing the size of the matrix element $\langle \bar{K}^0 | (\bar{s}d)_{V-A} (\bar{s}d)_{V-A} | K^0 \rangle$. In our numerical analysis, we will choose

$$B_{\text{K}} = 0.65 \pm 0.15, \quad (7.7)$$

which is in the ballpark of most recent estimates [56]. For the QCD-factors η_i , we will use

$$\eta_1 = 0.85, \quad \eta_2 = 0.58, \quad \eta_3 = 0.36, \quad (7.8)$$

where η_2 includes next-to-leading order corrections calculated in ref. [32]. Because the second term in eq. (7.6) is the dominant one, we included next-to-leading order corrections in η_2 although for the other two smaller terms they are still unknown. Without these corrections one would have $(\eta_2)_{\text{lo}} \approx 0.62$.

For fixed values of the parameters in (7.2), (7.3), (7.7) and (7.8), and for a fixed value of m_{t} comparison of (7.4) with the experimental data for ε gives two solutions for the phase δ in the first and second quadrant. With the experimental constraint from $B^0 - \bar{B}^0$ -mixing it is sometimes possible to exclude one of the two solutions. In particular for $m_{\text{t}} > 150 \text{ GeV}$ and $F_{\text{B}} > 200 \text{ MeV}$ the solution in the first quadrant is favoured. Due to remaining substantial uncertainties in F_{B} and m_{t} , we will however not use the constraint

coming from $B^0 - \bar{B}^0$ -mixing and we will present the results for ε'/ε corresponding to two solutions for δ .

In the left half of fig. 16, we show $\text{Im}\lambda_t$ as a function of m_t when $|V_{cb}|$, $|V_{ub}/V_{cb}|$ and B_K are varied in the ranges given by (7.2), (7.3), and (7.7). In the right half of fig. 16 similar plots are given for the parameter ranges to be expected in a few years time

$$|V_{cb}| = 0.043 \pm 0.002, \quad |V_{ub}/V_{cb}| = 0.10 \pm 0.01, \quad B_K = 0.65 \pm 0.05, \quad (7.9)$$

We observe that $\text{Im}\lambda_t$ decreases with m_t and is larger for the solution $0 < \delta < \pi/2$. The uncertainty in $\text{Im}\lambda_t$ is considerable at present.

8 ε'/ε Beyond Leading Logarithms

8.1 Basic Formulae

The parameter ε' is given in terms of the amplitudes A_0 and A_2 as follows

$$\varepsilon' = -\frac{\omega}{\sqrt{2}} \xi (1 - \Omega) \exp^{i\phi}, \quad (8.1)$$

where

$$\xi = \frac{\text{Im}A_0}{\text{Re}A_0}, \quad \omega = \frac{\text{Re}A_2}{\text{Re}A_0}, \quad \Omega = \frac{1}{\omega} \frac{\text{Im}A_2}{\text{Im}A_0}, \quad (8.2)$$

and $\phi = \pi/2 + \delta_2 - \delta_0 \approx \pi/4$.

Using $\mathcal{H}_{\text{eff}}(\Delta S = 1)$ and the experimental data for ω , $\text{Re}A_0$ and ε , we find

$$\frac{\varepsilon'}{\varepsilon} = 10^{-4} \left[\frac{\text{Im}\lambda_t}{1.7 \cdot 10^{-4}} \right] \left[P^{(1/2)} - P^{(3/2)} \right], \quad (8.3)$$

where

$$P^{(1/2)} = \sum P_i^{(1/2)} = r \sum y_i \langle Q_i \rangle_0 (1 - \Omega_{\eta+\eta'}), \quad (8.4)$$

$$P^{(3/2)} = \sum P_i^{(3/2)} = \frac{r}{\omega} \sum y_i \langle Q_i \rangle_2, \quad (8.5)$$

with

$$r = 1.7 \frac{G_F \omega}{2 |\varepsilon| \text{Re}A_0} = 594 \text{ GeV}^{-3}. \quad (8.6)$$

In (8.4) and (8.5) the sum runs over all contributing operators. This means for $\mu > m_c$ also the contribution from operators $Q_{1,2}^c$ to $P^{(1/2)}$ and $P^{(3/2)}$ have to be taken into account. This is necessary for $P^{(1/2)}$ and $P^{(3/2)}$ to be independent of μ . Next

$$\Omega_{\eta+\eta'} = \frac{1}{\omega} \frac{(\text{Im}A_2)_{I.B.}}{\text{Im}A_0}, \quad (8.7)$$

represents the contribution of the isospin breaking in the quark masses ($m_u \neq m_d$). For $\Omega_{\eta+\eta'}$, we will take

$$\Omega_{\eta+\eta'} = 0.25 \pm 0.05 \quad (8.8)$$

which is in the ballpark of the values obtained in the $1/N$ approach [25] and in chiral perturbation theory [57, 27]. $\Omega_{\eta+\eta'}$ is independent of m_t .

Now the formulation of the phenomenology of ε'/ε found in refs. [5]–[8] and [17, 18, 19] uses instead of $P^{(1/2)}$ and $P^{(3/2)}$ defined in (8.4) and (8.5) the ratios

$$\Omega_i^{(1/2)} \equiv -\frac{P_i^{(1/2)}}{P_6^{(1/2)}}, \quad \Omega_i^{(3/2)} \equiv \frac{P_i^{(3/2)}}{P_6^{(1/2)}} (1 - \Omega_{\eta+\eta'}), \quad (8.9)$$

with $\Omega_{\eta+\eta'}$ being treated separately.

We would like to point out one drawback of this formulation: The separate contributions $\Omega_i^{(1/2)}$ and $\Omega_i^{(3/2)}$ depend on μ and on the renormalization scheme. In this respect the example of the operator Q_2^c is very instructive. As pointed out in ref. [19], Q_2^c can have some impact on ε'/ε for $\mu \approx \mathcal{O}(2 \text{ GeV})$. Yet, for $\mu \leq m_c$ the operator Q_2^c is absent in the effective theory, hence $\Omega_{2,c}^{(1/2)} = 0$, and its effects are hidden in the contributions of operators present in the effective three quark theory.

On the other hand, $P^{(1/2)}$ and $P^{(3/2)}$ in (8.4) and (8.5) are independent of μ and the renormalization scheme considered. We have verified numerically that this is always the case. Consequently, they are more suitable for the phenomenological analysis. $P^{(1/2)}$ is dominated by the contribution of the Q_6 operator but receives also important contributions from Q_4 . $P^{(3/2)}$ receives only contributions from electroweak operators Q_i ($i = 7 \dots 10$). Although Q_8 dominates $P^{(3/2)}$, the operators Q_7 , Q_9 and Q_{10} have also some impact on the final result for ε'/ε .

8.2 B_i -Expansions and the Four Dominant Contributions to ε'/ε

The contributions $P^{(1/2)}$ and $P^{(3/2)}$ can be written as linear combinations of the B_i -parameters introduced in section 5. In our approach of section 6, there are only three relevant B_i -parameters introduced in (6.21). We then find

$$P^{(1/2)} = a_0^{(1/2)} + a_2^{(1/2)} B_2^{(1/2)} + a_6^{(1/2)} B_6^{(1/2)}, \quad (8.10)$$

$$P^{(3/2)} = a_0^{(3/2)} + a_8^{(3/2)} B_8^{(3/2)}, \quad (8.11)$$

where the parameters B_i will be taken at $\mu = m_c$. Then the coefficients $a_i^{(1/2)}$ and $a_i^{(3/2)}$ depend only on $\Lambda_{\overline{\text{MS}}}$, m_t , and the renormalization scheme considered. These dependencies are given in tabs. 14 and 15.

Looking at the expression (8.10) and (8.11), we identify four contributions which govern the ratio ε'/ε :

- i) The contribution of $(V - A) \otimes (V - A)$ operators to $P^{(1/2)}$ is represented by the first two terms in (8.10). These two terms include also small contributions from $(V - A) \otimes (V + A)$ electroweak penguin operators, and if we would use $\mu \geq m_c$ also operators $Q_{1,2}^c$ would contribute here. These two terms are dominated by the contribution of the operator Q_4 . We observe that the sum of the two terms in question is *negative* and only weakly dependent on $B_2^{(1/2)}$, especially if we vary this parameter in the ranges given in (6.17). The dependence of $\Lambda_{\overline{\text{MS}}}$ is also weak. These weak dependences on renormalization scheme, $B_2^{(1/2)}$ and $\Lambda_{\overline{\text{MS}}}$ result from the fact that in our approach of section 6 the matrix elements entering the first two terms in $P^{(1/2)}$ are more or less fixed by the experimental value of A_0 . The weak dependence on m_t results from the contributions of electroweak penguin operators. It should be stressed that the constraint from CP -conserving data suppresses considerably ε'/ε . In order to see this we calculated the sum of the first two terms in (8.10) using the matrix elements with $B_i = 1$. Taking $\Lambda_{\overline{\text{MS}}} = 300$ MeV, $\mu = m_c$ and $m_t = 130$ GeV we have found $a_0^{(1/2)} + a_2^{(1/2)} B_2^{(1/2)}$ equal to -0.75, -0.72, -0.74 for LO, NDR and HV, respectively. This should be compared with -3.78, -3.99 and -3.92 used here.
- ii) The contribution of $(V - A) \otimes (V + A)$ QCD penguin operators to $P^{(1/2)}$ is given by the last term in (8.10). This contribution is large and *positive*. The coefficient $a_6^{(1/2)}$ depends sensitively on $\Lambda_{\overline{\text{MS}}}$ which is the result of the strong dependence of y_6 on the QCD scale. $a_6^{(1/2)}$ is suppressed by next-to-leading corrections at $\mu = m_c$ although due to matching effects discussed in section 4 it is somewhat enhanced for $\mu > m_c$ in the NDR scheme.
- iii) The contribution of the $(V - A) \otimes (V - A)$ electroweak penguin operators Q_9 and Q_{10} to $P^{(3/2)}$ is represented by the first term in $P^{(3/2)}$. As in the case of the contribution i), the matrix elements contributing to $a_0^{(3/2)}$ are fixed by the CP -conserving data. This time by the amplitude A_2 . Consequently, the scheme dependence and the $\Lambda_{\overline{\text{MS}}}$ dependence of $a_0^{(3/2)}$ are weak. The sizable m_t -dependence of $a_0^{(3/2)}$ results from the corresponding dependence of $y_9 + y_{10}$. $a_0^{(3/2)}$ contributes *positively* to ε'/ε . As seen in tab. 15 this contribution is slightly enhanced through next-to-leading order corrections. On the other hand it should be stressed that it is considerably suppressed by the constraint from CP -conserving data. Indeed as seen in fig. 8 $B^{(3/2)}(m_c)$ is by a factor of 2 below the vacuum insertion value.

- iv) The contribution of the $(V - A) \otimes (V + A)$ electroweak penguin operators Q_7 and Q_8 to $P^{(3/2)}$ is represented by the second term in (8.11). This contribution depends sensitively on m_t and $\Lambda_{\overline{\text{MS}}}$. It contributes *negatively* to ε'/ε . The m_t dependence of this contribution is governed roughly by $y_7/3 + y_8$. For $m_t < 150$ GeV enhancement through next-to-leading corrections is observed but for $m_t > 150$ GeV the leading and next-to-leading order results are quite similar to each other. For $m_t < 150$ GeV the operator Q_7 is important when next-to-leading corrections are taken into account but for $m_t \approx 200$ GeV its contribution can be neglected.

The competition between these four contributions depends on m_t and on the values of $B_6^{(1/2)}$ and $B_8^{(3/2)}$. Setting first $B_6^{(1/2)} = B_8^{(3/2)} = 1$, we observe that the contribution ii) is always largest and the contribution iii) smallest. For lower values of m_t the contribution i) is more important than iv), and it is this contribution which represents the main suppression of ε'/ε at $m_t \leq 150$ GeV together with $\Omega_{\eta+\eta'} \neq 0$. With increasing m_t , the contribution iv) grows and for $m_t \geq 170$ GeV, it is more important than the contribution i). At such high values of m_t , the collaboration of i) and iv) is so strong that it becomes as important as the contribution ii) and hence, ε'/ε becomes very small. For even higher values of m_t the sum i)+iv) wins the competition, and ε'/ε becomes negative.

8.3 The μ -Dependence of Various Contributions

It is instructive to study the μ -dependence of the various contributions in (8.4) and (8.5). In fig. 17 we show $P_5^{(1/2)}$, $P_6^{(1/2)}$, $P_7^{(3/2)}$, $P_8^{(3/2)}$ and the remaining contributions to $P^{(1/2)}$ and $P^{(3/2)}$ as functions of μ for $\Lambda_{\overline{\text{MS}}} = 300$ MeV, $m_t = 130$ GeV and $B_5^{(1/2)}(m_c) = B_6^{(1/2)}(m_c) = B_7^{(3/2)}(m_c) = B_8^{(3/2)}(m_c) = 1$. We observe

- i) The various contributions show visible μ -dependence. The sum of all contributions is however μ -independent. The discontinuities in NDR are the result of the matching at m_c .
- ii) The μ -dependence of $P_6^{(1/2)}(\mu)$ and $P_8^{(3/2)}(\mu)$ demonstrates the importance of $1/N$ corrections because in the large- N limit they should be μ -independent. These μ -dependence although visible is rather weak.
- iii) Substantially stronger μ dependence is observed for the remaining smaller contributions in accordance with our previous discussions. $P_5^{(1/2)}$ remains however always very small.

8.4 Final Numerical Results for ε'/ε

We are now in the position to present our final results for ε'/ε which are based on the Wilson coefficients of section 4, the hadronic matrix elements of section 6 and results on $\text{Im}\lambda_t$ of section 7.

Let us first emphasize that with the help of the CP -conserving data we were able to determine two out of four contributions to ε'/ε discussed in section 8.2. These are the contributions i) and iii). Taken together these two contributions give a *negative* value for ε'/ε which is very weakly dependent on $\Lambda_{\overline{\text{MS}}}$ and on the renormalization scheme (LO,NDR,HV). For instance for $\Lambda_{\overline{\text{MS}}} = 300$ MeV and $m_t = 130$ GeV we find $\varepsilon'/\varepsilon \approx -2.7 \times 10^{-4}$. We observe that with increasing m_t this part of ε'/ε becomes smaller.

We should also stress that these two contributions are very different in the vacuum insertion method. In fact in the latter method the sum of the contributions i) and iii) gives a *positive* $\varepsilon'/\varepsilon \approx 1.8 \times 10^{-4}$ for $m_t = 130$ GeV instead of the negative contribution found here.

The fate of ε'/ε in the Standard Model depends then mainly on the following quantities:

$$\text{Im}\lambda_t, \quad m_t, \quad \Lambda_{\overline{\text{MS}}}, \quad B_6^{(1/2)}(m_c), \quad B_8^{(3/2)}(m_c). \quad (8.12)$$

This dependence is shown in tabs. 16–21 and in figs. 18–20. In obtaining these results we have set $m_s(1 \text{ GeV}) = 175$ MeV but we varied the parameters $B_6^{(1/2)}(m_c)$ and $B_8^{(3/2)}(m_c)$ in a broad range which effectively could take into account variations in m_s . Recall that the relevant combinations are B_i/m_s^2 . $B_{6,8} = 0.75, 1, 1.25, 1.5$ and 2.0 corresponds then effectively to $m_s(1 \text{ GeV}) = 202, 175, 157, 143$ and 124 MeV if the matrix elements $\langle Q_{6,8} \rangle$ were kept at the vacuum insertion values. The tabs. 16–18 in which $B_6 = B_8$ show then effectively the variation of $m_s(1 \text{ GeV})$ in the range $143 \text{ MeV} \leq m_s(1 \text{ GeV}) \leq 202 \text{ MeV}$. Tabs. 19, 20 and 21 on the other hand show examples of $B_6 \neq B_8$. We observe the following main dependencies:

- ε'/ε decreases with increasing m_t and $B_8^{(3/2)}$.
- ε'/ε increases with increasing $\Lambda_{\overline{\text{MS}}}$ and $B_6^{(1/2)}$

Moreover as one can deduce from the analysis of $\text{Im}\lambda_t$

- ε'/ε increases with decreasing B_K, V_{cb} and V_{ub} .

The main conclusion which we can draw on the basis of these tables are as follows

- i) If $B_6 = B_8 = 1$ the values of ε'/ε are below 10^{-3} and fully consistent with the result of the experiment E731. The next-to-leading corrections calculated in the NDR scheme suppress ε'/ε by roughly 10–20% relative to the leading order result. Much stronger suppression is observed in the HV scheme, especially at higher values of m_t . Yet in the full range of the parameters considered, ε'/ε remains positive.
- ii) We stress however that the increase of $\langle Q_6(m_c) \rangle_0$ by only a factor of two with $\langle Q_8(m_c) \rangle_2$ kept fixed moves ε'/ε as shown in tab. 21 in the ball park of the NA31 result if $m_t < 150$ GeV, $\Lambda_{\overline{\text{MS}}} \geq 300$ MeV and the NDR scheme is considered. The values in the HV scheme are lower but still consistent with the NA31 result if the CKM phase δ is in the first quadrant.
- iii) For the intermediate choices of the B_i parameters shown in tabs. 17, 19 and 20 the ratio ε'/ε is found somewhere in between the values of the two experiments in question although for higher values of m_t and lower values of $\Lambda_{\overline{\text{MS}}}$ they certainly favour the E731 experiment.
- iv) An important point to be stressed here is the relatively strong dependence of ε'/ε on the value of $\Lambda_{\overline{\text{MS}}}$. It is a result of large anomalous dimensions of penguin operators. This dependence is evident in the tables but is even more clearly depicted in figs. 18, 19 and 20 where ε'/ε is plotted as a function of $\Lambda_{\overline{\text{MS}}}$ for various choices of m_t and B_i . We note that for the cases $(B_6 = B_8 = 1.5)$ and $(B_6 = 1.5, B_8 = 1)$ with $m_t = 130$ GeV the increase of $\Lambda_{\overline{\text{MS}}}$ from 150 MeV to 450 MeV moves essentially ε'/ε from the E731 value to the NA31 result.

We should stress that although our different contributions to ε'/ε have been presented for $\mu = m_c$ we have checked that the final result for ε'/ε does not depend on the actual choice of μ .

In summary, our results for ε'/ε are fully compatible with both experiments when $m_t < 150$ GeV but favour E731 when m_t is higher. The progress in predicting a more accurate value of ε'/ε can only be achieved through the reduction of the uncertainties in the values of the parameters listed in (8.12).

8.5 Comparison with Other Analyses

Our results for ε'/ε cover the range of values between those obtained by the Dortmund [17, 18] and Rome [19] groups. Depending on the choice of the parameters listed in (8.12) one can obtain the results of these two groups.

Here we would like to make a comparison with ref.[19] because this is the only other paper in which full next-to-leading order corrections to the $\Delta S = 1$ Hamiltonian have been computed.

Since these authors presented their results only for the HV scheme, only the comparison for this scheme is possible. Here are our findings:

- i) The results for y_6 and y_8 obtained in [19] agree with ours to better than 3%. Since the details on the two-loop anomalous dimensions are not yet available from the Rome group it is impossible for us to identify the origin of this difference³⁾. Fortunately this is immaterial for any phenomenological applications. We should however remark that the next-to-leading corrections in the HV scheme found by us are larger than those given in ref. [19] because there some of these corrections have been included in the leading order.
- ii) From the smooth μ -dependence of y_6 presented in [19] we conclude that the matching effects discussed in section 4.3 have not been taken into account there. In the case of the HV scheme as seen in fig. 4 this is fortunately only a small effect.

Next we would like to list several differences between our own analysis and the one of ref.[19] which are relevant when taken individually but which cancel each other to some extent when taken as a whole.

- iii) Our analysis of section 6.5 shows that the contributions of $Q_{1,2}^c$ operators to ε'/ε evaluated at $\mu \approx 2$ GeV lie at the lower end of the educated guess of ref. [19]. We find $\Omega_1^c \approx -0.01$, $\Omega_2^c \approx -0.04$ to be compared with $\Omega_1^c \approx 0.02$, $\Omega_2^c \approx -0.18$ quoted in [19]. This reduces the value of ε'/ε found by the Rome group.
- iv) Our analysis of $B_1^{(3/2)}$ shows that the lattice calculations overestimate the contributions of the operators $Q_{9,10}$ by almost a factor of two. When this is corrected for, the value of ε'/ε of ref. [19] is further reduced.
- v) The suppression of ε'/ε through the imposition of the $\Delta I = 1/2$ rule found by us is compatible with the one given in [19] although somewhat stronger.

³⁾ We have just been informed by Guido Martinelli that the Rome group confirmed our NDR two-loop results of refs. [14, 15]. The final results on two-loop anomalous dimensions in the HV scheme also agree, although there are apparently some differences at the intermediate stages of the calculations. We guess then that the 3% difference in the Wilson coefficients originates in the numerical integration of the renormalization group equations done in [19] which in our paper has been done analytically.

- vi) As discussed in section 5 the values of $m_s(1 \text{ GeV})$ used in [19] are higher than those used by us. With our values the results for ε'/ε obtained in [19] would be increased.
- vii) The values of $|V_{ub}/V_{cb}|$, B_K and in particular of $|V_{cb}|$ used in [19] are systematically higher than those used here which results in a smaller value of $\text{Im}\lambda_t$. With our choices of these parameters the authors of [19] would find a higher ε'/ε . In view of the increased B -meson life time and the decrease of B_K in the recent lattice calculations [58] we think that our estimate of $\text{Im}\lambda_t$ is better than the one of ref. [19].

As already stated above these effects cancel each other to some extent when taken as a whole and consequently our result given in tab. 16 for ε'/ε in the HV scheme with $B_6 = B_8 = 1$ are certainly consistent with the ones obtained in ref. [19]. We have however varied the parameters B_6 and B_8 in a larger range and did in addition the same analysis in the NDR scheme. Consequently we reached somewhat different conclusions than ref. [19] regarding the two experimental results for ε'/ε given in (1.1).

9 Wilson Coefficients for $\Delta B = 1$ Decays

This section can be viewed as the generalization of the leading order analyses of Grinstein [59] and Kramer and Palmer [60], beyond the leading order approximation. In addition, the coefficients of electroweak penguin operators will be calculated.

We will focus on the $\Delta B = 1$, $\Delta C = \Delta U = 0$ part of the effective Hamiltonian which is of particular interest for the study of CP violation, i.e., decays to CP self-conjugate final states.

At the tree level the effective Hamiltonian is simply given by

$$\mathcal{H}_{eff}(\Delta B = 1) = \frac{G_F}{\sqrt{2}} \sum_{q=u,c} \sum_{q'=d,s} V_{qb}^* V_{qq'} (\bar{b} q)_{V-A} (\bar{q} q')_{V-A}. \quad (9.1)$$

The cases $q' = d$ or s can be treated separately and have the same coefficients $C_i(\mu)$. Specifying to $q' = d$ and using the unitarity of the CKM matrix we find for $\mu \approx \mathcal{O}(m_b)$ ($\xi_i = V_{ib}^* V_{id}$)

$$\begin{aligned} \mathcal{H}_{eff}(\Delta B = 1) = \frac{G_F}{\sqrt{2}} \left\{ \right. & \xi_c \left(z_1(\mu) O_1^c + z_2(\mu) O_2^c \right) \\ & + \xi_u \left(z_1(\mu) O_1^u + z_2(\mu) O_2^u \right) \\ & \left. - \xi_t \left(\sum_{i=3}^{10} y_i(\mu) O_i \right) \right\}, \quad (9.2) \end{aligned}$$

where O_i , $i = 3, \dots, 10$, are obtained from Q_i , $i = 3, \dots, 10$ in (2.1) by replacing s by b ,

$$O_1^u = (\bar{b}_\alpha u_\beta)_{V-A} (\bar{u}_\beta d_\alpha)_{V-A} \quad ; \quad O_2^u = (\bar{b}u)_{V-A} (\bar{u}d)_{V-A} \quad (9.3)$$

and the O_i^c are obtained from (9.3) through the replacement $u \rightarrow c$.

In spite of the presence of the CKM factors in (9.2), it is an easy matter to convince oneself that for $\mu = m_b$ all ten coefficients building the vector $\vec{C}(\mu)$ can be found using

$$\vec{C}(m_b) = \hat{U}_5(m_b, M_W, \alpha) \vec{C}(M_W), \quad (9.4)$$

with the evolution matrix of eq. (2.17) given in an effective theory with 5 flavours and the initial conditions given in eqs. (4.8)–(4.17). The numerical results for $m_t = 130$ GeV are given in tab. 22. They have a structure similar to the results in tab. 3 and therefore do not require further discussion.

10 Ten Messages from This Paper

Using the two-loop anomalous dimension matrices of refs. [12]–[15], we have constructed the effective Hamiltonian for $\Delta S = 1$, $\Delta C = 1$, and $\Delta B = 1$ transitions with the Wilson coefficients $C_i(\mu)$ including leading and next-to-leading QCD corrections and leading order corrections in the electromagnetic coupling constant α . As the main application of the constructed $\Delta S = 1$ Hamiltonian, we have calculated the ratio ε'/ε as a function of m_t , $\Lambda_{\overline{\text{MS}}}$ and of a set of non-perturbative parameters B_i . This new anatomy of ε'/ε improves the leading order anatomy of 1989 [6] in two respects:

- The Wilson coefficients $C_i(\mu)$ include next-to-leading logarithmic corrections and consequently, the scale $\Lambda_{\overline{\text{MS}}}$ extracted from deep-inelastic scattering and from e^+e^- data at LEP can be meaningfully used for the first time in the evaluation of ε'/ε . Since ε'/ε , being dominated by penguin contributions with large anomalous dimensions, is sensitive to the strength of the QCD coupling constant, the meaningful use of $\Lambda_{\overline{\text{MS}}}$ increases considerably the precision of the theory provided the QCD scale can be extracted accurately from high energy data.
- The hadronic matrix elements $\langle Q_i(\mu) \rangle$ used in the analysis are at all stages consistent with the data on CP -conserving $K \rightarrow \pi\pi$ decays. In particular, $\Delta I = 1/2$ enhancement and $\Delta I = 3/2$ suppression are exactly built into our analysis.

We have presented a detailed renormalization group analysis of both the Wilson coefficient functions and of the hadronic matrix elements. In particular, we have stressed that

the Wilson coefficients are renormalization scheme dependent and that this scheme dependence can only be cancelled by the one present in $\langle Q_i(\mu) \rangle$. Since the existing methods are not capable to study this scheme and scale dependence accurately enough, we have presented a semi-phenomenological approach to hadronic matrix elements with the help of which we could determine several of these matrix elements from existing CP -conserving data.

To summarize, the ten main messages of our paper are as follows:

- i) The coefficients $z_-(\Delta I = 1/2)$ and $z_+(\Delta I = 3/2)$ calculated in the NDR and HV schemes are contrary to the common wisdom suppressed and enhanced by next-to-leading order corrections, respectively. These effects must be compensated by those present in the hadronic matrix elements so that the experimentally known $\Delta I = 1/2$ and $\Delta I = 3/2$ amplitudes are reproduced.
- ii) The contribution of QCD penguins to the $\Delta I = 1/2$ rule depends strongly on μ and the renormalization scheme considered, but is rather small with respect to the whole amplitude. For $\mu > m_c$ it vanishes, but even for $\mu \approx 1$ GeV it does not exceed 20% of A_0 for $m_s(1 \text{ GeV}) > 125$ MeV. In view of these features, relating the size of ε'/ε to the penguin contribution to A_0 is in our opinion not a good idea.
- iii) The coefficient $y_6(m_c)$ is suppressed by roughly 15% in the HV scheme but it is enhanced for $\mu > m_c$ by 10% in the NDR scheme relative to the leading order value. Simultaneously, for $m_t < 150$ GeV we find a strong enhancement of $y_8(m_c)$ calculated in the HV scheme, to be compared with modest enhancement of $y_8(m_c)$ obtained in the NDR scheme. These enhancements of y_8 become smaller for large m_t values.
- iv) The choice $\mu = m_c$ allows to extract efficiently several hadronic matrix elements from the data on CP -conserving $K \rightarrow \pi\pi$ decays. Indeed, at this scale the contributions of all penguin operators and furthermore $Q_{1,2}^c$ operators to the amplitudes A_0 and A_2 vanish for the HV scheme or are very small for the NDR scheme. This allows for obtaining the matrix elements $\langle Q_{1,2}(m_c) \rangle_2$ directly from A_2 as functions of $\Lambda_{\overline{\text{MS}}}$. The matrix elements $\langle Q_{1,2}(m_c) \rangle_0$ are given as a function of $B_2^{(1/2)}(m_c)$ which is found to be in the range $5 \leq B_2^{(1/2)}(m_c) \leq 7$. The relations between operators allow to obtain subsequently all matrix elements of $(V - A) \otimes (V - A)$ penguin operators. This analysis shows that the extracted matrix elements differ considerably from the ones obtained by the vacuum insertion method and in the case of $\langle Q_i \rangle_2$, $i = 1, 2, 9, 10$ also from the lattice results. We have also demonstrated that $\langle Q_{1,2}^c(\mu) \rangle_{0,2}$ can be calculated and that for $\mu \leq 2$ GeV the role of these operators in ε'/ε is small.

- v) Our renormalization group analysis of $\langle Q_i(\mu) \rangle$ shows an interesting result that the B_i parameters of all $(V - A) \otimes (V + A)$ operators are almost μ -independent. All B_i parameters of $(V - A) \otimes (V - A)$ operators show a substantial μ -dependence. The μ - and scheme dependences of $\langle Q_{1,2}(\mu) \rangle_2$ and $\langle Q_{9,10}(\mu) \rangle_2$ are given to a very good approximation by $1/z_+(\mu)$ in the range $1 \text{ GeV} < \mu < 2 \text{ GeV}$. The μ -dependences of $\langle Q_5(\mu) \rangle_0$, $\langle Q_6(\mu) \rangle_0$, $\langle Q_7(\mu) \rangle_2$ and $\langle Q_8(\mu) \rangle_2$ are given within 5% accuracy by $1/m_s^2(\mu)$. We also point out that the contributions $P_6^{(1/2)}(\mu)$ and $P_8^{(3/2)}(\mu)$, which are μ -independent in the large- N limit show visible μ -dependences when exact renormalization group analysis with mixing between operators is taken into account.
- vi) As a preparation for future developments in the evaluation of hadronic matrix elements, we have presented ε'/ε in form of an expansion in the independent non-perturbative parameters $B_i(m_c)$. The coefficients of this expansion are functions of renormalization scheme, $\Lambda_{\overline{\text{MS}}}$ and m_t and the values given in tabs. 14 and 15 are such that the CP -conserving A_0 and A_2 amplitudes are always consistent with the data.
- vii) Among several contributions to ε'/ε there are four which govern this ratio. Two of them can to a good accuracy be fixed by the CP -conserving data and consequently are only weakly dependent on $\Lambda_{\overline{\text{MS}}}$ and the renormalization scheme. These are the negative m_t -independent contribution of Q_4 and a smaller positive contribution of $Q_9 + Q_{10}$ which moderately increases with m_t . The former contribution is substantially enhanced when the $\Delta I = 1/2$ rule is taken into account as pointed out already in ref. [6], and recently reemphasized by the authors of [19]. On the other hand, Q_9 and Q_{10} contributions are similarly to A_2 suppressed substantially relatively to their vacuum insertion and lattice estimates. Consequently, if only the contributions of $(V - A) \otimes (V - A)$ penguins Q_4 , Q_9 and Q_{10} are taken into account ε'/ε is negative and of $\mathcal{O}(10^{-4})$.
- viii) The main uncertainties in ε'/ε result from $\text{Im}\lambda_t$ and from the contributions of the $(V - A) \otimes (V + A)$ penguin operators Q_6 and Q_8 which enter ε'/ε with opposite signs and are sensitive functions of $\Lambda_{\overline{\text{MS}}}$. None of them can be determined from the existing CP -conserving data. Their matrix elements depend on m_s and the parameters $B_6^{(1/2)}$ and $B_8^{(3/2)}$. For $m_s(m_c) = 150 \text{ MeV}$ and $B_6^{(1/2)}(m_c) = B_8^{(3/2)}(m_c) = 1$, the Q_6 contribution dominates for $m_t < 200 \text{ GeV}$, although this dominance is substantially suppressed in the HV scheme and moderately in the NDR scheme (see message iii) above). For $m_t < 150 \text{ GeV}$ the contribution of Q_8 is smaller than the one of Q_4 and consequently, for $m_t \approx \mathcal{O}(130 \text{ GeV})$ the ratio ε'/ε is mainly determined by the

QCD penguins Q_6 and Q_4 with Q_6 being stronger and giving a positive ε'/ε . With increasing m_t the role of Q_8 increases rapidly and for $m_t \approx \mathcal{O}(200 \text{ GeV})$ it is the competition of Q_6 and Q_8 which dominates ε'/ε . Q_8 being helped by the negative contribution of Q_4 wins this competition for $m_t > 200 \text{ GeV}$ and ε'/ε becomes negative similarly to the results of [6].

- ix) Although the parameters B_6 and B_8 are essentially μ -independent and in accordance with the vacuum insertion method and the $1/N$ approach, there is an important question whether their actual values are in the neighborhood of unity. Recall that other parameters B_i show substantial deviation from $B_i = 1$. In this respect, we sympathize with the efforts made by the authors of ref. [17, 18, 54] who questioned the use of $B_6 = B_8 = 1$. Yet, in our opinion the chapter on the actual values of B_6 and B_8 is just being opened and it may well turn out that these parameters are indeed special with values close to unity as given in the leading order of the $1/N$ approach, in the vacuum insertion method, and in lattice calculations. A closely related issue is the actual value of m_s .
- x) Our numerical analysis of ε'/ε summarized in tabs. 16–21 shows that for $B_6 = B_8 = 1$ and high values of m_t , at which strong cancellation takes place, the actual values for ε'/ε depend sensitively on whether the ratio y_8/y_6 is calculated in the NDR or HV scheme. This demonstrates very clearly the necessity of a solid evaluation of $\langle Q_6 \rangle_0$ and $\langle Q_8 \rangle_2$ which would cancel this dependence. For higher values of B_6 and lower values of m_t this scheme dependence is weaker. Generally, the values of ε'/ε obtained in the HV scheme are below the ones obtained in the NDR scheme and roughly in agreement with the results of ref. [19]. We have also stressed that ε'/ε depends sensitively on $\Lambda_{\overline{\text{MS}}}$.

In the NDR scheme for $B_6^{(1/2)}(m_c) = B_8^{(3/2)}(m_c) = 1$, $m_s(m_c) = 150 \text{ MeV}$, $\Lambda_{\overline{\text{MS}}} = 300 \text{ MeV}$, and $m_t = 130 \text{ GeV}$, we find

$$\varepsilon'/\varepsilon = \begin{cases} (6.7 \pm 2.6) \times 10^{-4} & 0 < \delta \leq \frac{\pi}{2}, \\ (4.8 \pm 2.2) \times 10^{-4} & \frac{\pi}{2} < \delta < \pi, \end{cases} \quad (10.1)$$

in perfect agreement with the E731 result. However, for $B_6^{(1/2)}(m_c) = 2$ and $B_8^{(3/2)}(m_c) = 1$ we find

$$\varepsilon'/\varepsilon = \begin{cases} (20.0 \pm 6.5) \times 10^{-4} & 0 < \delta \leq \frac{\pi}{2}, \\ (14.4 \pm 5.6) \times 10^{-4} & \frac{\pi}{2} < \delta < \pi, \end{cases} \quad (10.2)$$

in agreement with the findings of NA31. The LO results are slightly higher than these values. In the HV scheme somewhat lower values are found.

The fate of theoretical estimates of ε'/ε in the coming years depends crucially on whether it will be possible to reduce the uncertainties in the values of m_t , $\Lambda_{\overline{\text{MS}}}$, m_s , $B_6^{(1/2)}$, $B_8^{(3/2)}$, B_K , $|V_{cb}|$ and $|V_{ub}/V_{cb}|$. If the standard CP violating interactions parametrized by the CKM matrix are the main origin of $\varepsilon' \neq 0$ also the fate of experimental searches for $\varepsilon'/\varepsilon \neq 0$ depends crucially on these parameters. They should pray that the top quark will be found soon or that $B_6 > 1.5$, $m_s(1 \text{ GeV}) < 175 \text{ MeV}$ and $\Lambda_{\overline{\text{MS}}} > 250 \text{ MeV}$.

Acknowledgement

We are grateful to Gerhard Buchalla, Robert Fleischer and Peter Weisz for several stimulating and illuminating discussions. M. J. would like to thank Toni Pich for discussions and A.J. B. would like to thank Guido Martinelli for e-mail discussions.

References

- [1] F. J. GILMAN and M. B. WISE, *Phys. Lett.* **83B** (1979) 83.
- [2] B. GUBERINA and R. D. PECCEI, *Nucl. Phys.* **B163** (1980) 289.
- [3] F. J. GILMAN and J. S. HAGELIN, *Phys. Lett.* **126B** (1983) 111.
- [4] A. J. BURAS and J.-M. GÉRARD, *Phys. Lett.* **203B** (1988) 272.
- [5] J. M. FLYNN and L. RANDALL, *Phys. Lett.* **224B** (1989) 221, Erratum **235B** (1990) 412.
- [6] G. BUCHALLA, A. J. BURAS, and M. K. HARLANDER, *Nucl. Phys.* **B337** (1990) 313.
- [7] E. A. PASCHOS and Y. L. WU, *Mod. Phys. Lett.* **A6** (1991) 93.
- [8] M. LUSIGNOLI, L. MAIANI, G. MARTINELLI, and L. REINA, *Nucl. Phys.* **B369** (1992) 139.
- [9] G. BARR (NA31), talk presented at the XV Int. Symposium on Lepton Photon Interaction, Geneva, July 1991.
- [10] L. K. GIBBONS *et al.*, *EFI preprint*, **EFI 93-06** (1993).
- [11] L. WOLFENSTEIN, *Phys. Rev. Lett.* **13** (1964) 562.
- [12] A. J. BURAS and P. H. WEISZ, *Nucl. Phys.* **B333** (1990) 66.
- [13] A. J. BURAS, M. JAMIN, M. E. LAUTENBACHER, and P. H. WEISZ, *Nucl. Phys.* **B370** (1992) 69; addendum *ibid.* *Nucl. Phys.* **B375** (1992) 501.
- [14] A. J. BURAS, M. JAMIN, M. E. LAUTENBACHER, and P. H. WEISZ, Two-Loop Anomalous Dimension Matrix for $\Delta S = 1$ Weak Non-Leptonic Decays I: $\mathcal{O}(\alpha_s^2)$, *Technical University Munich preprint*, **TUM-T31-18/92**; *Max-Planck-Institut preprint*, **MPI-PAE/PTh 106/92**, to appear in *Nucl. Phys.* **B** .
- [15] A. J. BURAS, M. JAMIN, and M. E. LAUTENBACHER, Two-Loop Anomalous Dimension Matrix for $\Delta S = 1$ Weak Non-Leptonic Decays II: $\mathcal{O}(\alpha \alpha_s)$, *Technical University Munich preprint*, **TUM-T31-30/92**; *Max-Planck-Institut preprint*, **MPI-PAE/PTh 107/92**, to appear in *Nucl. Phys.* **B** .

- [16] G. ALTARELLI, G. CURCI, G. MARTINELLI, and S. PETRARCA, *Nucl. Phys.* **B187** (1981) 461.
- [17] J. FRÖHLICH, J. HEINRICH, E. A. PASCHOS, and J.-M. SCHWARZ, *University of Dortmund preprint*, **DO-TH 02/91** (1991).
- [18] J. HEINRICH, E. A. PASCHOS, J.-M. SCHWARZ, and Y. L. WU, *Phys. Lett.* **B279** (1992) 140.
- [19] M. CIUCHINI, E. FRANCO, G. MARTINELLI, and L. REINA, *Phys. Lett.* **B301** (1993) 263.
- [20] M. K. GAILLARD and B. W. LEE, *Phys. Rev. Lett.* **33** (1974) 108.
- [21] G. ALTARELLI and L. MAIANI, *Phys. Lett.* **52B** (1974) 351.
- [22] A. I. VAINSHTEIN, V. I. ZAKHAROV, and M. A. SHIFMAN, *JEPT* **45** (1977) 670.
- [23] F. J. GILMAN and M. B. WISE, *Phys. Rev.* **D20** (1979) 2392.
- [24] J. BIJNENS and M. B. WISE, *Phys. Lett.* **137 B** (1984) 245.
- [25] A. J. BURAS and J.-M. GÉRARD, *Phys. Lett.* **192B** (1987) 156.
- [26] S. R. SHARPE, *Phys. Lett.* **194B** (1987) 551.
- [27] M. LUSIGNOLI, *Nucl. Phys.* **B325** (1989) 33.
- [28] M. CIUCHINI, E. FRANCO, and R. ONOFRIO, *Mod. Phys. Lett.* **A5** (1990) 2173.
- [29] W. A. BARDEEN, A. J. BURAS, and J.-M. GÉRARD, *Nucl. Phys.* **B293** (1987) 787.
- [30] H.-Y. CHENG, *Phys. Rev.* **D37** (1988) 1908.
- [31] G. ALTARELLI, *CERN preprint* **CERN-TH 6623/92** (1992).
- [32] A. J. BURAS, M. JAMIN, and P. H. WEISZ, *Nucl. Phys.* **B347** (1990) 491.
- [33] W. A. BARDEEN, A. J. BURAS, and J.-M. GÉRARD, *Phys. Lett.* **192B** (1987) 138.
- [34] A. PICH and E. DE RAFAEL, *Nucl. Phys.* **B358** (1991) 311.
- [35] J. KAMBOR, J. MISSIMER, and D. WYLER, *Phys. Lett.* **261B** (1991) 496.
- [36] W. A. BARDEEN, A. J. BURAS, and J.-M. GÉRARD, *Phys. Lett.* **180B** (1986) 133.

- [37] M. BAUER and B. STECH, *Phys. Lett.* **152B** (1985) 380.
- [38] A. J. BURAS, J.-M. GÉRARD, and R. RÜCKL, *Phys. Lett.* **B268** (1986) 16.
- [39] R. S. CHIVUKULA, J. M. FLYNN, and H. GEORGI, *Phys. Lett.* **171B** (1986) 453.
- [40] J.-M. GÉRARD, *proceedings of the XXIV. International Conference on High Energy Physics, Munich, 1988, editors R. Kotthaus and J. H. Kühn, page 840* .
- [41] S. R. SHARPE, *Nucl. Phys. B (Proc. Suppl.)* **17** (1990) 146.
- [42] C. BERNARD *et al.*, *Nucl. Phys. (Proc. Suppl.)* **17** (1990) 495.
- [43] M. B. GAVELA *et al.*, *Nucl. Phys.* **B306** (1988) 677.
- [44] G. W. KILCUP *et al.*, *Phys. Rev. Lett.* **64** (1990) 25.
- [45] G. W. KILCUP, *Nucl. Phys. B (Proc. Suppl.)* **20** (1991) 417.
- [46] S. R. SHARPE, *Nucl. Phys. B (Proc. Suppl.)* **20** (1991) 429.
- [47] G. MARTINELLI, *Phys. Lett.* **B141** (1984) 395.
- [48] C. BERNARD, A. SONI, and T. DRAPER, *Phys. Rev.* **D36** (1987) 3224.
- [49] M. F. L. GLOTERMAN and J. SMIT, *Nucl. Phys.* **B245** (1984) 61.
- [50] D. DANIEL and S. SHEARD, *Nucl. Phys.* **B302** (1988) 471.
- [51] S. SHEARD, *Nucl. Phys.* **B314** (1989) 238.
- [52] G. CURCI, E. FRANCO, L. MAIANI, and G. MARTINELLI, *Phys. Lett.* **B 202** (1988) 363.
- [53] PARTICLE DATA GROUP, Review of Particle Properties, *Phys. Rev.* **D45** (1992).
- [54] Y. L. WU, *Int. J. Mod. Phys.* **A7** (1992) 2863.
- [55] M. JAMIN and M. MÜNZ, *in preparation* .
- [56] A. J. BURAS and M. K. HARLANDER, A Top Quark Story, in *Heavy Flavours*, eds. A.J. Buras and M. Lindner, World Scientific (1992) , page 58.
- [57] J. F. DONOGHUE, E. GOLOWICH, B. R. HOLSTEIN, and J. TRAMPETIC, *Phys. Lett.* **179B** (1986) 361.

- [58] R. GUPTA, G. W. KILCUP, and S. R. SHARPE, *Nucl. Phys. B (Proc. Suppl.)* **26** (1992) 197.
- [59] B. GRINSTEIN, *Phys. Lett.* **229B** (1989) 280.
- [60] G. KRAMER and W. F. PALMER, *Phys. Rev.* **D45** (1992) 193.

Appendices

A Quark Threshold Matching Matrices

The matrix $\delta\hat{r}_s$ in (4.36) has the following non-vanishing rows.

$\mu = m_b$:

$$\delta\hat{r}_s(Q_4) = \delta\hat{r}_s(Q_6) = -2 \delta\hat{r}_s(Q_8) = -2 \delta\hat{r}_s(Q_{10}) = -\frac{5}{9} P \quad (\text{A.1})$$

$\mu = m_c$:

$$\delta\hat{r}_s(Q_4) = \delta\hat{r}_s(Q_6) = \delta\hat{r}_s(Q_8) = \delta\hat{r}_s(Q_{10}) = -\frac{5}{9} P \quad (\text{A.2})$$

where

$$P = (0, 0, -\frac{1}{3}, 1, -\frac{1}{3}, 1, 0, 0, 0, 0). \quad (\text{A.3})$$

The matrix $\delta\hat{r}_e$ has the following non-vanishing rows.

$\mu = m_b$:

$$\delta\hat{r}_e(Q_3) = 3 \delta\hat{r}_e(Q_4) = \delta\hat{r}_e(Q_5) = 3 \delta\hat{r}_e(Q_6) = \frac{20}{27} \bar{P} \quad (\text{A.4})$$

$$\delta\hat{r}_e(Q_7) = 3 \delta\hat{r}_e(Q_8) = \delta\hat{r}_e(Q_9) = 3 \delta\hat{r}_e(Q_{10}) = -\frac{10}{27} \bar{P} \quad (\text{A.5})$$

$\mu = m_c$:

$$\delta\hat{r}_e(Q_3) = \delta\hat{r}_e(Q_5) = \delta\hat{r}_e(Q_7) = \delta\hat{r}_e(Q_9) = -\frac{40}{27} \bar{P} \quad (\text{A.6})$$

$$\delta\hat{r}_e(Q_4) = \delta\hat{r}_e(Q_6) = \delta\hat{r}_e(Q_8) = \delta\hat{r}_e(Q_{10}) = -\frac{40}{81} \bar{P} \quad (\text{A.7})$$

where

$$P = (0, 0, 0, 0, 0, 0, 1, 0, 1, 0). \quad (\text{A.8})$$

B Numerical Results for Wilson Coefficients, ε'/ε and B_i -Expansion

Table 1: $\Delta S = 1$ Wilson coefficients at $\mu = 1$ GeV for $m_t = 130$ GeV. In our approach $y_1 = y_2 \equiv 0$ holds.

Scheme	$\Lambda_{\overline{\text{MS}}} = 0.2$ GeV			$\Lambda_{\overline{\text{MS}}} = 0.3$ GeV			$\Lambda_{\overline{\text{MS}}} = 0.4$ GeV		
	LO	NDR	HV	LO	NDR	HV	LO	NDR	HV
z_1	-0.587	-0.397	-0.477	-0.715	-0.486	-0.606	-0.854	-0.588	-0.774
z_2	1.319	1.204	1.256	1.409	1.262	1.345	1.511	1.333	1.472
z_3	0.004	0.008	0.004	0.005	0.013	0.008	0.007	0.021	0.015
z_4	-0.010	-0.023	-0.011	-0.014	-0.035	-0.018	-0.018	-0.054	-0.030
z_5	0.003	0.006	0.003	0.004	0.007	0.004	0.006	0.009	0.006
z_6	-0.011	-0.023	-0.010	-0.015	-0.035	-0.016	-0.020	-0.056	-0.026
z_7/α	0.005	0.000	-0.005	0.008	0.008	-0.003	0.012	0.017	-0.002
z_8/α	0.001	0.009	0.007	0.001	0.016	0.011	0.002	0.028	0.018
z_9/α	0.005	0.005	-0.001	0.009	0.016	0.004	0.013	0.030	0.010
z_{10}/α	-0.001	-0.006	-0.007	-0.001	-0.009	-0.011	-0.001	-0.015	-0.017
z_-	1.907	1.600	1.733	2.123	1.748	1.951	2.365	1.921	2.245
z_+	0.732	0.807	0.779	0.694	0.776	0.740	0.657	0.746	0.698
z_-/z_+	2.604	1.982	2.226	3.060	2.252	2.638	3.597	2.576	3.217
y_3	0.027	0.022	0.025	0.034	0.029	0.033	0.042	0.036	0.043
y_4	-0.048	-0.044	-0.046	-0.056	-0.052	-0.055	-0.064	-0.060	-0.065
y_5	0.011	0.005	0.013	0.012	0.001	0.015	0.013	-0.008	0.018
y_6	-0.078	-0.071	-0.065	-0.102	-0.099	-0.087	-0.130	-0.142	-0.118
y_7/α	-0.025	-0.083	-0.082	-0.017	-0.080	-0.079	-0.009	-0.078	-0.076
y_8/α	0.053	0.069	0.081	0.074	0.095	0.110	0.101	0.133	0.154
y_9/α	-1.160	-1.161	-1.161	-1.222	-1.225	-1.226	-1.297	-1.314	-1.318
y_{10}/α	0.488	0.400	0.407	0.592	0.502	0.512	0.706	0.634	0.647

Table 2: $\Delta S = 1$ Wilson coefficients at $\mu = 1.4$ GeV for $m_t = 130$ GeV. In our approach $y_1 = y_2 \equiv 0$ holds.

Scheme	$\Lambda_{\overline{\text{MS}}} = 0.2$ GeV			$\Lambda_{\overline{\text{MS}}} = 0.3$ GeV			$\Lambda_{\overline{\text{MS}}} = 0.4$ GeV		
	LO	NDR	HV	LO	NDR	HV	LO	NDR	HV
z_1	-0.486	-0.321	-0.383	-0.573	-0.379	-0.459	-0.660	-0.438	-0.543
z_2	1.252	1.158	1.195	1.310	1.193	1.244	1.369	1.231	1.301
z_-	1.738	1.479	1.578	1.883	1.571	1.704	2.030	1.669	1.844
z_+	0.766	0.836	0.812	0.736	0.814	0.785	0.709	0.793	0.758
z_-/z_+	2.269	1.769	1.943	2.558	1.930	2.170	2.862	2.105	2.432

y_3	0.024	0.020	0.022	0.029	0.025	0.028	0.035	0.030	0.035
y_4	-0.047	-0.044	-0.045	-0.055	-0.052	-0.054	-0.063	-0.060	-0.063
y_5	0.013	0.007	0.013	0.014	0.006	0.015	0.015	0.004	0.017
y_6	-0.068	-0.061	-0.056	-0.085	-0.077	-0.070	-0.102	-0.097	-0.087
y_7/α	-0.023	-0.082	-0.081	-0.014	-0.080	-0.079	-0.006	-0.078	-0.076
y_8/α	0.041	0.059	0.067	0.054	0.076	0.085	0.068	0.097	0.106
y_9/α	-1.103	-1.110	-1.110	-1.139	-1.144	-1.143	-1.179	-1.182	-1.182
y_{10}/α	0.403	0.320	0.325	0.474	0.379	0.385	0.545	0.443	0.450

Table 3: $\Delta S = 1$ Wilson coefficients at $\mu = 2$ GeV for $m_t = 130$ GeV. In our approach $y_1 = y_2 \equiv 0$ holds.

Scheme	$\Lambda_{\overline{\text{MS}}} = 0.2$ GeV			$\Lambda_{\overline{\text{MS}}} = 0.3$ GeV			$\Lambda_{\overline{\text{MS}}} = 0.4$ GeV		
	LO	NDR	HV	LO	NDR	HV	LO	NDR	HV
z_1	-0.403	-0.261	-0.311	-0.465	-0.300	-0.362	-0.523	-0.338	-0.413
z_2	1.200	1.123	1.152	1.238	1.145	1.182	1.276	1.168	1.214
z_-	1.603	1.384	1.463	1.703	1.445	1.545	1.798	1.505	1.627
z_+	0.797	0.862	0.840	0.773	0.845	0.820	0.752	0.830	0.801
z_-/z_+	2.010	1.606	1.741	2.202	1.710	1.884	2.390	1.814	2.030

y_3	0.019	0.019	0.018	0.023	0.022	0.021	0.026	0.026	0.025
y_4	-0.039	-0.045	-0.038	-0.045	-0.052	-0.044	-0.050	-0.060	-0.050
y_5	0.011	0.010	0.011	0.012	0.010	0.013	0.013	0.011	0.014
y_6	-0.053	-0.056	-0.045	-0.064	-0.067	-0.054	-0.074	-0.080	-0.063
y_7/α	-0.023	-0.077	-0.073	-0.016	-0.073	-0.072	-0.010	-0.069	-0.071
y_8/α	0.032	0.047	0.054	0.040	0.057	0.065	0.048	0.068	0.076
y_9/α	-1.060	-1.073	-1.070	-1.084	-1.092	-1.091	-1.108	-1.111	-1.114
y_{10}/α	0.333	0.264	0.268	0.384	0.304	0.309	0.432	0.344	0.349

Table 4: $\Delta S = 1$ Wilson coefficient y_7/α at $\mu = 1$ GeV for various m_t values.

m_t [GeV]	$\Lambda_{\overline{\text{MS}}} = 0.2$ GeV			$\Lambda_{\overline{\text{MS}}} = 0.3$ GeV			$\Lambda_{\overline{\text{MS}}} = 0.4$ GeV		
	LO	NDR	HV	LO	NDR	HV	LO	NDR	HV
110	-0.045	-0.102	-0.102	-0.036	-0.100	-0.099	-0.028	-0.097	-0.094
130	-0.025	-0.083	-0.082	-0.017	-0.080	-0.079	-0.009	-0.078	-0.076
150	-0.002	-0.058	-0.058	0.006	-0.057	-0.056	0.014	-0.056	-0.053
170	0.025	-0.031	-0.031	0.033	-0.030	-0.029	0.039	-0.030	-0.027
190	0.056	-0.000	-0.000	0.062	-0.000	0.001	0.068	-0.001	0.002

Table 5: $\Delta S = 1$ Wilson coefficient y_8/α at $\mu = 1$ GeV for various m_t values.

m_t [GeV]	$\Lambda_{\overline{\text{MS}}} = 0.2$ GeV			$\Lambda_{\overline{\text{MS}}} = 0.3$ GeV			$\Lambda_{\overline{\text{MS}}} = 0.4$ GeV		
	LO	NDR	HV	LO	NDR	HV	LO	NDR	HV
110	0.031	0.050	0.062	0.045	0.070	0.085	0.062	0.098	0.119
130	0.053	0.069	0.081	0.074	0.095	0.110	0.101	0.133	0.154
150	0.079	0.090	0.102	0.109	0.124	0.140	0.145	0.174	0.195
170	0.109	0.115	0.126	0.148	0.158	0.173	0.196	0.221	0.242
190	0.142	0.142	0.153	0.191	0.195	0.210	0.252	0.273	0.293

Table 6: $\Delta S = 1$ Wilson coefficient sum $(y_9 + y_{10})/\alpha$ at $\mu = 1$ GeV for various m_t values.

m_t [GeV]	$\Lambda_{\overline{\text{MS}}} = 0.2$ GeV			$\Lambda_{\overline{\text{MS}}} = 0.3$ GeV			$\Lambda_{\overline{\text{MS}}} = 0.4$ GeV		
	LO	NDR	HV	LO	NDR	HV	LO	NDR	HV
110	-0.567	-0.652	-0.646	-0.531	-0.620	-0.613	-0.497	-0.585	-0.576
130	-0.672	-0.760	-0.754	-0.630	-0.722	-0.715	-0.591	-0.680	-0.671
150	-0.779	-0.872	-0.866	-0.732	-0.828	-0.820	-0.688	-0.779	-0.770
170	-0.891	-0.987	-0.981	-0.838	-0.937	-0.929	-0.788	-0.881	-0.872
190	-1.008	-1.108	-1.102	-0.948	-1.051	-1.043	-0.893	-0.988	-0.978

Table 7: $\Delta S = 1$ Wilson coefficient y_7/α at $\mu = 1.4$ GeV for various m_t values.

m_t [GeV]	$\Lambda_{\overline{\text{MS}}} = 0.2$ GeV			$\Lambda_{\overline{\text{MS}}} = 0.3$ GeV			$\Lambda_{\overline{\text{MS}}} = 0.4$ GeV		
	LO	NDR	HV	LO	NDR	HV	LO	NDR	HV
110	-0.043	-0.102	-0.102	-0.034	-0.100	-0.099	-0.025	-0.098	-0.096
130	-0.023	-0.082	-0.081	-0.014	-0.080	-0.079	-0.006	-0.078	-0.076
150	0.001	-0.057	-0.057	0.010	-0.056	-0.054	0.018	-0.054	-0.052
170	0.029	-0.029	-0.029	0.037	-0.028	-0.027	0.044	-0.027	-0.025
190	0.060	0.002	0.003	0.067	0.003	0.004	0.074	0.003	0.005

Table 8: $\Delta S = 1$ Wilson coefficient y_8/α at $\mu = 1.4$ GeV for various m_t values.

m_t [GeV]	$\Lambda_{\overline{\text{MS}}} = 0.2$ GeV			$\Lambda_{\overline{\text{MS}}} = 0.3$ GeV			$\Lambda_{\overline{\text{MS}}} = 0.4$ GeV		
	LO	NDR	HV	LO	NDR	HV	LO	NDR	HV
110	0.024	0.045	0.053	0.032	0.059	0.068	0.042	0.075	0.085
130	0.041	0.059	0.067	0.054	0.076	0.085	0.068	0.097	0.106
150	0.061	0.075	0.084	0.079	0.097	0.106	0.099	0.122	0.132
170	0.084	0.094	0.102	0.107	0.120	0.129	0.133	0.151	0.161
190	0.109	0.115	0.123	0.139	0.146	0.155	0.172	0.183	0.193

Table 9: $\Delta S = 1$ Wilson coefficient sum $(y_9 + y_{10})/\alpha$ at $\mu = 1.4$ GeV for various m_t values.

m_t [GeV]	$\Lambda_{\overline{\text{MS}}} = 0.2$ GeV			$\Lambda_{\overline{\text{MS}}} = 0.3$ GeV			$\Lambda_{\overline{\text{MS}}} = 0.4$ GeV		
	LO	NDR	HV	LO	NDR	HV	LO	NDR	HV
110	-0.591	-0.677	-0.672	-0.560	-0.655	-0.649	-0.532	-0.634	-0.627
130	-0.700	-0.791	-0.785	-0.665	-0.764	-0.758	-0.633	-0.739	-0.732
150	-0.812	-0.907	-0.902	-0.773	-0.877	-0.871	-0.738	-0.847	-0.840
170	-0.929	-1.028	-1.023	-0.886	-0.993	-0.987	-0.846	-0.959	-0.952
190	-1.052	-1.155	-1.149	-1.003	-1.115	-1.109	-0.959	-1.076	-1.069

Table 10: $\Delta S = 1$ Wilson coefficient y_7/α at $\mu = 2$ GeV for various m_t values.

m_t [GeV]	$\Lambda_{\overline{\text{MS}}} = 0.2$ GeV			$\Lambda_{\overline{\text{MS}}} = 0.3$ GeV			$\Lambda_{\overline{\text{MS}}} = 0.4$ GeV		
	LO	NDR	HV	LO	NDR	HV	LO	NDR	HV
110	-0.043	-0.098	-0.094	-0.036	-0.093	-0.093	-0.030	-0.089	-0.091
130	-0.023	-0.077	-0.073	-0.016	-0.073	-0.072	-0.010	-0.069	-0.071
150	0.002	-0.051	-0.048	0.008	-0.048	-0.047	0.014	-0.044	-0.046
170	0.030	-0.023	-0.020	0.036	-0.020	-0.019	0.041	-0.017	-0.018
190	0.062	0.009	0.013	0.067	0.012	0.013	0.072	0.015	0.013

Table 11: $\Delta S = 1$ Wilson coefficient y_8/α at $\mu = 2$ GeV for various m_t values.

m_t [GeV]	$\Lambda_{\overline{\text{MS}}} = 0.2$ GeV			$\Lambda_{\overline{\text{MS}}} = 0.3$ GeV			$\Lambda_{\overline{\text{MS}}} = 0.4$ GeV		
	LO	NDR	HV	LO	NDR	HV	LO	NDR	HV
110	0.019	0.036	0.043	0.024	0.044	0.052	0.029	0.052	0.061
130	0.032	0.047	0.054	0.040	0.057	0.065	0.048	0.068	0.076
150	0.048	0.059	0.067	0.059	0.072	0.080	0.070	0.086	0.095
170	0.066	0.074	0.081	0.081	0.090	0.098	0.096	0.106	0.115
190	0.086	0.090	0.098	0.104	0.109	0.117	0.124	0.129	0.138

Table 12: $\Delta S = 1$ Wilson coefficient sum $(y_9 + y_{10})/\alpha$ at $\mu = 2$ GeV for various m_t values.

m_t [GeV]	$\Lambda_{\overline{\text{MS}}} = 0.2$ GeV			$\Lambda_{\overline{\text{MS}}} = 0.3$ GeV			$\Lambda_{\overline{\text{MS}}} = 0.4$ GeV		
	LO	NDR	HV	LO	NDR	HV	LO	NDR	HV
110	-0.613	-0.693	-0.685	-0.589	-0.674	-0.669	-0.569	-0.656	-0.653
130	-0.727	-0.810	-0.802	-0.700	-0.788	-0.782	-0.676	-0.767	-0.764
150	-0.844	-0.931	-0.923	-0.814	-0.905	-0.900	-0.787	-0.882	-0.879
170	-0.966	-1.056	-1.048	-0.932	-1.028	-1.022	-0.902	-1.001	-0.998
190	-1.093	-1.187	-1.179	-1.055	-1.155	-1.150	-1.022	-1.125	-1.123

Table 13: $\Delta S = 1$ Wilson coefficient ratio $\frac{-(y_7/3+y_8)/\alpha}{y_6}$ at $\mu = 1.4$ GeV for various m_t values.

m_t [GeV]	$\Lambda_{\overline{\text{MS}}} = 0.2$ GeV			$\Lambda_{\overline{\text{MS}}} = 0.3$ GeV			$\Lambda_{\overline{\text{MS}}} = 0.4$ GeV		
	LO	NDR	HV	LO	NDR	HV	LO	NDR	HV
110	0.144	0.183	0.349	0.252	0.331	0.499	0.330	0.443	0.615
130	0.492	0.525	0.714	0.582	0.644	0.838	0.646	0.730	0.935
150	0.898	0.923	1.138	0.964	1.007	1.233	1.013	1.066	1.308
170	1.352	1.370	1.619	1.395	1.418	1.680	1.426	1.445	1.729
190	1.855	1.867	2.146	1.870	1.871	2.173	1.883	1.864	2.195

Table 14: Coefficients in the expansion of $P^{(1/2)}$.

$\Lambda_{\overline{\text{MS}}}$	m_t [GeV]	LO			NDR			HV			
		$a_0^{(1/2)}$	$a_2^{(1/2)}$	$a_6^{(1/2)}$	$a_0^{(1/2)}$	$a_2^{(1/2)}$	$a_6^{(1/2)}$	$a_0^{(1/2)}$	$a_2^{(1/2)}$	$a_6^{(1/2)}$	
	110	-6.49	0.48	9.84	-7.66	0.57	8.97	-7.59	0.60	8.03	
	130	-6.18	0.45	9.97	-7.29	0.53	9.07	-7.22	0.56	8.13	
	200	150	-5.84	0.41	10.07	-6.89	0.49	9.15	-6.82	0.52	8.20
		170	-5.46	0.38	10.15	-6.45	0.45	9.21	-6.38	0.48	8.26
		190	-5.05	0.34	10.21	-5.97	0.41	9.26	-5.90	0.43	8.32
	110	-6.62	0.47	12.29	-7.94	0.57	11.56	-7.84	0.61	10.07	
	130	-6.33	0.44	12.44	-7.61	0.54	11.68	-7.51	0.57	10.19	
	300	150	-6.00	0.42	12.56	-7.24	0.51	11.77	-7.14	0.54	10.28
		170	-5.65	0.39	12.66	-6.84	0.47	11.85	-6.74	0.50	10.36
		190	-5.26	0.35	12.74	-6.41	0.43	11.91	-6.31	0.46	10.42
	110	-6.68	0.46	14.94	-8.13	0.57	14.78	-8.00	0.60	12.49	
	130	-6.40	0.44	15.13	-7.82	0.54	14.92	-7.69	0.57	12.64	
	400	150	-6.08	0.41	15.27	-7.48	0.51	15.03	-7.35	0.54	12.75
		170	-5.73	0.39	15.39	-7.10	0.48	15.12	-6.97	0.51	12.84
		190	-5.35	0.36	15.48	-6.70	0.45	15.19	-6.57	0.48	12.91

Table 15: Coefficients in the expansion of $P^{(3/2)}$.

$\Lambda_{\overline{\text{MS}}}$	m_t [GeV]	LO		NDR		HV	
		$a_0^{(3/2)}$	$a_8^{(3/2)}$	$a_0^{(3/2)}$	$a_8^{(3/2)}$	$a_0^{(3/2)}$	$a_8^{(3/2)}$
	110	-1.01	0.66	-1.04	0.87	-1.08	1.35
	130	-1.19	1.97	-1.22	2.01	-1.26	2.49
200	150	-1.38	3.52	-1.41	3.36	-1.45	3.84
	170	-1.58	5.28	-1.60	4.89	-1.64	5.37
	190	-1.79	7.24	-1.80	6.59	-1.84	7.07
	110	-0.99	1.29	-1.03	1.68	-1.08	2.22
	130	-1.18	2.84	-1.21	3.02	-1.26	3.55
300	150	-1.37	4.67	-1.40	4.59	-1.45	5.13
	170	-1.57	6.76	-1.59	6.38	-1.64	6.92
	190	-1.78	9.07	-1.79	8.37	-1.84	8.91
	110	-0.98	1.96	-1.02	2.66	-1.08	3.24
	130	-1.16	3.78	-1.20	4.23	-1.26	4.81
400	150	-1.36	5.92	-1.39	6.07	-1.44	6.66
	170	-1.56	8.36	-1.58	8.17	-1.64	8.75
	190	-1.76	11.06	-1.78	10.50	-1.84	11.09

Table 16: ε'/ε in units of 10^{-4} for $B_6^{(1/2)} = 1.0$ and $B_8^{(3/2)} = 1.0$.

$\Lambda_{\overline{\text{MS}}}$	m_t	LO		NDR		HV	
		1. Quad.	2. Quad.	1. Quad.	2. Quad.	1. Quad.	2. Quad.
	130	6.4 ± 2.4	4.6 ± 2.0	5.2 ± 2.2	3.7 ± 1.8	3.7 ± 1.7	2.6 ± 1.4
200	150	4.6 ± 1.9	3.2 ± 1.6	3.7 ± 1.7	2.6 ± 1.4	2.4 ± 1.3	1.6 ± 1.0
	170	3.0 ± 1.3	2.0 ± 1.1	2.3 ± 1.2	1.6 ± 1.0	1.1 ± 0.8	0.8 ± 0.6
	130	8.0 ± 2.9	5.8 ± 2.5	6.7 ± 2.6	4.8 ± 2.2	4.6 ± 2.0	3.3 ± 1.6
300	150	5.8 ± 2.2	4.1 ± 1.9	4.9 ± 2.0	3.4 ± 1.7	2.9 ± 1.5	2.0 ± 1.2
	170	3.8 ± 1.6	2.6 ± 1.4	3.1 ± 1.5	2.1 ± 1.2	1.4 ± 0.9	1.0 ± 0.7
	130	9.9 ± 3.4	7.1 ± 2.9	8.8 ± 3.2	6.3 ± 2.7	5.7 ± 2.3	4.1 ± 1.9
400	150	7.2 ± 2.7	5.0 ± 2.3	6.5 ± 2.5	4.5 ± 2.2	3.7 ± 1.7	2.6 ± 1.4
	170	4.7 ± 1.9	3.2 ± 1.6	4.3 ± 1.9	3.0 ± 1.6	1.8 ± 1.1	1.3 ± 0.9

Table 17: ε'/ε in units of 10^{-4} for $B_6^{(1/2)} = 1.5$ and $B_8^{(3/2)} = 1.5$.

$\Lambda_{\overline{\text{MS}}}$	m_t	LO		NDR		HV	
		1. Quad.	2. Quad.	1. Quad.	2. Quad.	1. Quad.	2. Quad.
	130	10.9 ± 3.8	7.9 ± 3.2	9.2 ± 3.3	6.6 ± 2.8	6.9 ± 2.7	5.0 ± 2.2
200	150	8.0 ± 2.9	5.6 ± 2.5	6.6 ± 2.6	4.6 ± 2.2	4.6 ± 1.9	3.2 ± 1.6
	170	5.2 ± 2.1	3.6 ± 1.8	4.3 ± 1.8	2.9 ± 1.6	2.5 ± 1.2	1.7 ± 1.0
	130	13.5 ± 4.5	9.7 ± 3.9	11.6 ± 4.1	8.3 ± 3.4	8.3 ± 3.1	6.0 ± 2.6
300	150	9.9 ± 3.5	6.9 ± 3.0	8.5 ± 3.2	5.9 ± 2.7	5.6 ± 2.3	3.9 ± 1.9
	170	6.5 ± 2.5	4.5 ± 2.2	5.6 ± 2.3	3.8 ± 2.0	3.0 ± 1.4	2.0 ± 1.2
	130	16.3 ± 5.4	11.8 ± 4.6	14.8 ± 5.0	10.6 ± 4.3	10.2 ± 3.7	7.3 ± 3.1
400	150	12.0 ± 4.1	8.4 ± 3.6	11.0 ± 3.9	7.7 ± 3.4	6.9 ± 2.7	4.8 ± 2.3
	170	8.0 ± 3.0	5.5 ± 2.6	7.5 ± 2.9	5.1 ± 2.5	3.7 ± 1.7	2.5 ± 1.4

Table 18: ε'/ε in units of 10^{-4} for $B_6^{(1/2)} = 0.75$ and $B_8^{(3/2)} = 0.75$.

		LO		NDR		HV	
$\Lambda_{\overline{\text{MS}}}$	m_t	1. Quad.	2. Quad.	1. Quad.	2. Quad.	1. Quad.	2. Quad.
	130	4.1 ± 1.8	3.0 ± 1.4	3.2 ± 1.6	2.3 ± 1.3	2.1 ± 1.3	1.5 ± 1.0
200	150	2.9 ± 1.4	2.0 ± 1.1	2.2 ± 1.2	1.6 ± 1.0	1.2 ± 0.9	0.9 ± 0.7
	170	1.8 ± 1.0	1.2 ± 0.8	1.3 ± 0.9	0.9 ± 0.7	0.4 ± 0.6	0.3 ± 0.4
	130	5.3 ± 2.1	3.8 ± 1.7	4.3 ± 1.9	3.1 ± 1.6	2.7 ± 1.4	1.9 ± 1.2
300	150	3.8 ± 1.6	2.6 ± 1.4	3.1 ± 1.5	2.1 ± 1.2	1.6 ± 1.0	1.1 ± 0.8
	170	2.4 ± 1.2	1.6 ± 1.0	1.9 ± 1.1	1.3 ± 0.9	0.6 ± 0.7	0.4 ± 0.5
	130	6.6 ± 2.5	4.8 ± 2.1	5.8 ± 2.4	4.2 ± 2.0	3.5 ± 1.7	2.5 ± 1.4
400	150	4.8 ± 1.9	3.4 ± 1.6	4.2 ± 1.9	2.9 ± 1.5	2.2 ± 1.2	1.5 ± 1.0
	170	3.1 ± 1.4	2.1 ± 1.2	2.8 ± 1.4	1.9 ± 1.1	0.9 ± 0.8	0.6 ± 0.6

Table 19: ε'/ε in units of 10^{-4} for $B_6^{(1/2)} = 1.25$ and $B_8^{(3/2)} = 0.75$.

		LO		NDR		HV	
$\Lambda_{\overline{\text{MS}}}$	m_t	1. Quad.	2. Quad.	1. Quad.	2. Quad.	1. Quad.	2. Quad.
	130	9.8 ± 3.4	7.0 ± 2.9	8.3 ± 3.1	6.0 ± 2.6	6.7 ± 2.6	4.8 ± 2.2
200	150	8.1 ± 2.9	5.6 ± 2.5	6.9 ± 2.7	4.8 ± 2.3	5.4 ± 2.2	3.8 ± 1.9
	170	6.6 ± 2.5	4.5 ± 2.2	5.6 ± 2.3	3.8 ± 1.9	4.3 ± 1.8	2.9 ± 1.5
	130	12.4 ± 4.2	8.9 ± 3.6	10.9 ± 3.9	7.8 ± 3.3	8.5 ± 3.2	6.1 ± 2.7
300	150	10.3 ± 3.6	7.1 ± 3.1	9.1 ± 3.3	6.3 ± 2.9	6.9 ± 2.7	4.8 ± 2.3
	170	8.3 ± 3.1	5.7 ± 2.7	7.4 ± 2.9	5.0 ± 2.5	5.4 ± 2.2	3.7 ± 1.9
	130	15.3 ± 5.0	11.0 ± 4.3	14.2 ± 4.9	10.2 ± 4.1	10.7 ± 3.8	7.7 ± 3.2
400	150	12.7 ± 4.3	8.8 ± 3.8	11.9 ± 4.2	8.3 ± 3.7	8.7 ± 3.2	6.1 ± 2.8
	170	10.3 ± 3.7	7.0 ± 3.2	9.8 ± 3.6	6.6 ± 3.2	6.9 ± 2.7	4.7 ± 2.3

Table 20: ε'/ε in units of 10^{-4} for $B_6^{(1/2)} = 1.5$ and $B_8^{(3/2)} = 1.0$.

$\Lambda_{\overline{\text{MS}}}$	m_t	LO		NDR		HV	
		1. Quad.	2. Quad.	1. Quad.	2. Quad.	1. Quad.	2. Quad.
	130	12.1 ± 4.1	8.7 ± 3.5	10.3 ± 3.7	7.4 ± 3.1	8.3 ± 3.1	6.0 ± 2.6
200	150	9.8 ± 3.5	6.8 ± 3.0	8.4 ± 3.1	5.8 ± 2.7	6.6 ± 2.6	4.6 ± 2.2
	170	7.7 ± 2.9	5.2 ± 2.5	6.6 ± 2.6	4.5 ± 2.2	5.0 ± 2.1	3.4 ± 1.7
	130	15.1 ± 5.0	10.9 ± 4.3	13.3 ± 4.6	9.6 ± 3.9	10.4 ± 3.7	7.5 ± 3.1
300	150	12.3 ± 4.2	8.6 ± 3.7	10.9 ± 3.9	7.6 ± 3.4	8.2 ± 3.1	5.7 ± 2.6
	170	9.7 ± 3.5	6.6 ± 3.1	8.6 ± 3.3	5.9 ± 2.8	6.2 ± 2.5	4.2 ± 2.1
	130	18.5 ± 6.0	13.3 ± 5.1	17.2 ± 5.7	12.4 ± 4.9	12.9 ± 4.5	9.3 ± 3.8
400	150	15.1 ± 5.1	10.5 ± 4.5	14.2 ± 4.9	9.9 ± 4.3	10.3 ± 3.7	7.2 ± 3.2
	170	11.9 ± 4.3	8.1 ± 3.7	11.3 ± 4.2	7.7 ± 3.6	7.8 ± 3.0	5.3 ± 2.6

Table 21: ε'/ε in units of 10^{-4} for $B_6^{(1/2)} = 2.0$ and $B_8^{(3/2)} = 1.0$.

$\Lambda_{\overline{\text{MS}}}$	m_t	LO		NDR		HV	
		1. Quad.	2. Quad.	1. Quad.	2. Quad.	1. Quad.	2. Quad.
	130	17.8 ± 5.8	12.8 ± 5.0	15.5 ± 5.2	11.1 ± 4.4	12.9 ± 4.5	9.3 ± 3.8
200	150	15.0 ± 5.0	10.4 ± 4.4	13.1 ± 4.5	9.1 ± 4.0	10.8 ± 3.8	7.5 ± 3.3
	170	12.4 ± 4.4	8.5 ± 3.9	10.9 ± 4.0	7.4 ± 3.5	8.8 ± 3.3	6.0 ± 2.9
	130	22.2 ± 7.1	16.0 ± 6.1	20.0 ± 6.5	14.4 ± 5.6	16.2 ± 5.4	11.6 ± 4.6
300	150	18.8 ± 6.2	13.1 ± 5.5	16.9 ± 5.7	11.8 ± 5.0	13.5 ± 4.7	9.4 ± 4.1
	170	15.6 ± 5.4	10.6 ± 4.8	14.1 ± 5.1	9.6 ± 4.4	11.1 ± 4.1	7.5 ± 3.5
	130	27.1 ± 8.5	19.5 ± 7.4	25.7 ± 8.2	18.5 ± 7.1	20.1 ± 6.6	14.5 ± 5.6
400	150	22.9 ± 7.5	16.0 ± 6.6	21.8 ± 7.2	15.2 ± 6.4	16.8 ± 5.7	11.7 ± 5.0
	170	19.1 ± 6.6	13.0 ± 5.8	18.3 ± 6.4	12.5 ± 5.6	13.8 ± 5.0	9.4 ± 4.3

Table 22: $\Delta B = 1$ Wilson coefficients at $\mu = m_b$ for $m_t = 130$ GeV.

Scheme	$\Lambda_{\overline{\text{MS}}} = 0.2$ GeV			$\Lambda_{\overline{\text{MS}}} = 0.3$ GeV			$\Lambda_{\overline{\text{MS}}} = 0.4$ GeV		
	LO	NDR	HV	LO	NDR	HV	LO	NDR	HV
z_1	-0.255	-0.152	-0.187	-0.286	-0.170	-0.210	-0.312	-0.185	-0.230
z_2	1.115	1.066	1.083	1.131	1.075	1.095	1.146	1.082	1.106
y_3	0.011	0.011	0.010	0.012	0.013	0.011	0.014	0.014	0.013
y_4	-0.025	-0.029	-0.024	-0.028	-0.033	-0.027	-0.030	-0.036	-0.029
y_5	0.007	0.008	0.008	0.008	0.008	0.008	0.009	0.009	0.009
y_6	-0.030	-0.033	-0.026	-0.034	-0.037	-0.030	-0.038	-0.041	-0.033
y_7/α	-0.011	-0.056	-0.045	-0.008	-0.054	-0.046	-0.006	-0.053	-0.046
y_8/α	0.019	0.028	0.033	0.022	0.032	0.037	0.025	0.035	0.041
y_9/α	-0.981	-1.003	-0.992	-0.991	-1.010	-1.001	-1.000	-1.017	-1.009
y_{10}/α	0.210	0.166	0.169	0.235	0.185	0.188	0.256	0.201	0.204

C Collection of Numerical Input Parameters

Quark Masses

$$\begin{array}{ll}
 m_t & = 100 - 200 \text{ GeV} & m_t^{\text{central}} & = 130 \text{ GeV} \\
 m_b & = 4.8 \text{ GeV} & m_c & = 1.4 \text{ GeV} \\
 m_d(m_c) & = 8 \text{ MeV} & m_s(m_c) & = 150 \text{ MeV}
 \end{array}$$

Scalar Meson Masses and Decay Constants

$$\begin{array}{ll}
 m_K & = 498 \text{ MeV} & F_K & = 161 \text{ MeV} \\
 m_\pi & = 135 \text{ MeV} & F_\pi & = 132 \text{ MeV}
 \end{array}$$

QCD and Electroweak Parameters

$$\begin{array}{ll}
 \Lambda_{\overline{\text{MS}}} & = 200 - 400 \text{ MeV} & \Lambda_{\overline{\text{MS}}}^{\text{central}} & = 300 \text{ MeV} \\
 \alpha & = 1/128 & M_W & = 80.0 \text{ GeV}
 \end{array}$$

CKM Elements

$$\begin{array}{ll}
 |V_{us}| & = 0.221 & |V_{ud}| & = 0.9753 \\
 |V_{cb}| & = 0.043 \pm 0.004 & |V_{ub}/V_{cb}| & = 0.10 \pm 0.03 \quad (\text{range I}) \\
 |V_{cb}| & = 0.043 \pm 0.002 & |V_{ub}/V_{cb}| & = 0.10 \pm 0.01 \quad (\text{range II})
 \end{array}$$

$K \rightarrow \pi\pi$ Decays and $K^0 - \bar{K}^0$ Mixing

$$\begin{array}{ll}
 \text{Re}A_0 & = 3.33 \times 10^{-7} \text{ GeV} & \text{Re}A_2 & = 1.50 \times 10^{-8} \text{ GeV} \\
 \omega & = 1/22.2 & \Omega_{\eta\eta'} & = 0.25 \\
 \varepsilon & = (2.258 \pm 0.018) \times 10^{-3} & \Delta M_K & = 3.5 \times 10^{-15} \text{ GeV} \\
 B_K & = 0.65 \pm 0.15 \quad (\text{range I}) & B_K & = 0.65 \pm 0.05 \quad (\text{range II}) \\
 \eta_1 & = 0.85 & \eta_2 & = 0.58 \\
 \eta_3 & = 0.36 & &
 \end{array}$$

Hadronic Matrix Elements

$$B_{2,LO}^{(1/2)}(m_c) = 5.8 \pm 1.1 \quad B_{2,NDR}^{(1/2)}(m_c) = 6.7 \pm 0.9 \quad B_{2,HV}^{(1/2)}(m_c) = 6.3 \pm 1.0$$

$$B_3^{(1/2)} = B_5^{(1/2)} = B_6^{(1/2)} = B_7^{(1/2)} = B_8^{(1/2)} = B_7^{(3/2)} = B_8^{(3/2)} = 1 \quad (\text{central values})$$

D Figures

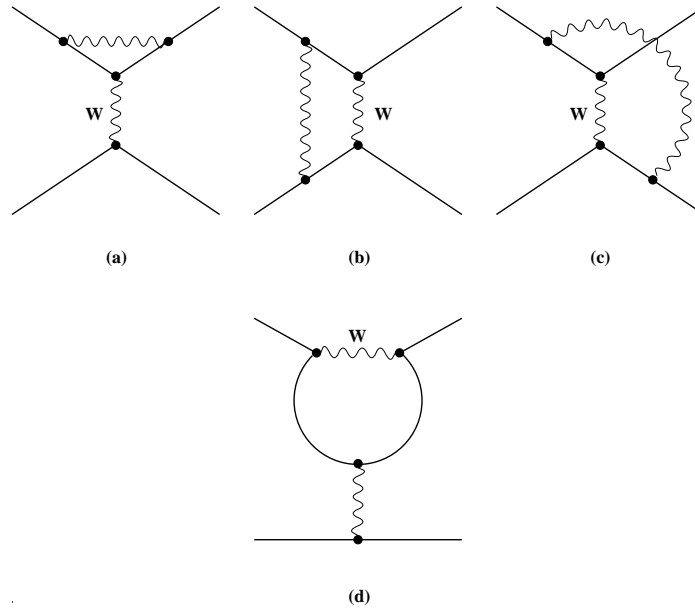


Figure 1:

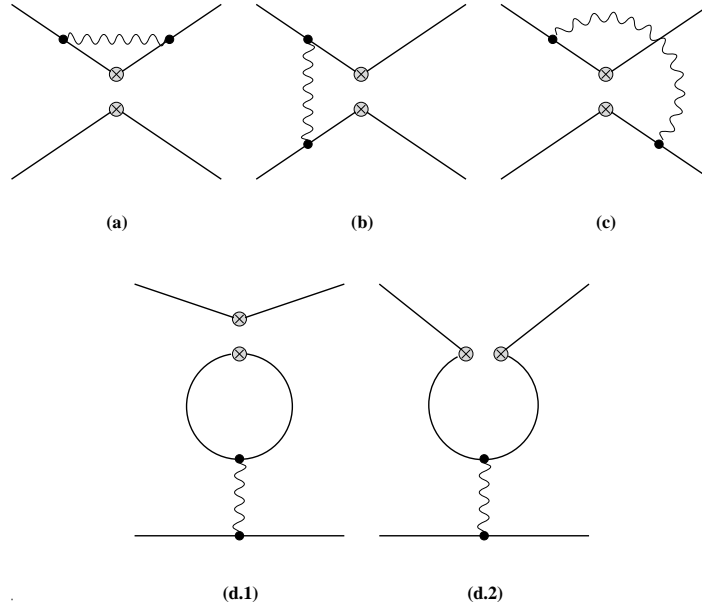


Figure 2:

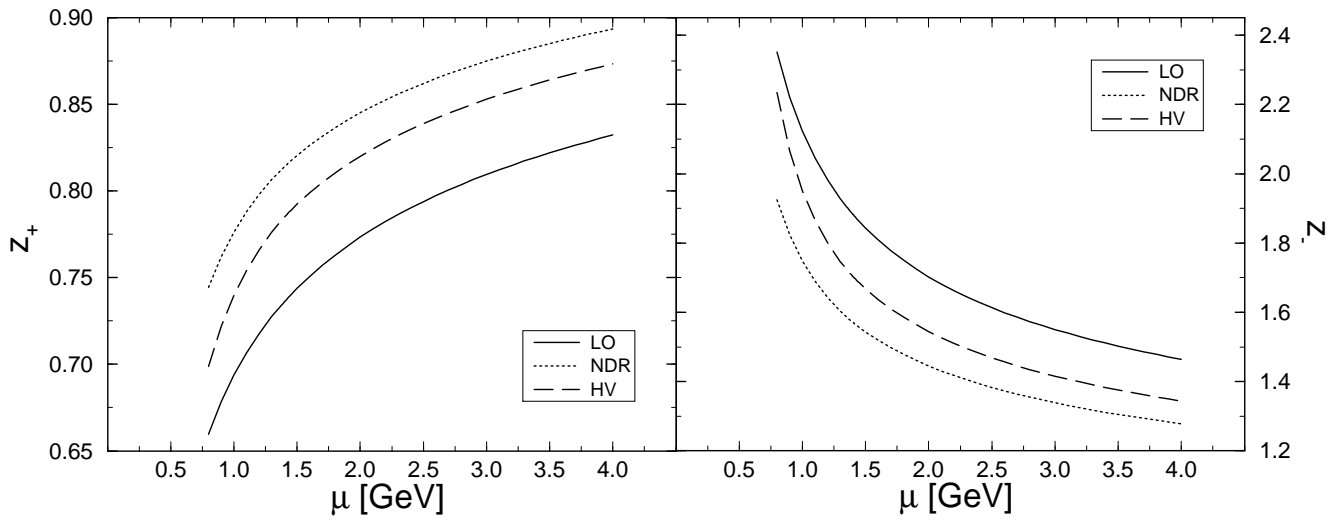


Figure 3:

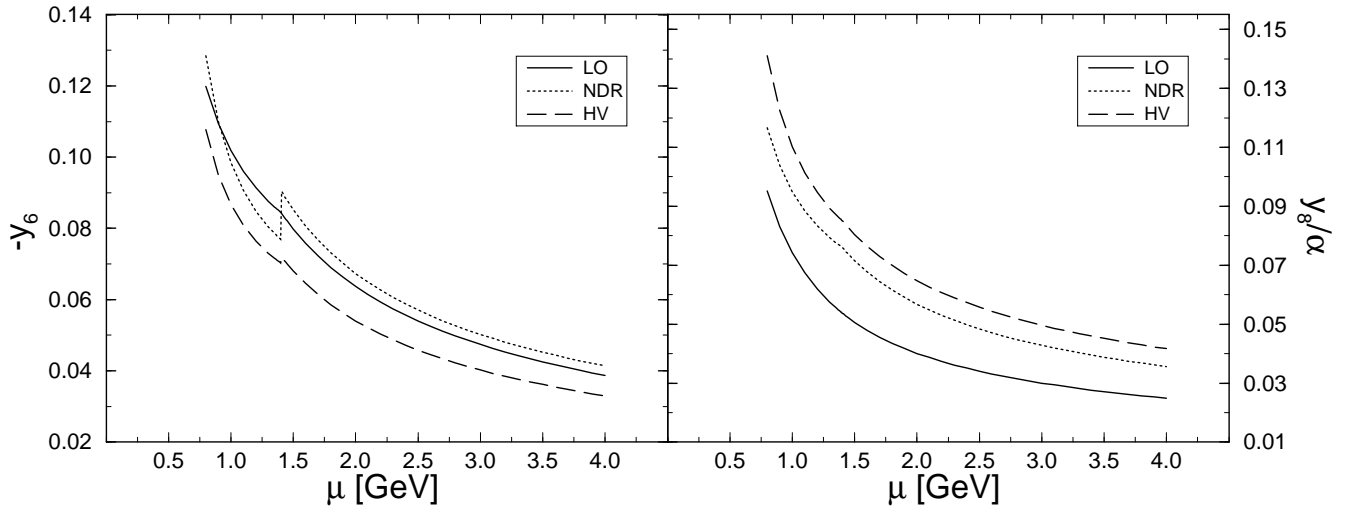


Figure 4:

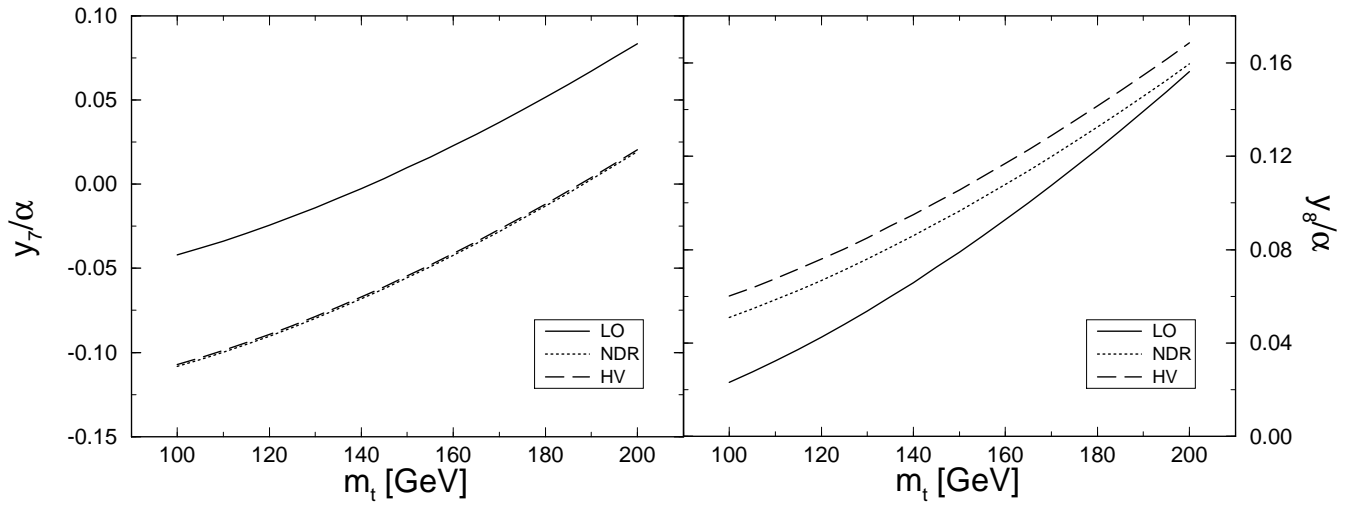


Figure 5:

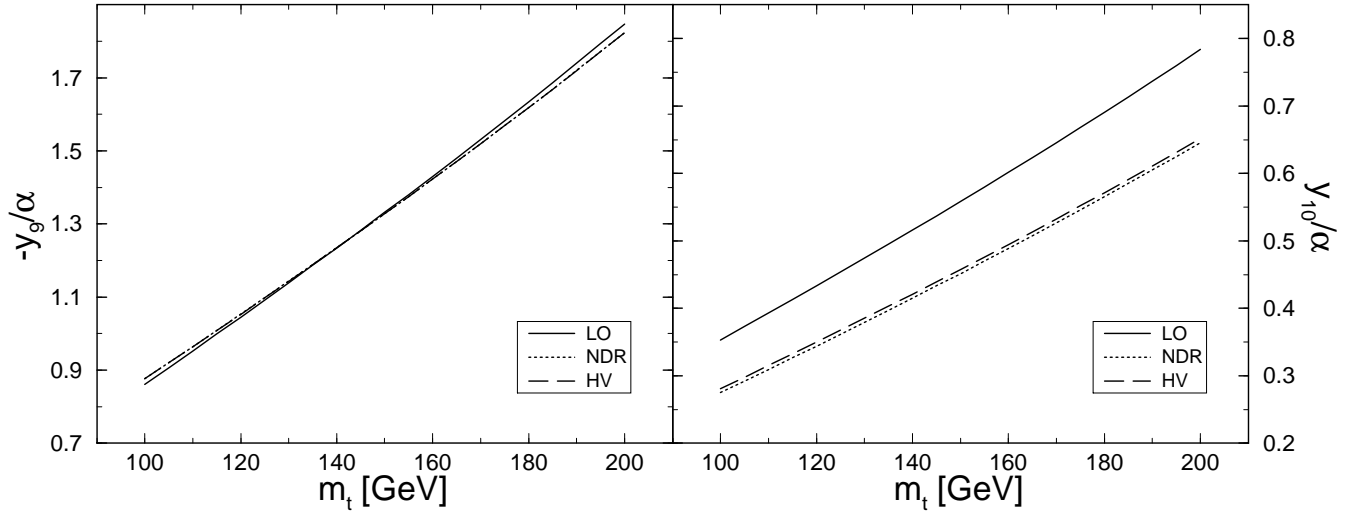


Figure 6:

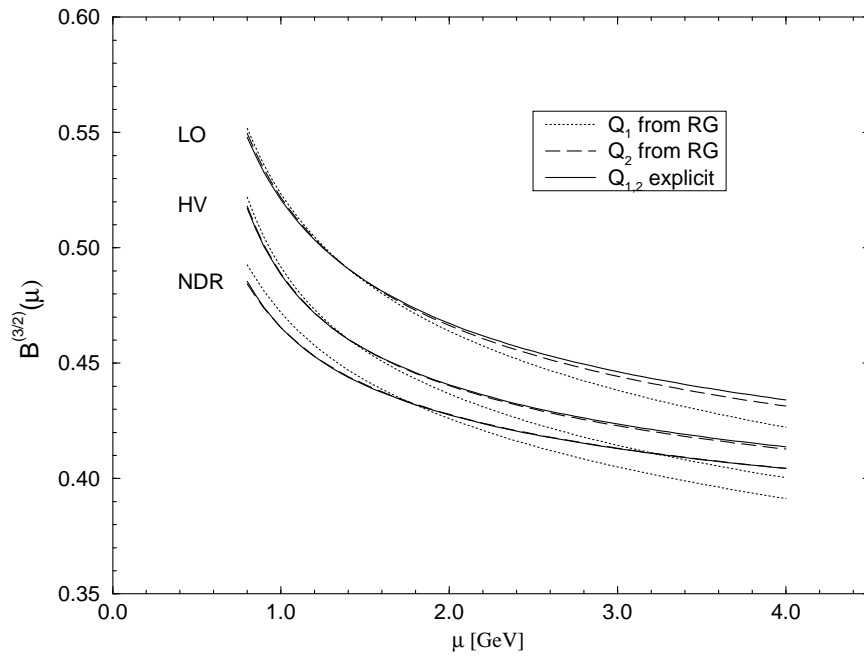


Figure 7:

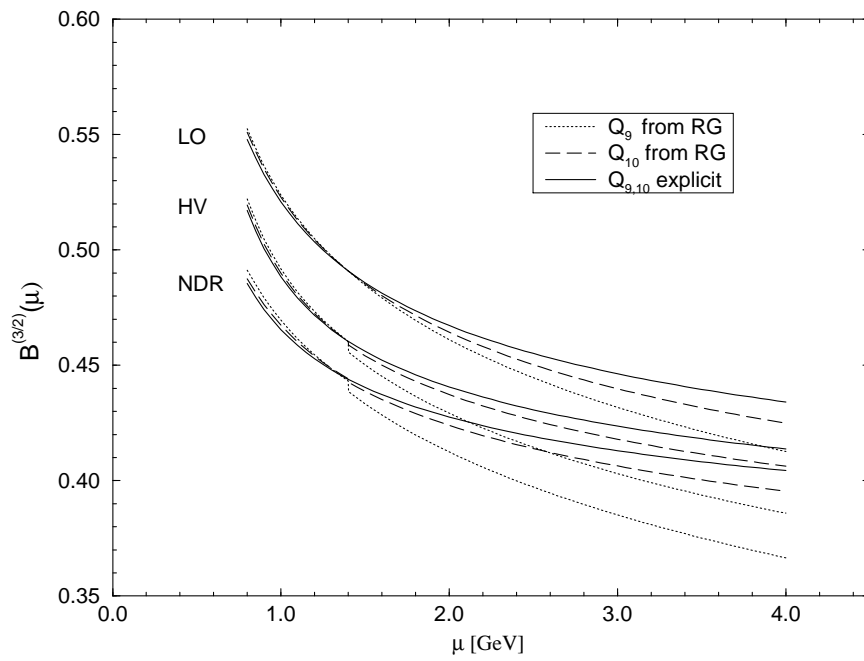


Figure 8:

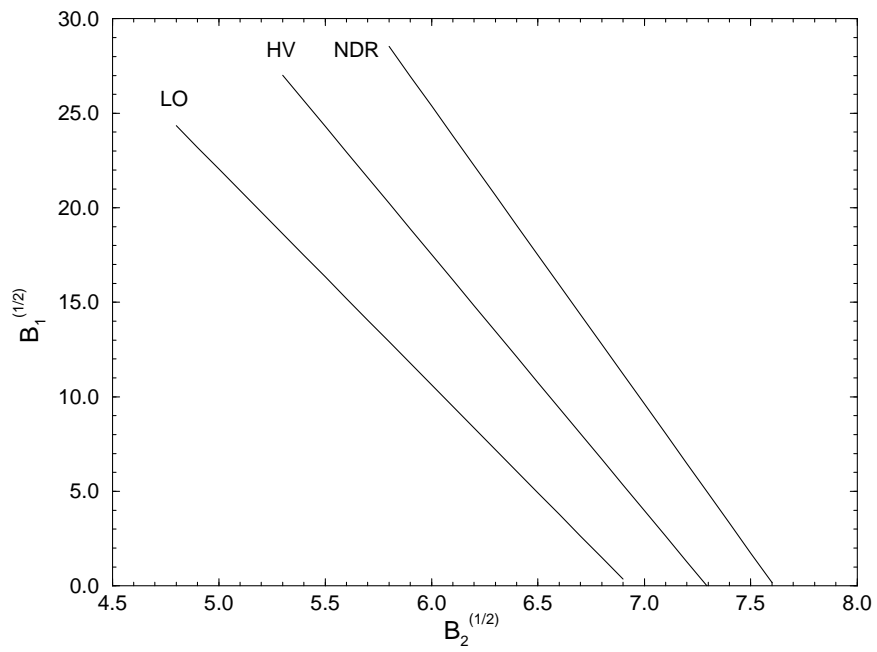


Figure 9:

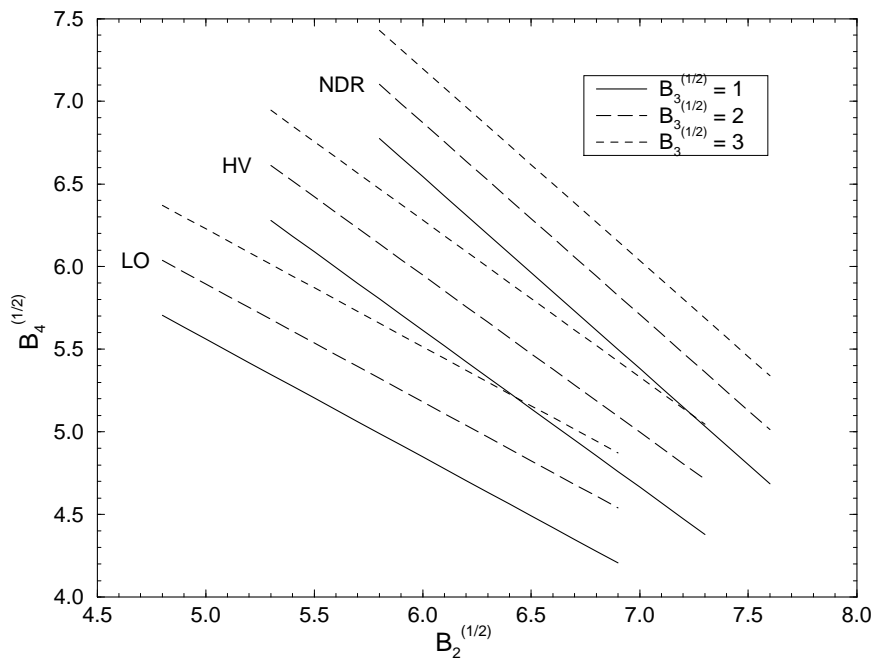


Figure 10:

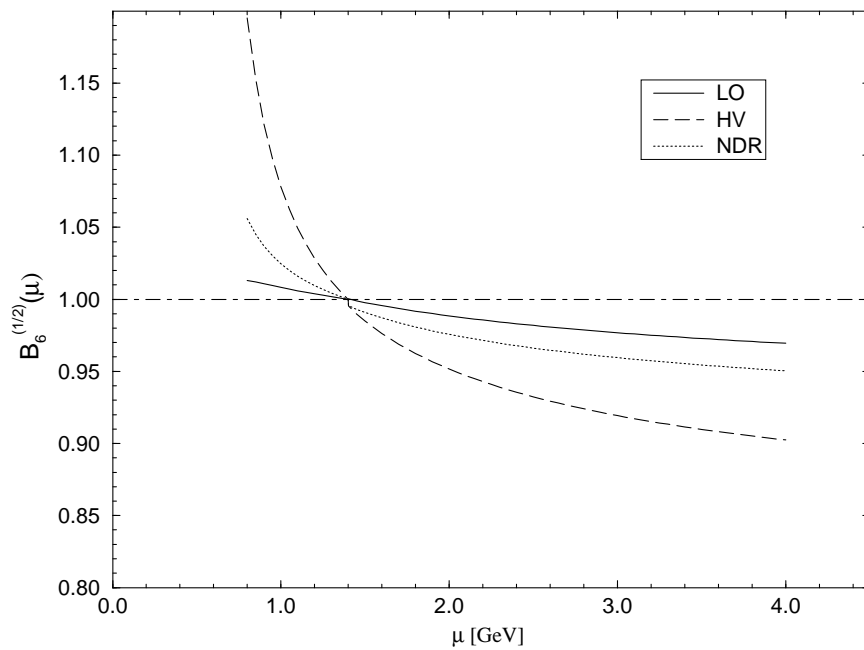


Figure 11:

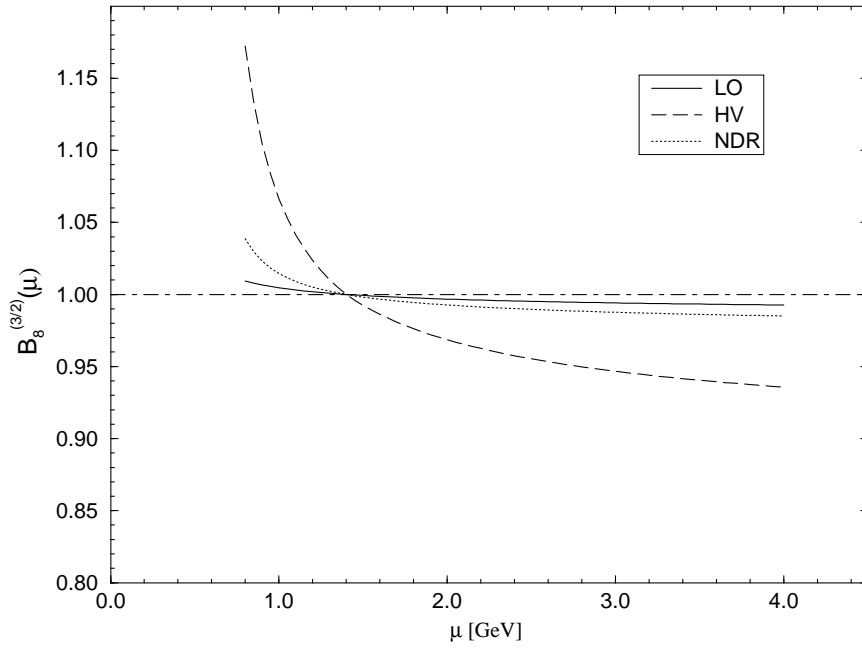


Figure 12:

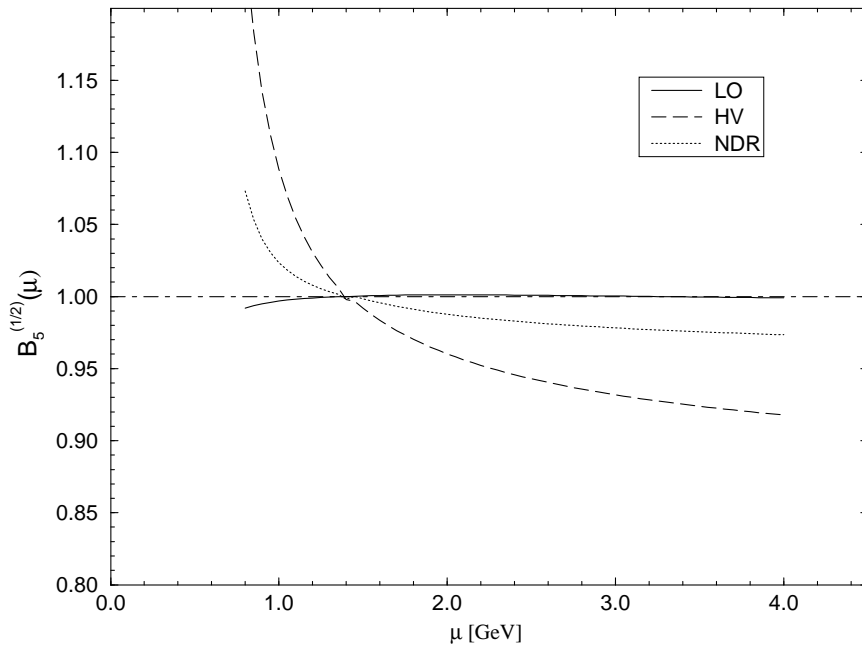


Figure 13:

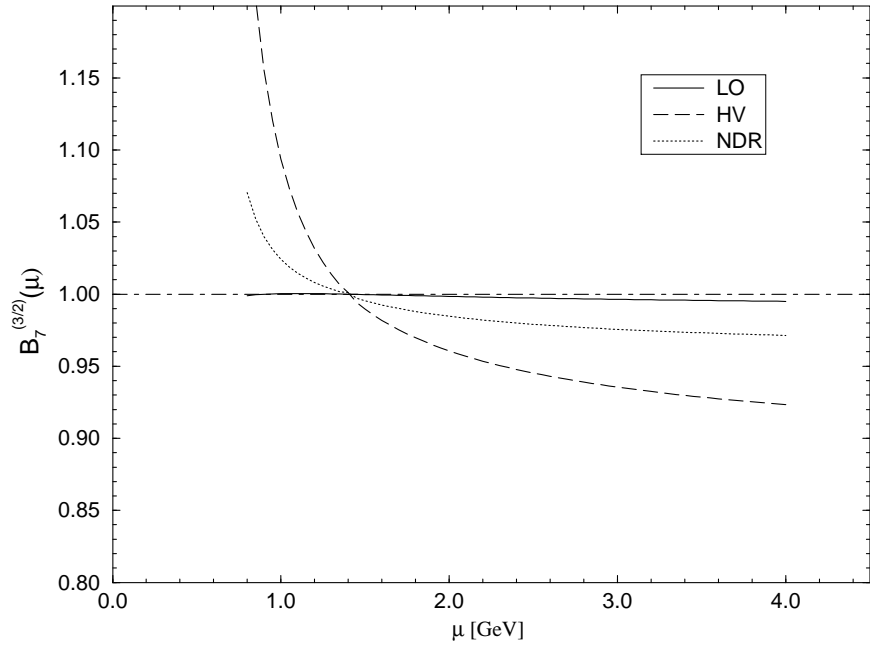


Figure 14:

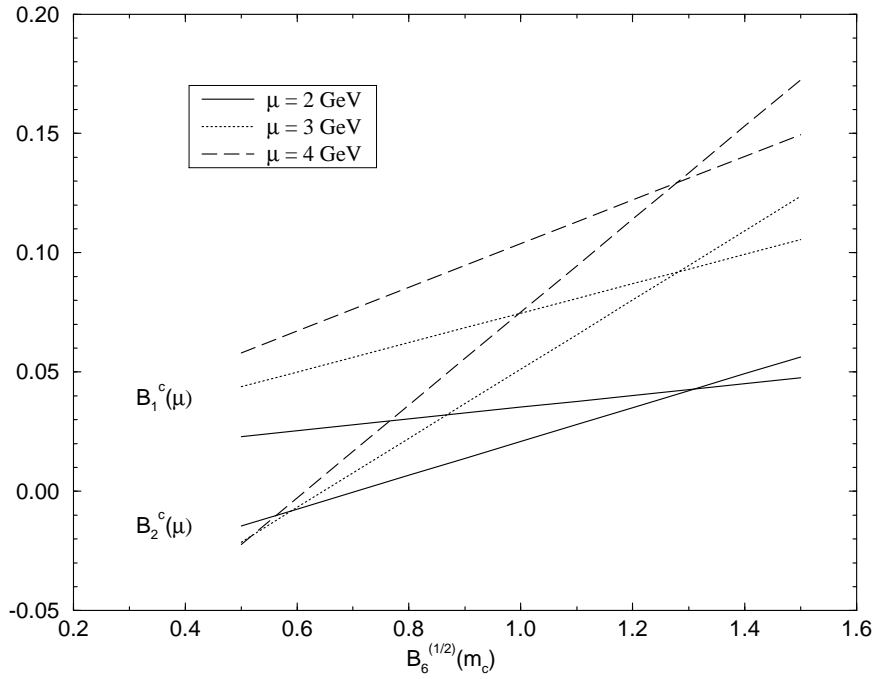


Figure 15:

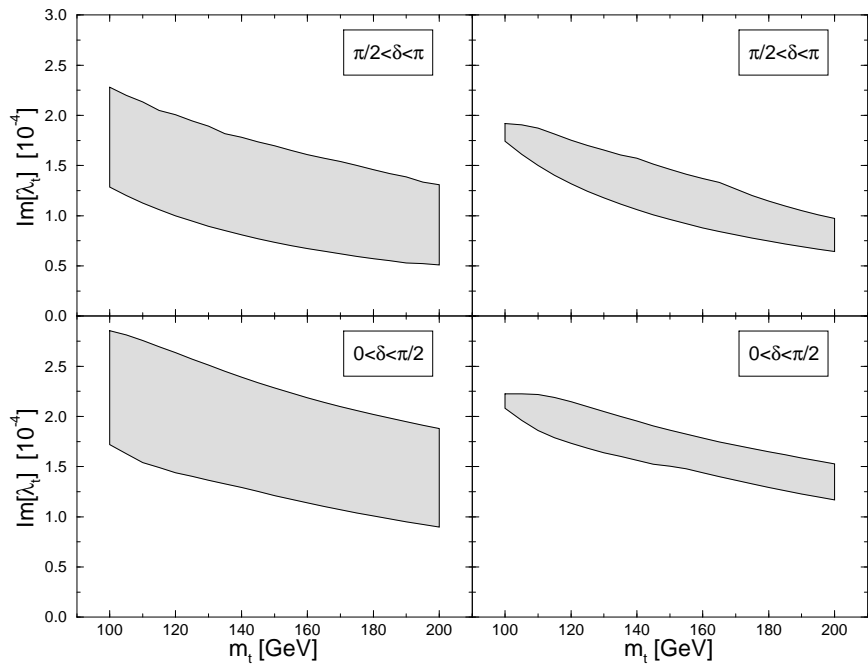
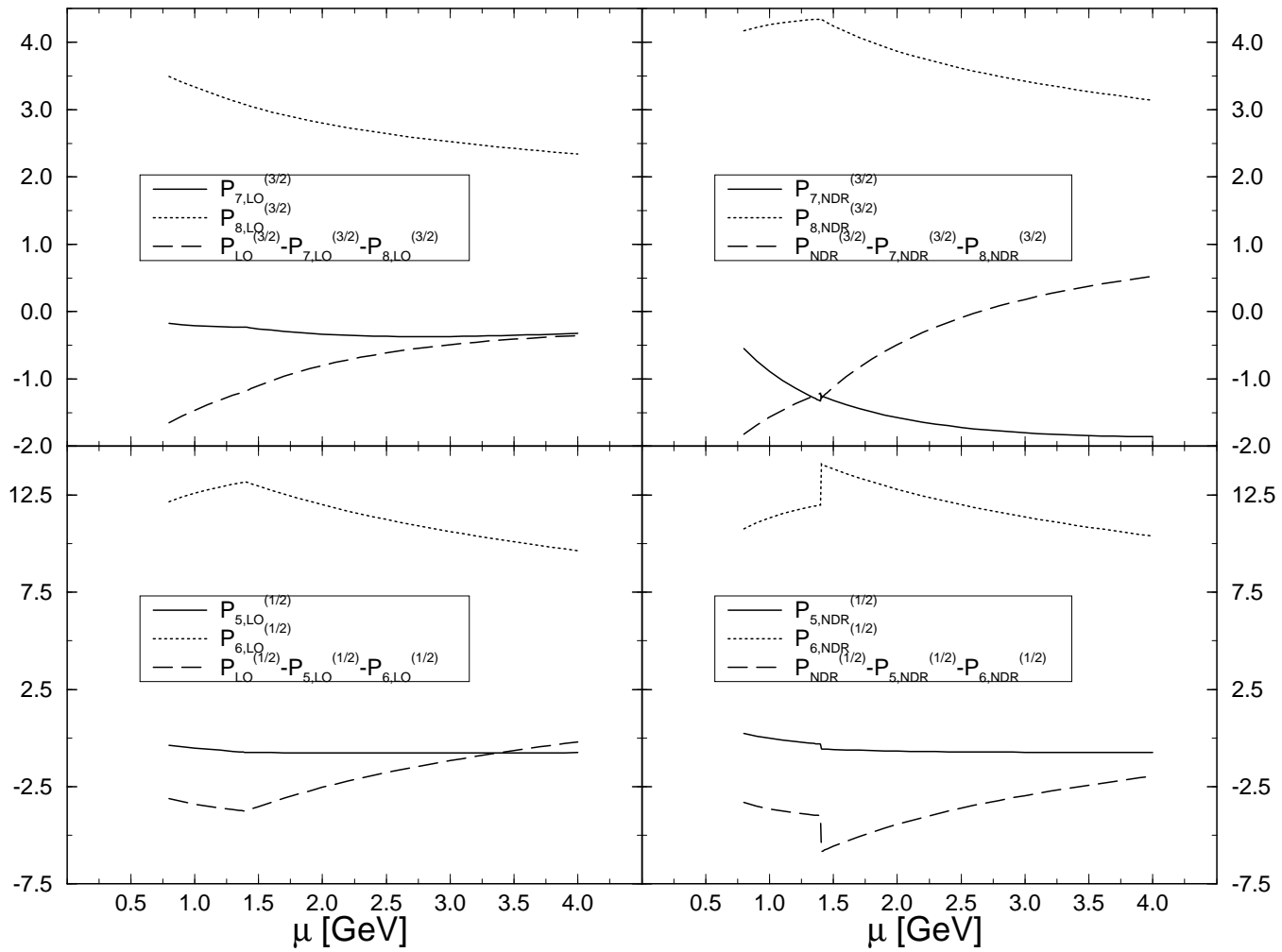


Figure 16:

Figure 17:



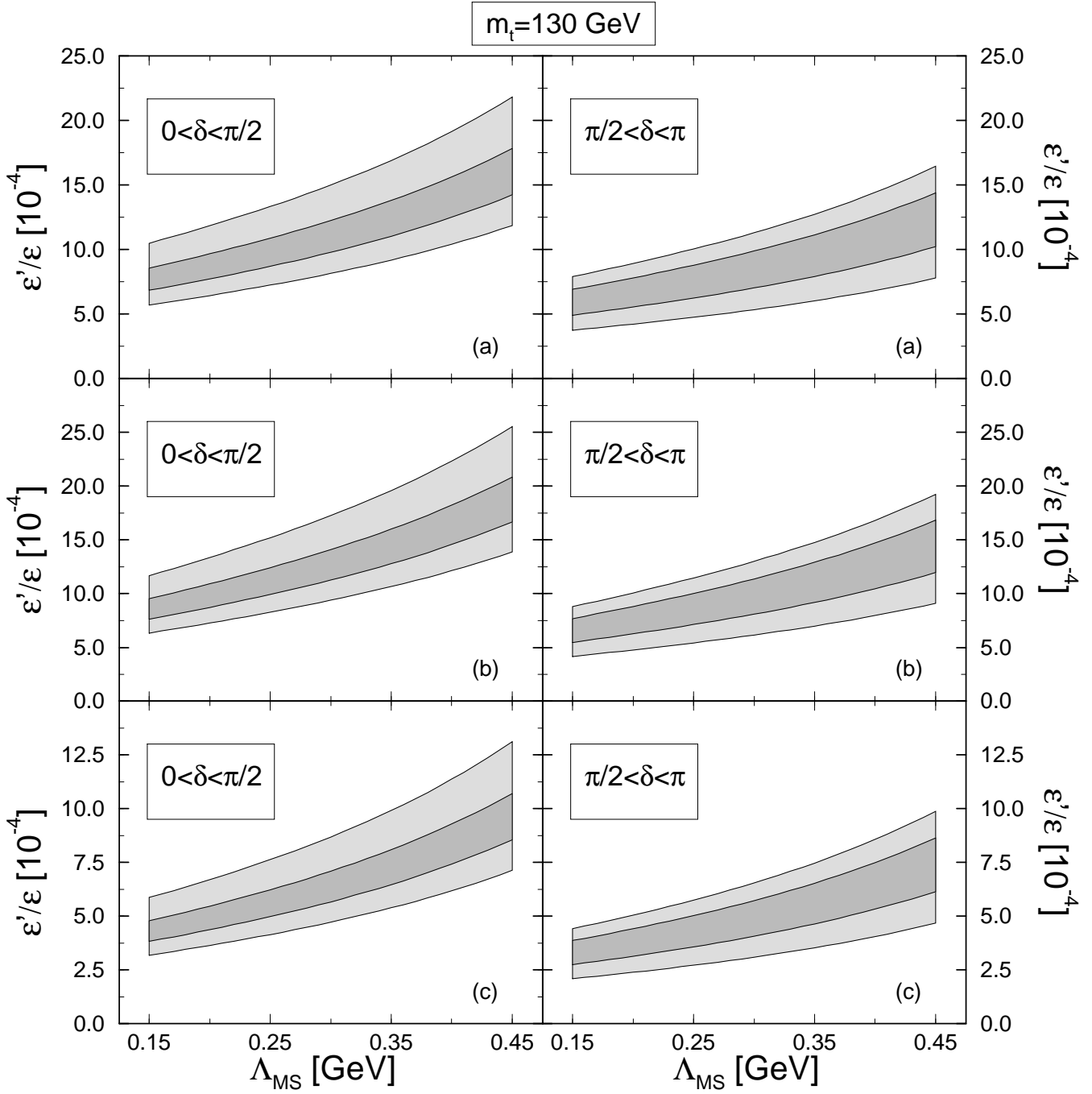


Figure 18:

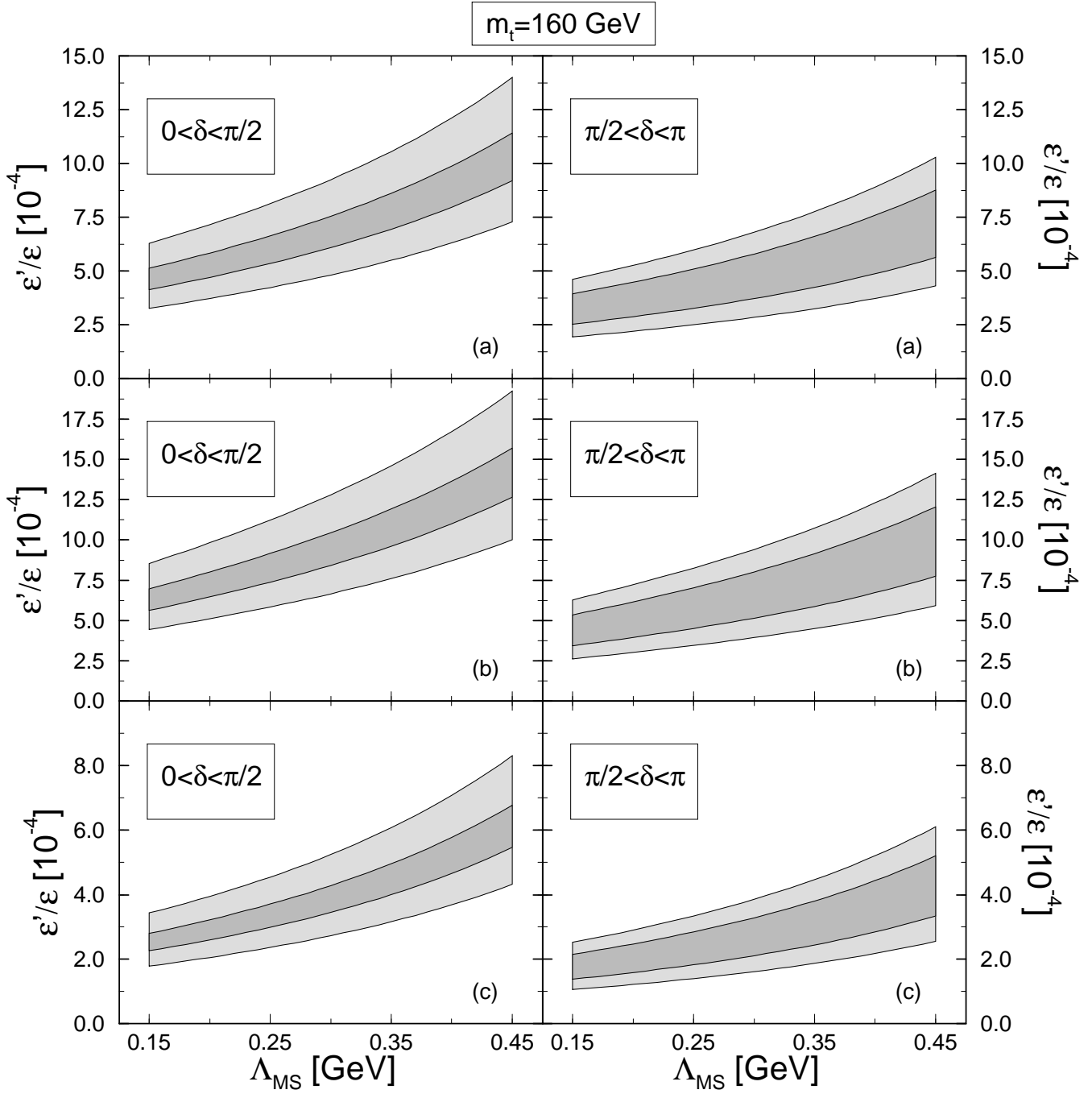


Figure 19:

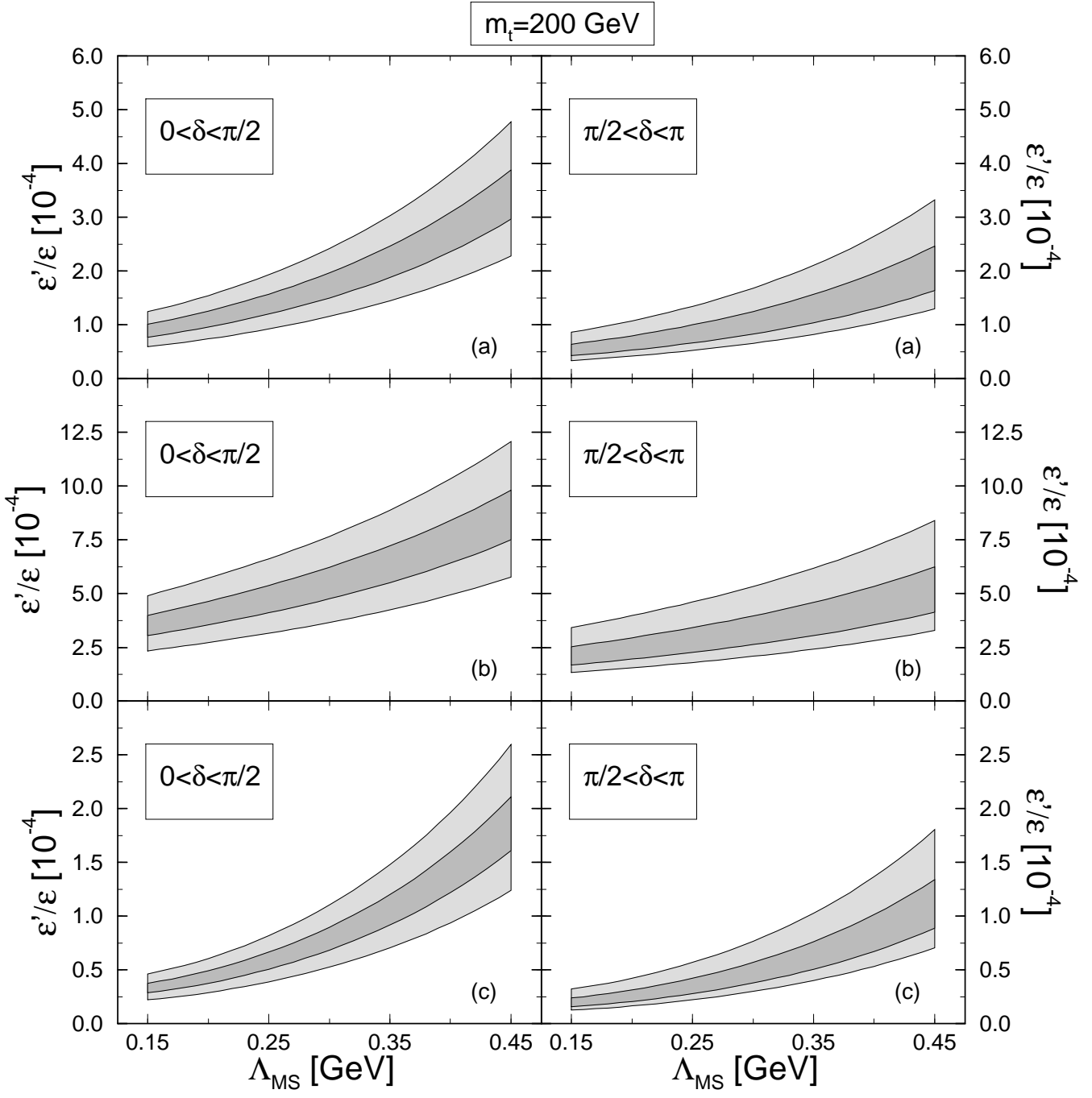


Figure 20:

Figure Captions

Figure 1: Current-current and penguin 1-loop diagrams in the full theory. The wavy lines labeled with “W” denote W^\pm bosons, the unlabeled wavy lines denote either a gluon or a photon.

Figure 2: Current-current and penguin 1-loop diagrams in the effective theory. The unlabeled wavy lines denote either a gluon or a photon.

Figure 3: $z_\pm(\mu)$ for various schemes and $\Lambda_{\overline{\text{MS}}} = 300 \text{ MeV}$.

Figure 4: $y_6(\mu)$ and $y_8(\mu)/\alpha$ for various schemes and $\Lambda_{\overline{\text{MS}}} = 300 \text{ MeV}$.

Figure 5: $y_7(m_c)/\alpha$ and $y_8(m_c)/\alpha$ as functions of m_t for various schemes and $\Lambda_{\overline{\text{MS}}} = 300 \text{ MeV}$.

Figure 6: $y_9(m_c)/\alpha$ and $y_{10}(m_c)/\alpha$ as functions of m_t for various schemes and $\Lambda_{\overline{\text{MS}}} = 300 \text{ MeV}$.

Figure 7: $B^{(3/2)}(\mu)$ entering $\langle Q_{1,2}(\mu) \rangle_2$ extracted from $\text{Re}A_2$ for different schemes, $\Lambda_{\overline{\text{MS}}} = 300 \text{ MeV}$ and different cases discussed in the text.

Figure 8: $B^{(3/2)}(\mu)$ entering $\langle Q_{9,10}(\mu) \rangle_2$ extracted from $\text{Re}A_2$ for different schemes, $\Lambda_{\overline{\text{MS}}} = 300 \text{ MeV}$ and different cases discussed in the text.

Figure 9: $B_1^{(1/2)}(m_c)$ as a function of $B_2^{(1/2)}(m_c)$ for $\Lambda_{\overline{\text{MS}}} = 300 \text{ MeV}$ and various schemes.

Figure 10: $B_4^{(1/2)}$ as a function of $B_2^{(1/2)}(m_c)$ for various values of $B_3^{(1/2)}(m_c)$.

Figure 11: $B_6^{(1/2)}(\mu)$ for different schemes, $\Lambda_{\overline{\text{MS}}} = 300 \text{ MeV}$ and common normalization $B_6^{(1/2)}(m_c) = 1$.

Figure 12: $B_8^{(1/2)}(\mu)$ for different schemes, $\Lambda_{\overline{\text{MS}}} = 300 \text{ MeV}$ and common normalization $B_8^{(1/2)}(m_c) = 1$.

Figure 13: $B_5^{(1/2)}(\mu)$ for different schemes, $\Lambda_{\overline{\text{MS}}} = 300 \text{ MeV}$ and common normalization $B_5^{(1/2)}(m_c) = 1$.

Figure 14: $B_7^{(1/2)}(\mu)$ for different schemes, $\Lambda_{\overline{\text{MS}}} = 300 \text{ MeV}$ and common normalization $B_7^{(1/2)}(m_c) = 1$.

Figure 15: $B_{1,2}^c(\mu)$ as a function of $B_6^{(1/2)}(m_c)$ in the HV scheme for $\Lambda_{\overline{\text{MS}}} = 300 \text{ MeV}$.

Figure 16: The ranges of $\text{Im}\lambda_t$ as a function of m_t for parameter ranges I (left) and II (right) given in appendix C.

Figure 17: The most important contributions to $P^{(1/2)}$ and $P^{(3/2)}$ as a function of μ for LO and the NDR scheme. m_t , $\Lambda_{\overline{\text{MS}}}$ and the various hadronic parameters B_i were taken at their central value given in appendix C.

Figure 18: The ranges of ε'/ε in the NDR scheme as a function of $\Lambda_{\overline{\text{MS}}}$ for $m_t = 130$ GeV and parameter ranges I (light grey) and II (dark grey) given in appendix C. The three pairs of ε'/ε plots correspond to hadronic parameters (a) $B_6^{(1/2)}(m_c) = B_8^{(3/2)}(m_c) = 1.5$, (b) $B_6^{(1/2)}(m_c) = 1.5$, $B_8^{(3/2)}(m_c) = 1$ and (c) $B_6^{(1/2)}(m_c) = B_8^{(3/2)}(m_c) = 1$, respectively.

Figure 19: Same as fig. 18 but for $m_t = 160$ GeV.

Figure 20: Same as fig. 18 but for $m_t = 200$ GeV.